FINITE-STATE MODELS OF TRANSPORT PHENOMENA IN HYDROLOGIC SYSTEMS

by

Michael Emerson Campana

A Dissertation Submitted to the Faculty of the

DEPARTMENT OF HYDROLOGY AND WATER RESOURCES

In Partial Fulfillment of the Requirements
For the Degree of

DOCTOR OF PHILOSOPHY
WITH A MAJOR IN HYDROLOGY

In the Graduate College

THE UNIVERSITY OF ARIZONA

1 9 7 5

THE UNIVERSITY OF ARIZONA

GRADUATE COLLEGE

I hereby recommend that this dissertation prepared under my direction by Michael Emerson Campana

entitled FINITE-STATE MODELS OF TRANSPORT PHENOMENA IN HYDROLOGIC SYSTEMS

be accepted as fulfilling the dissertation requirement of the degree of DOCTOR OF PHILOSOPHY

Eugene S Simpson — Dissertation Director — 30 Oct 75 — Date

After inspection of the final copy of the dissertation, the following members of the Final Examination Committee concur in its approval and recommend its acceptance:*

Samuel N. Lavenue	9/29/75
Eugene S Simpson	30 Oct 75
Donald R Davis	10 Oct 75

*This approval and acceptance is contingent on the candidate's adequate performance and defense of this dissertation at the final oral examination. The inclusion of this sheet bound into the library copy of the dissertation is evidence of satisfactory performance at the final examination.

STATEMENT BY AUTHOR

This dissertation has been submitted in partial fulfillment of requirements for an advanced degree at The University of Arizona and is deposited in the University Library to be made available to borrowers under rules of the Library.

Brief quotations from this dissertation are allowable without special permission, provided that accurate acknowledgment of source is made. Requests for permission for extended quotation from or reproduction of this manuscript in whole or in part may be granted by the head of the major department or the Dean of the Graduate College when in his judgment the proposed use of the material is in the interests of scholarship. In all other instances, however, permission must be obtained from the author.

SIGNED: Michael E. Campana

To Tricia

ACKNOWLEDGMENTS

This dissertation would not have been possible without the generous assistance of certain individuals and organizations.

The author is extremely grateful to Dr. Eugene S. Simpson, his dissertation director and advisor, whose encouragement and assistance made this dissertation a reality. Dr. Simpson is responsible for much of the theory in this work, and he was a source of great inspiration and many ideas throughout the author's graduate education. Many of the simulations contained in this work were suggested by him. His patience and understanding were greatly appreciated by the author. The author is also indebted to Drs. Daniel D. Evans and Donald R. Davis, who, along with Dr. Simpson, critically read the manuscript and made numerous suggestions to improve it. Dr. Davis deserves thanks for persuading the Department of Systems and Industrial Engineering to provide the author with the computer time necessary to complete certain aspects of this work. The author would also like to thank Drs. D. Trifan and Clark Benson of the Department of Mathematics for serving on the author's committee.

The author benefitted from many hours of discussion with his colleague and friend, Roger W. Peebles. Many of

the concepts embodied in the author's computer program were originally devised by Mr. Peebles. He was also of tremendous aid in developing certain aspects of the author's model.

Without the help of Dr. F. J. Pearson, Jr., of the U.S. Geological Survey, the chapter on the Edwards Limestone would not have been possible. He provided the author with most of the data, as well as the initial cell network, and made many suggestions for improving the Edwards model, most of which were incorporated by the author in his model.

The author would like to acknowledge the financial assistance afforded by The University of Arizona and a NDEA Title IV Fellowship. The author is also grateful to the Departments of Hydrology and Water Resources and Systems and Industrial Engineering for providing computer time.

All computer calculations were performed on the Control Data Corporation 6400 computer at The University of Arizona Computer Center.

Finally, the author wishes to thank a truly outstanding woman, his wife Tricia, who was a continual source of inspiration, encouragement, and strength throughout the author's graduate career. Without her, none of this would have been possible.

TABLE OF CONTENTS

TABLE OF CONTENTS--Continued

TABLE OF CONTENTS--Continued

TABLE OF CONTENTS--Continued

TABLE OF CONTENTS--Continued

LIST OF TABLES

LIST OF TABLES--Continued

LIST OF TABLES--Continued

LIST OF ILLUSTRATIONS

LIST OF ILLUSTRATIONS--Continued

ABSTRACT

Transport phenomena in hydrologic systems are simulated with finite-state models (FSMs), which are similar to mixing cell models in that they utilize a mixing cell as their basic subdivision, yet are more flexible, capable of modeling more complex systems, and easier to manipulate than previous mixing cell models. The basic FSM equations are discrete, recursive forms of the continuity equation for mass transport and the storage equation for fluid transport. Different types of mixing and flow can be simulated by specifying appropriate algorithms for use in the basic equations. Finite-state models thus have a physical basis, although they avoid the use of differential equations. The FSM digital computer model can simulate systems in one, two, or three spatial dimensions with relative facility. In many important cases, transit number and age number distributions can be calculated. These distributions, and especially their means, are useful in determining fluid residence times in hydrologic systems.

Two aquifer systems are modeled using finite-state models. In a portion of the Tucson Basin Aquifer of southern Arizona a three-dimensional, steady flow FSM is used to account for the observed carbon-14 age distribution in the aquifer without assuming piston flow in the aquifer

and without evaluating dispersion parameters. This model provides a first approximation of the three-dimensional flow distribution, an estimate of the long-term average annual recharge, and fluid residence times in the aquifer. The second FSM, two-dimensional and non-steady flow, accounts for the transient distribution of tritium in the Edwards Limestone of south-central Texas. This aquifer is a highly anisotropic, nonhomogeneous karst aquifer that is difficult to model by traditional methods. In both models, first guesses for cell volumes and flow distributions were made on the basis of available hydrogeological data.

Saturated, unsaturated, and open-channel flow also are examined. Flow algorithms for the basic FSM storage equation follow the theory of linear systems, although in certain regimes, especially those involving unsaturated flow, it may be necessary to develop nonlinear flow algorithms. This was not attempted. It is also shown that the finite-state model can simultaneously model the transport of mass and fluid in a hydrologic system. The FSM also has the potential for modeling heat transport, which may prove useful in simulating geothermal reservoirs as well as other systems involving heat transport.

CHAPTER 1

INTRODUCTION

1.1 Transport in Hydrologic Systems

The analysis of mass and energy transport in hydrologic systems is basic to efficient water resources exploitation and management. "Energy" as herein considered and called hydraulic energy is that energy contained in a unit weight or unit mass of water by virtue of its vertical position relative to a horizontal datum, its pressure relative to atmospheric pressure, and its velocity relative to a set of coordinate axes fixed to the earth's surface. When defined in terms of unit weight of water, hydraulic energy is measured by hydraulic head. Hydraulic energy may be transported and dissipated, or dissipated only (mainly to heat) in flow through hydrologic systems. "Mass" as herein considered refers primarily to substances dissolved in water, including isotopes of the water molecule, rather than to the water itself. This mass is considered to move with the water (molecular thermokinetic motion is normally neglected); hence, the flow system must be determined. The flow system, in turn, depends mainly upon the hydraulic head distribution. Thus, energy distribution and transport and mass transport are intimately interrelated. Finally, a

"hydrologic system" as used herein is any watershed, soil, or aquifer having definable boundaries and definable inputs and outputs of mass and energy.

The modeling of heat transport will also be considered. Heat transport can be an important consideration in the study of hydrologic systems, particularly surface water bodies which receive large quantities of thermal effluent, which can have pronounced effects on the biological and physicochemical regimes of the water bodies. Heat transport is also an important factor in the assessment of geothermal resources, which are especially significant now as society searches for new sources of energy.

This dissertation deals with the elaboration and generalization of a basically simple approach to modeling transport in hydrologic systems. Particular attention will be given to mass transport in aquifers, although the method employed will be applicable to mass transport in any hydrologic system. In addition, a chapter is devoted to energy transport in hydrologic systems.

1.2 Modeling Mass Transport in Aquifer Systems

1.2.1 Background

In solving problems involving mass transport in aquifer systems, the most common approach consists of formulating and solving deterministic partial differential

equations (PDEs) with the concomitant initial and boundary conditions. Although analytical solutions to the PDEs exist for certain sample cases, such solutions are usually inadequate for describing mass transport on an aquifer-wide scale. In addition, it is unlikely that rigorous analytical solutions to these PDEs will be developed in the near future, owing to the complexities of these equations (Reddell and Sunada, 1970). Therefore, it will be necessary to resort to numerical techniques and digital computer simulation to adequately describe mass transport in aquifers under most conditions.

1.2.2 Numerical Techniques

Before one can solve a mass transport PDE, it will be necessary to obtain the ground-water velocity distribution in the aquifer, which will serve as one of the inputs to the mass transport model. The velocity distribution can be obtained from the hydraulic head distribution. The latter can be determined from data, although the requirements of the mass transport model usually dictate that it be obtained from a hydraulic model of the aquifer. This model usually consists of a partial differential equation describing flow in the aquifer which is solved numerically. Finite-difference techniques of solution are popular (Freeze, 1969; Prickett and Lonnquist, 1971; Remson, Hornberger, and Molz, 1971, Chapters 3-5), although

finite-element methods have also been used to solve flow PDEs (Neuman and Witherspoon, 1971; Pinder, 1973).

Once the velocity distribution has been obtained from the flow PDE, the mass transport equation can be solved, usually in two spatial dimensions. Numerical solutions can be effected using finite-difference methods (Reddell and Sunada, 1970), finite-element techniques (Guymon, 1970; Guymon, Scott, and Herrmann, 1970; Pinder, 1973), or the method of characteristics (Garder, Peaceman, and Pozzi, 1964; Pinder and Cooper, 1970; Reddell and Sunada, 1970; Bredehoeft and Pinder, 1973). Sagar (1973, Chapter 2) contains an excellent review of ground-water modeling in general.

In order to calibrate and validate the mass transport model, it is necessary to have sufficient data on the movement of mass in the aquifer. The model must be calibrated so that the dispersion coefficients in the mass transport PDE can be obtained. The dispersion coefficients are usually obtained by trial-and-error, that is, different values of these coefficients are used in the PDE until the model output approximates the calibration data. Once this has been accomplished, data other than the calibration data are used to validate the model.

The dispersion coefficient may be a measure of the ignorance of the detailed velocity distribution. For example, Nelson (1973) attempted to model dispersion without

recourse to a dispersion coefficient. He instead attempted a sufficiently detailed velocity ("micro-flow") distribution by solving a so-called "permeability integral." However, the method requires the detailed determination of the permeability distribution along a plane that intersects the flow field and a detailed map of the hydraulic head distribution. Uncertainties in these measurements and high computer costs make the method unfeasible for most problems.

1.2.3 Dispersion Coefficients

The dispersion coefficient takes into account two distinct effects: molecular diffusion, or that movement of mass caused by the thermokinetic motions of the mass particles themselves (Brownian motion), and hydrodynamic or convective dispersion, that movement of the mass particles caused by the motion of the fluid in which the mass is carried. For most field problems, Bredehoeft and Pinder (1973) state that molecular diffusion is negligible compared to hydrodynamic dispersion. Disregarding the molecular component of dispersion simplifies the estimation of dispersion coefficients.

As far as dispersion coefficients are concerned, calibration of a mass transport model is simplified considerably by assuming that the aquifer is isotropic. In such a case, the dispersion coefficient, ordinarily a second rank tensor, reduces to two independent terms: the

longitudinal dispersion coefficient D_L and the transverse dispersion coefficient D_T (Scheidegger, 1961). D_T is sometimes estimated as $.10D_L$ (Simpson, 1970), although Bredehoeft and Pinder (1973) used $D_T = .30D_L$. If one assumes one of these relationships between D_T and D_L and abides by it, then only one dispersion parameter must be adjusted during the calibration process. D_T and D_L can also be related to quantities called the longitudinal and transverse dispersivities by multiplying the appropriate dispersivity by the magnitude of the velocity (Reddell and Sunada, 1970). The dispersivity is in fact a fourth rank tensor, although Scheidegger (1961) showed that in the isotropic case, it reduces to just two components, the transverse and longitudinal dispersivities. Scheidegger also demonstrated that for the general anisotropic case, the dispersivity tensor can be reduced to 36 independent components and also suggested a relationship between the components of the dispersion tensor and the components of the dispersivity tensor. Reddell and Sunada (1970) also gave relationships between the components of the dispersion tensor and D_T, D_L, and the molecular diffusion coefficient, although they stated that relationships other than theirs had been derived.

Because of the large number of dispersion-related parameters involved, the calibration of a mass transport model for an anisotropic aquifer would probably be awkward, particularly if the model were large and required great

expense to simulate on a digital computer. Ideally, one would like to be able to get dispersion coefficients from the properties of the medium and the fluid, and much research has been conducted with that in mind (Reddell and Sunada, 1970), with little agreement among the different investigations. In light of this disagreement and the calibration difficulties for anisotropic aquifers it is perhaps not difficult to see why researchers such as Bredehoeft and Pinder (1973) confined themselves to consideration of the isotropic case and its concomitant simplifications. One might also wonder how the introduction of nonhomogeneity as well as anisotropy would further complicate matters. Clearly, any mass transport model that would not depend upon dispersion coefficients and the confusion surrounding their evaluation would be a welcome addition to ground-water hydrology. Such a model would also be of great help in mass transport studies in other hydrologic systems, since dispersion coefficients are necessary in these systems as well. The author will introduce a model which neither requires a micro-flow analysis nor the use of dispersion coefficients, yet which is not a "black box" model.

1.3 Environmental Tracers

All models require real-world data for calibration and validation. To date, the mass transport models described in the literature all were calibrated and validated against

the transport of a pollutant after several decades of record. It is necessary to obtain some documentation of pollution in a hydrologic system before one can calibrate and validate a model for use in predicting future contamination of the system. One takes the risk that the system may be ruined by pollution or irreversibly contaminated by the time enough data are obtained for calibration and validation. It would therefore be advantageous to know something about the mass transport properties of a hydrologic system by utilizing environmental (naturally-occurring) tracers and their distributions in a system. Radioactive environmental tracers such as carbon-14, tritium, and silicon-32 may be particularly useful in this regard, though it is not necessary to restrict oneself to radioactive tracers. Certain artificially-produced but naturally-introduced tracers such as the fluorocarbons can also be used.

CHAPTER 2

MIXING CELL MODELS

2.1 The Mixing Cell Concept

The modeling concept developed in this dissertation has its roots in the concept of a mixing cell, in which the flow of mass or energy in a system is modeled by subdividing the system into one or more mixing cells. A mathematical algorithm is then formulated to describe movement into, out of, and within the cell system. In a multi-cell system, each cell is connected to at least one other cell by a flow path. There is normally at least one input to the cell system from the outside environment and one output from the cell system. The cell system may be arranged in one-, two-, or three-dimensional networks. Three-dimensional networks are uncommon, due in part to the difficulty of mathematically describing the flow in such a complex system. Sometimes a three-dimensional cell network can be reduced to a two-dimensional one by invoking symmetry arguments (Deans and Lapidus, 1960).

In addition to the above properties, each mixing cell is usually assumed to have impermeable walls, except, of course, for connections to other cells or to the outside environment. The volume of each cell is often assumed

constant, and there are no gradients of concentration or energy within a given cell. Any quantity entering the cell is instantaneously dispersed throughout the entire cell, and therefore the output stream has the same concentration as that of the cell itself. These assumptions are not universal for all mixing cell models; however, they are made in most mixing cell models with which the writer is familiar.

2.2 Mixing Cell and Related Models in Various Fields

2.2.1 Chemical Engineering

The field of chemical engineering was perhaps the first discipline to make extensive use of mixing cell and related models to simulate the movement of and chemical changes in substances within and among reactor vessels. These models are known in the literature by a variety of names: tanks-in-series models (Levenspiel, 1972, p. 290), constant flow stirred tank reactors or CFSTRs (Levenspiel, 1972, p. 97), continuous stirred tank reactors or CSTRs (Levenspiel, 1972, p. 571), finite-stage models (Deans and Lapidus, 1960), and population-balance models (Himmelblau and Bischoff, 1968, Chapter 4). These models differ from one another in terms of the algorithms used, the mixing assumptions, etc., although they are all similar in that they utilize a cell or some other mixing unit as the basic subdivision of the system. It should be noted that chemical

engineers are generally concerned with systems much smaller than hydrologic systems.

2.2.2 Hydrology and Other Fields

Most of the early hydrologic mixing cell and related models dealt with surface water systems. Nash (1957) pointed out that the gamma distribution could be considered as the impulse response function for a cascade of equal cells which he referred to as linear reservoirs. Dooge (1959) assumed that the action of a watershed could be represented by linear distortionless channels and linear storage elements or reservoirs. Banks (1974) obtained a result for the definition of a dispersion unit in open channels by constructing a model composed of equal cells arranged in series.

Hydrologists have also been modeling subsurface flow with mixing cell and related models. Wentworth (1948) suggested that the creation of a transition zone at a moving interface between fresh and salt water in a coastal aquifer could be explained by perfect mixing in an array of cells. Bear and Todd (1960) showed that dispersion may be regarded as a combination of two processes: complete mixing in the elementary cells and translation at the average flow velocity from one cell to the next through the channels connecting them. Dooge (1960) assumed that the action of a ground water reservoir consisted of storage alone and modeled an aquifer as a linear storage element or linear

reservoir. Eliasson (1971) modeled unsteady ground-water flow in an aquifer of limited horizontal extent by assuming that the aquifer could be represented by linear reservoirs. Eliasson et al. (1973) described the unsteady ground-water level in an aquifer by a differential equation, the solution of which included the solution of an eigenvalue problem. They also showed that for an aquifer of limited horizontal extent and arbitrary shape, ground-water runoff behaved as a sum of flows through infinitely many linear reservoirs, and corresponded to the eigenfunctions. Gelhar and Wilson (1974) modeled a phreatic aquifer as a single well-mixed linear reservoir (mixing cell) in order to account for the effects of highway deicing salts on ground-water quality. Their model included both mass transport and fluid flow. Przewlocki and Yurtsever (1974) modeled tritium movement in two different aquifers using one-dimensional arrays of mixing cells. They also determined an estimate of the total volume of one of the aquifers and turnover times for both aquifers.

Other examples of mixing cell and related models as applied to hydrology and other fields can be found in Craig (1957), Kraijenhoff van de Leur (1958), Eriksson (1971), and Bolin and Rodhe (1973). Dooge (1973) contains much information on linear and nonlinear reservoirs as applied to hydrologic systems, many of which can be adapted to mixing cell models.

2.3 Two Common Mixing Cell Models

Before presenting the theory of finite-state mixing cell models, the author believes that it would be useful to mention two common mixing cell models and their analytical solutions. Both of these models are given in Himmelblau and Bischoff (1968, Chapter 4).

Figure 1(a) shows a single mixing cell in which there are no concentration gradients and where the concentration of the output stream is identical to the concentration within the cell. The differential equation describing this flow and its solution for an instantaneous pulse input of tracer are

$$QC_{in} - QC = \frac{VdC}{dt} \tag{1}$$

and

$$C = C_o \exp(-t/\bar{t}) \tag{2}$$

where

V = cell volume, a constant;

Q = volumetric flow rate, a constant;

C = concentration of material in the cell, initially equal to zero;

C_o = average concentration of the input tracer pulse if uniformly distributed throughout the system;

t = time;

$\bar{t}$ = V/Q, the residence time of the fluid in the cell; and

C_{in} = input concentration, = 0 for $t > 0$.

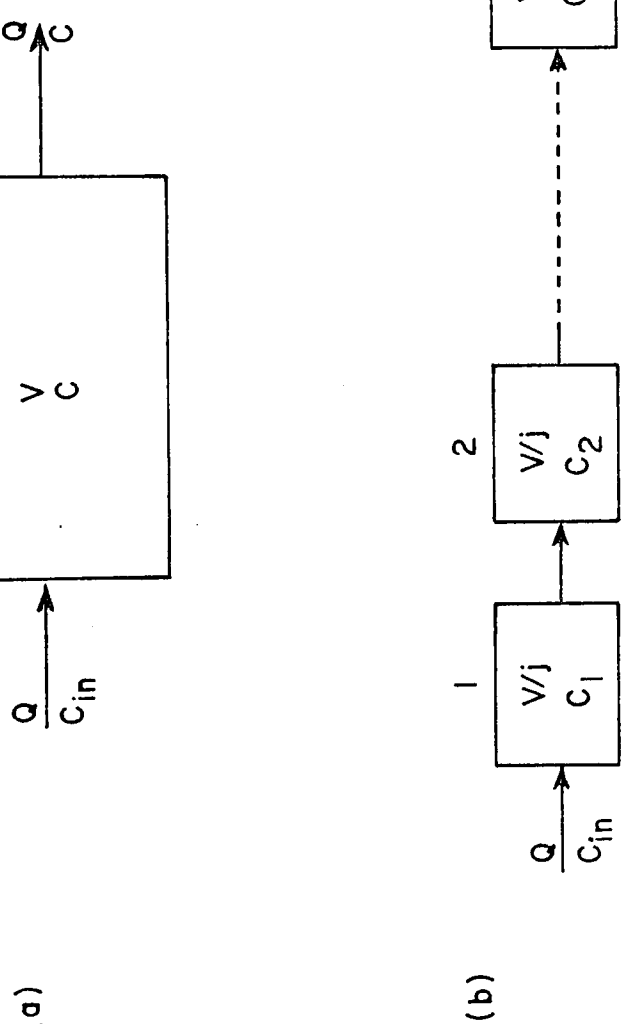

Figure 1. Single mixing cell (a), and series of equi-volume mixing cells (b).

Figure 1(b) shows j equi-volume mixing cells arranged in series. For an instantaneous pulse input of tracer with no tracer initially present in the system, the concentration of the output stream from the last cell in the series is given by

$$C_j = [C_o j^j (t/\bar{t})^{j-1} \exp(-jt/\bar{t})]/(j-1)! \qquad (3)$$

where

C_j = concentration of tracer in the last cell and of the output stream of this cell;

j = total number of cells; and

$\bar{t}$ = V/Q, where V = total volume of the system.

Equation (3) can be generalized for the ith cell ($1 \leq i \leq j$) by replacing j with i and noting that $\bar{t}$ will equal iV'/Q, where V' is the volume of each cell. C_o must also be adjusted for the new i-cell system.

2.4 Limitations on the Hydrologic Applications of Current Mixing Cell Models

The two models described in the previous section are very simple in terms of the geometric configurations of the cell networks. Indeed, the model in Figure 1(a) is the simplest possible case, whereas the model in Figure 1(b) is merely an extension of the first model to a series of j equi-volume cells. Models incorporating more complex configurations can be found in Himmelblau and Bischoff (1968, Chapter 4) and in Levenspiel (1972, Chapter 9). However,

these models were formulated by chemical engineers for chemical engineering problems and the hydrologist seeking to use them might be hard-pressed to find a real-world hydrologic system that conformed to their geometric configurations. The hydrologist might be able to model certain simple hydrologic systems using a model similar to the one shown in Figure 1(b), but complex systems would present problems.

There are also other restrictions on existing mixing cell models that limit their use in modeling hydrologic systems. Cell volumes are usually assumed to be equal and are not allowed to vary with time. Some two-dimensional cell network models composed of two or more series of cells arranged in parallel do allow the cell volumes to vary from series to series, though within a given series all cell volumes must be equal. When cell volumes within a series are allowed to vary, they are usually restricted to varying according to a geometric or arithmetic series. Even for such cases, the mathematical expressions describing the system become quite awkward (Fan et al., 1969).

Current mixing cell models usually restrict the modeler to employing only a certain number of inputs to and outputs from the cell network. Spatial and temporal variations in inputs and outputs are also restricted, as are variations in and complexities of the flow paths among the

cells. The inclusion of sources and sinks within the cells also presents difficulties.

2.5 The Ideal Hydrologic Mixing Cell Model

In light of the preceding discussion, the author can list the properties of the ideal hydrologic mixing cell model. It should be able to accomplish the following objectives:

1. Give the amount of the particular tracer, either mass or energy, in each cell as a function of time or iteration number.
2. Allow any arbitrary number and volumes of cells.
3. Allow any arbitrary cell network in one, two, or three spatial dimensions.
4. Allow inputs to and outputs from the cell network to be placed anywhere in the network.
5. Permit variations in the input flow volumes and/or the amount of tracer contained in these inputs.
6. Permit complex flow paths among the cells in the network.
7. Allow changes in the volumes of any or all cells as a function of time or iteration number.
8. Account for sources or sinks in some or all of the cells.

9. Be sufficiently general so that a wide variety of hydrologic systems can be modeled without having to make major changes in the model.
10. Be able to model the transport of mass and/or energy in a hydrologic system.
11. Keep the mathematical algorithms relatively simple and easy to manipulate so that hydrologists of varying mathematical proficiencies can understand and use the model with confidence and a minimum of difficulty.
12. Be relatively inexpensive to operate.
13. Have some physical basis.
14. Provide acceptable answers.

The author feels that any mixing cell model capable of meeting all fourteen objectives will prove to be extremely worthwhile to hydrologists. The last objective is undoubtedly the most important, because any model, no matter how simple or complex, is worthless if it unable to provide the modeler with acceptable answers. The definition of "acceptable answers" rests with the individual modeler. The writer is confident that the finite-state mixing cell models described in the following chapters meet all fourteen of the above criteria.

CHAPTER 3

FINITE-STATE MIXING CELL MODELS

3.1 Introduction

A finite-state mixing cell model (or simply, finite-state model or FSM) consists of a set of interconnected cells of any desired size through which the transport of an incompressible fluid (water) and dissolved matter is represented by a sequence of finite states. In theory, the states can assume an infinite number of values, but operationally the states will be restricted to a finite number of values. The transformation from one state to the next is governed by a set of recursive equations. The transport of the fluid itself can be effected by algorithms governing the change of cell volume from one iteration to the next. The type of mixing in a cell, whether perfect mixing, piston flow, or some intermediate type, is determined by specific mixing algorithms.

3.2 Basic Mathematical Algorithm

The basic equation for any cell in an array of cells is (Simpson, 1973):

$$S(N+1) = S(N) + BRV(N+1)*BRC(N+1) - BDV(N+1)*BDC(N+1) \pm R(N+1) \quad (4)$$

where

S(N+1) = cell state or the amount of material in the cell at iteration N+1;

S(N) = cell state at iteration N;

N = iteration number;

BRV(N+1) = boundary recharge volume at iteration N+1, the volume of water entering the cell;

BRC(N+1) = boundary recharge concentration at iteration N+1, the concentration of material in the water entering the cell (the BRV(N+1));

BDV(N+1) = boundary discharge volume at iteration N+1, the volume of water leaving the cell;

BDC(N+1) = boundary discharge concentration at iteration N+1, the concentration of material in the water leaving the cell (the BDV(N+1));

R(N+1) = source or sink term for iteration N+1; more than one such term is permissible; and

* = symbol denoting multiplication.

In words, Equation (4) states that the amount of material in the cell at iteration N+1 equals the amount of material in the cell at iteration N plus the amount that entered at iteration N+1 minus the amount that left at iteration N+1 plus or minus any material that was created or destroyed within the cell at iteration N+1. Simply stated, Equation (4) is a discrete form of the continuity

equation. The fact that this equation is a recursive equation makes it especially easy to program on a digital computer. The author has written a computer program in FORTRAN IV (see Appendix B) that applies Equation (4) to an arbitrary number of cells arranged in any fashion in one-, two-, or three-dimensional cell networks. The maximum number of cells in the network will be limited by the memory capacity of the particular computer used, the availability and amount of data, and the size of the system being modeled.

The volumetric quantities BRV, BDV, cell volumes (which will be denoted by the term VOL), and all other volumes not specified here are expressed as multiples of an arbitrary unit reference volume, the URV. The size of the URV is selected to give convenient numbers to all volumes for computational purposes. For example, in modeling a large aquifer system with a FSM, a suitable URV might be one cubic kilometer. The reader should note that the BRV and the BDV always have concentration terms associated with them, the BRC and the BDC, respectively. These concentration terms may at times assume values of zero. It should also be indicated that the product of the BRV or the BDV and its associated concentration term yields a number with the dimensions of an absolute amount of material.

3.3 FSM Terminology

Before continuing the discussion of FSMs, it will be necessary to define some terms critical to the understanding of these models. Unless otherwise indicated, these definitions are modified after Simpson (1973).

By cell state is meant the amount of substance, other than water and the cell matrix, if any, contained in the cell. The particular substance moving through the system will determine the units of the cell state (grams, moles, curies, etc.). When considering mass transport, it may be more convenient to work with concentration units rather than mass units. Cell states are readily converted to cell concentrations by dividing the cell state at any iteration by the effective volume of the cell at that iteration. The initial state of a cell is its state prior to the first iteration of the FSM.

The author will define the effective volume of a cell as the portion of the cell volume that is filled with fluid which can participate in the processes of mixing and/or flow. For a surface water system, the effective volume of a cell will probably be identical to or very close to the total volume of the cell. For a saturated porous medium system, the effective volume of the cell will equal the total volume of the cell multiplied by the effective porosity of the medium.

A tracer is any substance that is dissolved in the water of the real-world hydrologic system. This term includes water molecules containing deuterium, tritium, or oxygen-18. Tracers in the FSM and the real world are assumed to occupy zero volume. The term numerical tracer will refer to the dimensionless numbers used in FSM simulation experiments. A tracer is said to be conservative if it is unaffected by physical or chemical reactions occurring within the FSM or real-world system, and non-conservative if it is so affected. A tracer can also be a form of energy, such as heat.

The finite-state model is defined by: (1) the arrangement and effective volumes of all cells and the manner in which they are interconnected with one another and with the FSM boundaries, and (2) the set of algorithms governing the changes of state and/or volume of each cell from one iteration to the next.

An iteration is one performance of the set of algorithms that govern changes of state and/or volume in each of the cells of the FSM.

Steady state is the condition in which the state of every cell, as displayed to the desired number of significant figures, remains constant from one iteration to the next. If the state of at least one cell varies with the iteration number, the FSM is in a non-steady state.

Steady flow is the condition in which the volumetric input of water to each cell (the BRV) is constant from one iteration to the next. This condition also requires that for each cell, BRV = BDV. The FSM is in a condition of non-steady flow when the volumetric input to at least one cell varies with the iteration number or when BRV $\neq$ BDV as displayed to the desired number of significant figures.

A condition of steady volume exists when the effective volume of each cell, as displayed to the desired number of significant figures, remains constant from one iteration to the next. The FSM is in a non-steady volume regime if the effective volume of at least one cell varies with the iteration number.

The definitions for steady state, steady flow, steady volume, and their opposite cases are operational in the sense that they are dependent upon the number of significant figures used by the modeler.

In the analysis to be given in Chapter 4, it will be necessary to assume that the water may be subdivided into a large number of small elements called fluid elements, each of which retains its identity in moving through the system of cells, and to each of which may be assigned a very small but finite and constant volume. As it enters the system, each fluid element is associated with a small amount of tracer. The tracer is contained in the fluid element, and the amount of tracer may be any finite amount down to and including

zero. The term "retaining identity" means that the amount of tracer contained in a fluid element does not change except by chemical reaction with other contained tracers, reaction with solids in the system, or by radioactive decay. In other words, fluid elements do not intermix with one another.

The author will use the word "system" (abbreviated "S") as a prefix to denote quantities which enter the FSM from the outside environment or are discharged by the FSM to the outside environment. Thus, a boundary recharge volume entering a cell from outside the FSM becomes a system boundary recharge volume or SBRV, and a BDV discharged from a cell to the outside environment becomes a system boundary discharge volume or SBDV. The concentrations associated with these volumes become the SBRC and SBDC, respectively. This terminology will be used only when it is imperative to distinguish between quantities entering or leaving the system and those entering cells from other cells or leaving cells destined for other cells.

3.4 FSM Regimes

In the preceding section, six possible conditions were specified: steady or non-steady state, steady or non-steady flow, and steady or non-steady volume. By taking any combination of these six possibilities, eight FSM regimes are obtained. However, two of these eight regimes, the

steady state, non-steady volume, steady flow and non-steady state, non-steady volume, steady flow regimes are not permissible. It is possible to pass from one regime to another as the iterative process proceeds, or to restrict the FSM to certain regimes only.

Changes of state, flow, or volume are affected by the precision of the definitions. For example, when approaching steady state a system whose states are defined by three significant figures will attain steady state before an identical system whose states are defined by five significant figures.

3.5 Mixing Algorithms

If one assumes that a particular FSM is restricted to steady volume and steady flow, then by definition BRV = BDV = a constant for each cell. The state can either be steady or non-steady. The BRV as well as the BRC either are specified inputs to the model that enter the FSM from outside the system (SBRV and SBRC) or are calculated outputs from one or more upstream connecting cells within the model. If one assumes for the moment that there are no sources or sinks within any of the cells, then the only unknown on the right side of Equation (4) is BDC(N+1). This quantity may be specified by writing an algorithm describing the manner in which the input mixes with the tracer already in the cell. Simpson (1973) described two different algorithms:

one entirely analogous to the mixing cell shown in Figure 1(a) and herein called a simple mixing cell or SMC, and the other for a cell somewhere between the perfect mixing of the SMC and pure piston flow (i.e., no mixing). This latter cell will be called a modified mixing cell or MMC.

3.5.1 The Simple Mixing Cell

In the case of the SMC it is assumed that at each iteration the cell expands to accommodate the incoming BRV. The expanded cell volume is now equal to VOL + BRV, where VOL is the original (unexpanded) effective volume of the cell. After this expansion, the tracer in the BRV then mixes completely with the contents of the cell. The cell then contracts to its original effective volume, and in the process discharges a volume of water (the BDV) equal to the volume that entered (the BRV). Figure 2(a) illustrates this process. The BDC will be equal to the concentration of the tracer in the cell in its expanded condition. The equation for the BDC is

$$BDC(N+1) = \frac{S(N) + BRV(N+1)*BRC(N+1)}{VOL + BRV(N+1)} \qquad (5)$$

The SMC can also be described as the "in-mix-out" algorithm since the incoming tracer mixes with the cell contents and is then discharged.

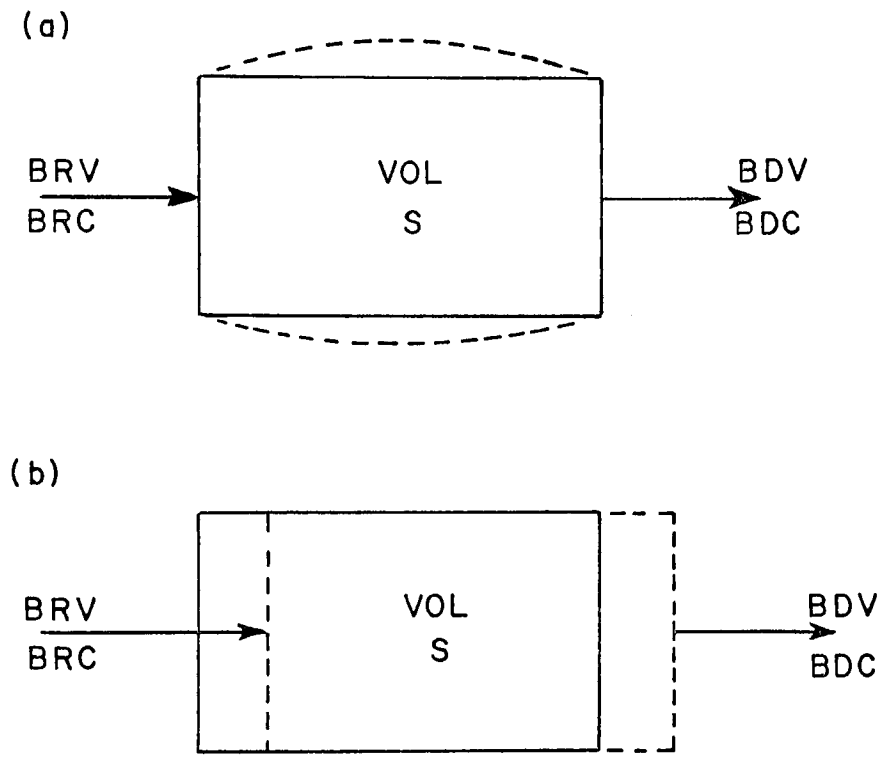

Figure 2. Types of mixing cells in finite-state models: (a) simple mixing cell; (b) modified mixing cell.

3.5.2 The Modified Mixing Cell

In the case of the MMC, the cell is assumed to be rigid. At each iteration, the incoming BRV first displaces an equal volume of water (the BDV) and then mixes with the remaining cell contents (Figure 2[b]). The BDC(N+1) is therefore identical to the concentration of tracer in the cell at iteration N. The equation for the BDC is

$$BDC(N+1) = \frac{S(N)}{VOL} \tag{6}$$

The MMC approaches pure piston flow as BRV approaches VOL, and approaches perfect mixing as BRV approaches zero. The BRV can equal VOL, but in general should not exceed it, else the cell may acquire a negative state.

The MMC can be termed the "in-out-mix" algorithm, since the BDV is discharged from the cell before the incoming BRV mixes with the cell contents.

3.5.3 Extension of the Mixing Algorithms to Other Regimes

Both the SMC and MMC algorithms are valid for any of the six possible FSM regimes. However, for any regime involving non-steady volume, it will be necessary to write Equations (5) and (6) in more general terms. The SMC algorithm thus becomes

$$BDC(N+1) = \frac{S(N) + BRV(N+1)*BRC(N+1)}{VOL(N) + BRV(N+1)} \tag{7}$$

and the MMC algorithm is

$$BDC(N+1) = \frac{S(N)}{VOL(N)} \tag{8}$$

where

VOL(N+1) = effective volume of the cell at iteration N+1;

VOL(N) = effective volume of the cell at iteration N.

In addition, for certain non-steady flow regimes (and the non-steady volume regime, as the reader shall see later on) the BRV and the BDV of a given cell are not necessarily equal at a given iteration. The SMC and the MMC still operate in the same manner, except that the volume of water discharged from the cell will not necessarily equal the amount of incoming water. The value of the BDV must be specified by a particular algorithm, to be discussed in a later section. In certain non-steady volume regimes, it is necessary to relax the requirement that the cells be rigid in the case of the MMC. For these regimes, it is best to view the MMC in terms of the phrase "in-out-mix," i.e., before the incoming BRV is allowed to mix with the cell contents, a BDV not necessarily equal to the BRV is discharged from the cell. For the SMC, the expanded cell will not be required to contract to its original effective volume. The effective volume it will assume will be dictated by the relative sizes of the BRV and BDV and the algorithm used to calculate the change in the effective volume.

In conclusion, the author should mention that in his computer program, no provision was made for combining the two mixing algorithms, either by having a cell alter its mixing algorithm as a function of iteration number or by combining simple and modified mixing cells in a FSM. All cells are restricted to using the same algorithm, nor are they allowed to change algorithms. The author cannot think of any theoretical reason for prohibiting combinations of and/or changes in mixing algorithms in a given FSM, and perhaps a system will be encountered which will demand such changes. The restrictions on mixing algorithms in the author's model were done for the sake of convenience and also because no reason was seen why these restrictions should not be made.

3.6 Operation of a FSM

Once the modeler selects a mixing algorithm, the state of a cell at iteration N+1 may be computed by knowing the state of the cell at iteration N, the inputs to the cell at iteration N+1, and the volumetric output from the cell at iteration N+1. In multi-cell models, interior cells receive their inputs from upstream connecting cells until eventually the upstream cell (or cells) is a boundary cell receiving its inputs from the outside environment. In order to operate a FSM, one must either know or assume the following:

1. The initial state for each of the cells.
2. The value and location of all inputs to the FSM as a function of iteration number.
3. The initial effective volumes of the cells.
4. The location of outputs from the FSM.
5. The flow paths within the FSM, that is, the spatial distribution of volumetric outputs from each cell and the fraction of the total volumetric output associated with each flow path.

Numbers 3 and 5 may be known a priori or they may be determined as part of the calibration process. It should go without saying that the hydrology of the real-world system, insofar as it is known, guides the setting up the flow paths, cell effective volumes, and the arrangement of the cells in the network.

The computer print-out consists of the succession of states or concentrations of each of the cells as well as the total amount of material entering the cell, the total amount leaving each cell, and the BDC of each cell. The program can also be instructed to output VOL, BRV, and BDV as functions of iteration number.

3.7 The FSM and Real Time

Until now, no attempt has been made to relate the FSM to real time. In and of itself, the FSM has no connection to real time. Naturally, if one intends to use a FSM

to model the evolution in time of a real-world hydrologic system, some length of time, which the author will call Δt, must be assigned as the amount of time required for the performance of one iteration. The choice of Δt is left up to the modeler and will depend upon the nature of the real-world hydrologic system, precision of the input data, and the purpose of the model. The following section will illustrate how one might determine Δt.

3.7.1 Choice of Δt

Suppose a hydrologist is using a FSM to model the movement of chloride in an aquifer. From data the hydrologist knows that 10^6 cubic meters of water is recharged to the aquifer each year and that the chloride concentration of this water is 10^4 parts per million (ppm). The chloride-laden recharge water is injected into the aquifer at a single location. Since the modeler's data are on an annual basis, an appropriate choice for Δt might be one year. Furthermore, if the modeler chose a URV = 10^6 cubic meters, the model would be programmed to receive a single SBRV = 1.0 with a SBRC = 10^4 at the beginning of each iteration. This would correspond to the real-world annual recharge of 10^6 cubic meters with a chloride concentration of 10^4 ppm. The SBRC is injected into the FSM as a dimensionless number; it is up to the modeler to assign appropriate units to the SBRC

and to keep these units in mind when examining the model output.

Some knowledge of the hydrology of a system is also important when choosing Δt. Since the FSM assumes that the contents of a cell are completely mixed with the incoming material at each iteration, it is also imperative to assign reasonable values to Δt in light of the system being simulated. Supposed that a hydrologist is modeling an aquifer in which the ground-water velocities are very low, and that he chooses his cells to be very large, on the order of one cubic kilometer or so. If the hydrologist then chooses Δt = one day, he would be assuming that every day, the contents of each of the cells mixes completely with any incoming material. In physical terms, such an assumption is a poor one and the modeler should choose another Δt, perhaps one month or one year. If the hydrologist were modeling a surface water body in which the flow velocities were fast, a Δt of one day might be acceptable.

3.7.2 The Discrete Nature of the FSM

It should be evident by now that the FSM operates in the realm of discrete time. Both the input and output variables are discrete functions of time, whereas in a real-world hydrologic system these variables may be either discrete or continuous functions of time. The discrete-time

nature of the FSM may be a factor in the choice of Δt, as will be illustrated in the following discussion

Recall the aquifer example given in 3.7.1. Suppose the hydrologist had monthly recharge data available in addition to the average annual recharge information. In addition to this, the hydrologist had a record of the observed concentrations in each of the cells on a monthly basis. This latter information would be very useful in calibrating the FSM. Instead of choosing Δt = 1 year, the modeler might do better to choose Δt = 1 month. This latter choice might insure that the FSM will be a better approximation of the real-world system. But if the modeler had yearly recharge data and monthly concentration data, no advantage might be gained by choosing Δt = 1 month, in which case the annual recharge data would be divided into 12 equal amounts for a given year and injected into the FSM. The division of the annual recharge data into 12 equal portions would approximate the real-world system only if the recharge in the real-world were distributed uniformly throughout the year. If the recharge were not uniformly distributed in any given year, using the Δt of one month might yield worse results than if the modeler chose Δt = 1 year.

Another point that bears mentioning is the fact that although the real-world hydrologic system evolves in continuous time, it is usually sampled on a discrete time basis. So it can be stated that despite the fact that the

FSM discretely models a real-world system that evolves continuously, the system is usually sampled in discrete time, and it is these discrete time samples that are used to calibrate and validate the FSM.

In conclusion, all the considerations discussed in this section and the preceding section should be taken into account before a modeler chooses a Δt for a FSM. It is probably best to choose the smallest possible realistic value of Δt unless of course the modeler is not interested in obtaining information on the system so often. In other words, the purpose to which the model is put may be the ultimate arbiter of the size of Δt.

3.8 Radioactive Decay and First-Order Reactions

The movement of radioactive tracers through hydrologic systems is modeled in Chapters 7 and 8; therefore, a brief presentation on how the FSM can account for radioactive decay follows. Since the process of radioactive decay is a first-order reaction the manner in which the FSM accounts for radioactive decay can be extended to the general case of any first-order reaction.

3.8.1 The Radioactive Decay Equation

The equation governing the decay of a radioactive substance is

$$\frac{dn}{dt} = - \lambda n \qquad (9)$$

The solution of Equation (9) is (Garland, 1971, p. 308):

$$n = n_o \exp(-\lambda t) \tag{10}$$

where

t = time,

n = amount of substance remaining at time t,

n_o = amount of substance present at $t = 0$, and

λ = decay constant.

Another quantity often given in discussions of radioactive decay is the half-life, or the time required for one-half of the amount present at $t = 0$ to disintegrate. The half-life $t_{1/2}$ is related to the decay constant by

$$t_{1/2} = \frac{\ln 2}{\lambda} \tag{11}$$

3.8.2 Radioactive Decay and the FSM

For a given cell of a FSM containing a radioactive substance, Equation (10) can be rewritten as

$$\frac{S(N)}{S(0)} = \exp(-\lambda N \Delta t) \tag{12}$$

where

$S(N)$ = state of the cell at iteration N and

$S(0)$ = initial state of the cell.

Equation (12) assumes that the cell loses material by radioactive decay alone; i.e., no material is flowing into or out of the cell.

Knowing the time interval represented by Δt, one can calculate the amount of material lost by radioactive decay in each cell after each iteration by using the equation

$$RD = \exp(-\lambda \Delta t) \tag{13}$$

where

RD = radioactive decay correction factor.

This factor is used in the following manner: Equation (4) is used to calculate the change in cell state resulting from flow alone. The sink term R(N+1) is temporarily neglected. Once this change has been calculated, the new state of the cell S(N+1) is then adjusted to account for radioactive decay occurring during the interval Δt. This is done as follows:

$$S'(N+1) = S(N+1)*RD \tag{14}$$

where

S'(N+1) = state of the cell at iteration N+1 after flow and radioactive decay changes;

S(N+1) = state of the cell at iteration N+1 after flow changes only.

In terms of the sink term R(N+1) in Equation (4), the actual amount of mass lost by radioactive decay is

$$R(N+1) = S(N+1) - S(N+1)*RD = S(N+1)*(1-RD) \tag{15}$$

In the FSM computer model, Equation (14) is used, not Equation (15). When the radioactive decay subroutine of the model is used, Δt must remain constant throughout the

operation of the FSM. In accounting for changes caused by radioactive decay, all changes in state due to flow alone are calculated for each cell in the FSM. Then, at the end of iteration N+1, all cell states are adjusted using Equation (14). RD is calculated by

$$RD = \exp(-(\Delta t * \ln 2)/t_{1/2}) \qquad (16)$$

Equation (16) is obtained by substituting Equation (11) into Equation (13). Equation (16) is used instead of Equation (13) because radioactive substances are usually reported in terms of their half-lives, not their decay constants.

When compared to radioactive decay in a real-world system, the FSM tends to overcompensate for radioactive decay. When the FSM accounts for radioactive decay, it assumes that all the radioactive material in the system has been present for the entire iteration. As far as the FSM is concerned, this is true, since all inputs to the FSM are injected into it at the start of the iteration. This may not be true in the real-world system being modeled by the FSM. Quantities of radioactive material may be coming into the system at various times during the iteration interval (Δt), so at the end of a given Δt, not all the material in the real-world system may have undergone the amount of decay as expressed by Equation (16). In light of this fact, and based upon simulation experiments with a single-cell FSM, Simpson and Duckstein (1975) proposed the following rule of

thumb for choosing Δt when dealing with a radioactive tracer:

$$\frac{\Delta t}{t_{1/2}} < \frac{1}{100} \tag{17}$$

3.8.3 The General First-Order Reaction

Consider the chemical reaction

$$A \rightarrow B$$

This reaction can be termed a first-order reaction if (Moore, 1972, p. 334):

$$\tau_{1/2} = \frac{\ln 2}{k_1} \tag{18}$$

where

$\tau_{1/2}$ = the reaction half-life, the amount of time required to reduce A to half its initial amount;

k_1 = the first-order reaction rate constant.

Equation (18) is analogous to Equation (11), except that the radioactive substance's half-life is now the half-life of the reaction and λ, the decay constant, has been generalized to k_1. In other words, Equation (11) is just a specific case of Equation (18). The process of radioactive decay is therefore a first-order reaction. This fact enables one to apply the same principles developed in section 3.8.2 to model radioactive decay to account for gains or losses of material resulting from first-order chemical reactions. A general form of Equation (16) could

be written as

$$FOR = \exp(-(\Delta t * \ln 2)/k_1) \qquad (19)$$

where

FOR = the first-order reaction correction factor.

The quantity (FOR*S(N)) would then be added to S(N) or subtracted from it, depending upon whether the reaction was a source or sink for the material in question. The correction would be made after calculating changes in state due to flow alone.

Since Equation (19) has not been applied to the modeling of real-world systems, it is probable that a constraint on Δt, as in the case of radioactive decay, may be necessary. This constraint may introduce great difficulty in the case of non-radioactive decay first-order reactions, since reaction half-lives may be extremely short, perhaps much shorter than the half-lives of the radioactive substances commonly of interest in hydrology.

3.9 Comparison Between FSM and Analytical Solutions

In this section, comparisons between FSM and analytical solutions will be presented for two simple cases.

3.9.1 Case I

A steady flow, steady volume FSM consisting of three simple mixing cells in series (Figure 1[b] with j = 3) was constructed. Each cell had an effective volume of 2.00 and

an initial state of zero. A SBRC = 10,000 was injected into the first cell at the first iteration and zeroed thereafter. A SBRV = 0.01 was injected into this same cell at each iteration.

The analytical solution describing the concentration of material within and out of cell 3 is given by Equation (3) with j = 3. Time t in this equation was made equivalent to N, the iteration number of the FSM. Only integer values of t were used.

Table 1 shows the concentration of material in cell 3 as a function of N as calculated by the two different methods, and the excellent agreement between them.

3.9.2 Case II

Another type of simulation experiment illustrating the agreement between FSM and analytical solutions is a steady flow, steady volume FSM consisting of a single SMC with an effective volume = 1000 and an initial state of zero. A choice of Δt = 1 year was made, and at the beginning of each iteration a SBRV = 0.1 and a SBRC = 1.00 was injected into the cell. The FSM was operated for 50,000 iterations (years), by which time the cell had attained steady state.

With this basic FSM, three separate simulations were conducted: one with a stable tracer (no radioactive decay), one with a tracer of $t_{1/2}$ = 5000 years, and the third with a tracer of $t_{1/2}$ = 100 years. Each of these results was

Table 1. Comparison between FSM and analytical solutions for a three cell model.

	Concentration in cell 3	
Iteration	FSM solution	Analytical solution
100	3.80	3.79
200	9.17	9.20
300	12.52	12.55
400	13.50	13.53
500	12.80	12.83
600	11.19	11.20
700	9.25	9.25
800	7.34	7.33
900	5.64	5.62
1000	4.23	4.21
1500	.79	.78
2000	.12	.11
3000	.00	.00
5000	.00	.00

compared to the equilibrium (steady state) concentration calculated at infinite time using the equation

$$C_{\infty} = \frac{1}{1 + (\lambda V/Q)} \qquad (20$$

where

C_{∞} = equilibrium or steady state tracer concentration at infinite time;

V = total volume of the system = 1000;

λ = decay constant; and

Q = volumetric flow rate = 0.1/year.

Table 2 summarizes the results of the simulations and the excellent agreement between the FSM and analytical solutions.

Table 2. Equilibrium concentrations of tracers in a single mixing cell.

	Equilibrium concentration	
Type of tracer	FSM solution	Analytical solution
stable	1.00000	1.00000
$t_{1/2}$ = 100 years	.01417	.01422
$t_{1/2}$ = 5000 years	.41904	.41906

3.10 Concluding Remarks

This chapter started by presenting the basic concept behind finite-state models and presented the basic equation of FSMs. The author pointed out the recursive structure of the basic FSM algorithm, which, to his knowledge, is unique to the FSM among other mixing cell models and a property which facilitates construction of a digital computer program for a FSM. FSMs avoid the use of differential equations and are able to model a system composed of an arbitrary number of cells arranged in any type of network. Some of the basic tenets of FSM theory were promulgated, along with a brief presentation on how FSMs could account for material sinks resulting from radioactive decay and sources or sinks caused by first-order chemical reactions. The chapter concluded with two simple simulations illustrating the excellent agreement between FSM and existing analytical solutions. Throughout the chapter, mass transport was emphasized and this emphasis on mass transport, particularly in aquifer systems, will continue throughout the rest of this dissertation. Energy transport will not be totally neglected however, since in a later chapter the author will describe how FSMs can model the transport of energy in a variety of hydrologic systems.

In later chapters the author will consider some aspects of FSM theory that make finite-state models particularly attractive in the analysis of hydrologic systems.

Some idealized FSM simulations will be performed to illustrate these aspects. FSM theory will then be used to model two real-world hydrologic systems: the distribution of carbon-14 ages in a portion of the Tucson Basin Aquifer and the transport of tritium (tritiated water or HTO) in the Edwards Limestone Aquifer system of south-central Texas. The former is a steady flow, steady volume three-dimensional (cell network) FSM; whereas the latter is a steady volume, non-steady flow two-dimensional FSM. After the chapter on energy transport in hydrologic systems, the dissertation will conclude with a chapter summarizing the applications of FSM theory to the modeling of hydrologic systems and suggesting avenues of future research.

CHAPTER 4

DISTRIBUTION FUNCTIONS OF FINITE-STATE MODELS

4.1 Theory of FSM Distribution Functions

Based on the concepts of fluid elements and modifying the development given in Himmelblau and Bischoff (1968, Chapter 4), two FSM distribution functions may be defined: a normalized transit number distribution T(N) and a normalized age number distribution A(N). These two distributions and the concepts embodied in them can be clarified somewhat by assuming that as each fluid element enters the FSM it automatically displays a positive integer, starting with the number one. This integer increases by one at each iteration and continues to do so as long as the fluid element remains in the FSM. This integer shall be called the age number of the fluid element. The maximum age number of a given fluid element is that which it has at the iteration of its discharge from the FSM or some sub-region of the FSM. This maximum age number is called the transit number of the fluid element. In other words, each fluid element receives a number, called its age number, which increases by one unit for each iteration of the FSM, to a maximum value called the transit number, which is the number that coincides with the iteration at which the fluid element is discharged from the

FSM or some sub-region. Thus, A(N) describes the distribution of iteration numbers among all fluid elements within a cell or cells at a given iteration, and T(N) describes the distribution of iteration numbers among all fluid elements discharged from the FSM or some sub-region (cell or cells). Both distributions are functions of the iteration number, N.

Conceptually, T(N) could be determined by collecting the water discharged from the FSM or sub-region at any iteration after operating the FSM for a sufficient number of iterations, grouping the fluid elements according to their transit numbers, and then dividing the number of fluid elements in each group by the total number collected. For each group, one would then have the fraction of fluid elements within that group, and T(N) could then be obtained by plotting the fraction in each group against the group number, and

$$\sum_{i=1}^{N_m} T(N)_i = 1 \qquad (21)$$

where

$T(N)_i$ = fraction of fluid elements in transit group number i, and

N_m = maximum transit number in the entire population.

In a similar fashion, at any iteration after the sufficient number, all the fluid elements in the FSM or any of its cells could be collected and A(N) calculated, and

$$\sum_{i=1}^{N_m} A(N)_i = 1 \tag{22}$$

In Equation (22), N_m is interpreted as the maximum age number in the entire population.

The average or mean transit number and age number can be obtained by taking the first moments of their respective distributions:

$$\bar{T} = \sum_{i=1}^{N_m} iT(N)_i \tag{23}$$

$$\bar{A} = \sum_{i=1}^{N_m} iA(N)_i \tag{24}$$

where

$\bar{T}$ = average or mean transit number, and

$\bar{A}$ = average or mean age number.

In his experience with FSMs, the author has found that $\bar{A}$ and $\bar{T}$ are more useful than their respective distributions, and in fact, he has rarely calculated A(N) and T(N). The next section will show how $\bar{A}$ and $\bar{T}$ can be calculated by the impulse-response method,although it will also be shown how in certain cases A(N) and T(N) can be obtained using the same method.

4.2 Determination of A(N), T(N), $\bar{A}$ and $\bar{T}$ by the Impulse-Response Method

While the preceding section dealt with the theory of FSM distribution functions, the equations presented are of little use in determining the functions or their means. These quantities can be obtained using the impulse-response method. In this and future sections, the group number i will be identical to the iteration number N, and in most cases i will be used to designate both the group number and the iteration number.

4.2.1 Determination of A(N) and $\bar{A}$

Recall the FSM described in 3.9.1. The model was a steady flow, steady volume FSM composed of three simple mixing cells in series, each with VOL = 2.00 and an initial state of zero. A constant SBRV = 0.01 was injected into the first cell at each iteration. At N = 1, a SBRC = 10,000 was also injected into the first cell and zeroed for all following iterations. This SBRC is the impulse to the system. Therefore, at N = 1, 100 units of tracer (SBRC*SBRV = 10,000*.01 = 100) entered the FSM. If this amount of tracer is divided by VOL, then the concentration of tracer units entering the first cell at N = 1 equals 50. After inflow, mixing, and outflow, the concentration of tracer in cell 1 at the end of the first iteration is 49.75 (see Table 3). It is evident that .005 (SBRV/VOL = .005) part of the effective volume of cell 1 is tagged by the entering tracer.

Table 3. Cell concentrations and mean age numbers for a FSM composed of three simple mixing cells.

Iteration number	Cell concentration		
	Cell 1	Cell 2	Cell 3
1	49.75	.25	.00
100	30.36	15.11	3.80
200	18.44	18.35	9.17
300	11.20	16.71	12.52
400	6.80	13.53	13.50
500	4.13	10.27	12.80
600	2.51	7.49	11.19
700	1.52	5.30	9.25
800	.93	3.68	7.34
900	.56	2.52	5.64
1000	.34	1.70	4.23
1500	.03	.21	.79
2000	.00	.02	.11
3000	.00	.00	.00
5000	.00	.00	.00
$\bar{A}$	201.00	401.00	601.00

After the first iteration, 49.75/50.00 fractional part of the entering tagged amount remains. Thus, in cell 1 the fraction of fluid elements of age number 1 is $49.75*10^{-4}$. For all N > 1, SBRC = 0 and no more tagged fluid elements enter the system. At any iteration N, the concentration of tracer remaining in any cell is a measure of the fractional amount of fluid elements of age number N in that cell. That is, for any cell (Simpson and Duckstein, 1975)

$$A(N)_i = \frac{C(N)_i}{C'} * \frac{SBRV'}{VOL'} \qquad (25)$$

where

$C(N)_i$ = concentration of tracer in a given cell as a function of iteration number at iteration i;

VOL' = sum of the effective volumes of all boundary cells discharging directly or indirectly to the cell in question;

SBRV' = sum of the system boundary recharge volumes to the boundary cells whose effective volumes comprise VOL'; and

C' = mass of tracer introduced into the particular boundary cells divided by VOL'.

If the cell under consideration is itself a boundary cell, it must be included when calculating VOL', SBRV', and C'.

Equation (25) can be simplified by noting that

$$C' = \frac{SBRC*SBRV'}{VOL'} \qquad (26)$$

If Equation (26) is substituted into Equation (25), one obtains

$$A(N)_i = \frac{C(N)_i * VOL' * SBRV'}{SBRC * SBRV' * VOL'} \tag{27}$$

which simplifies to

$$A(N)_i = \frac{C(N)_i}{SBRC} \tag{28}$$

A particularly good choice of the system boundary recharge concentration is SBRC = 1.00, since in this case

$$A(N)_i = \text{(numerically) } C(N)_i \tag{29}$$

Equations (25) through (28) are valid for any steady flow, steady volume FSM subjected to a tracer impulse at the first iteration only and whose cells have zero initial states. The FSM is permitted to have multiple inputs from outside its boundaries, although the SBRCs must be non-zero and equal to each other. In the case of unit SBRCs, Equation (29) is valid.

In the impulse-response experiment previously described, $C(N)_i$ and $A(N)_i$ (see Figure 3) will attain values of zero to the number of significant figures desired after a sufficient number of iterations. In effect, each cell in the FSM becomes flushed of tracer for all practical purposes (see Table 3), although in theory an infinite number of iterations will be required for this. $C(N)_i$ will assume an operational value of zero in each cell regardless of the value chosen for the SBRC, just so long as the SBRC is zeroed for N > 1.

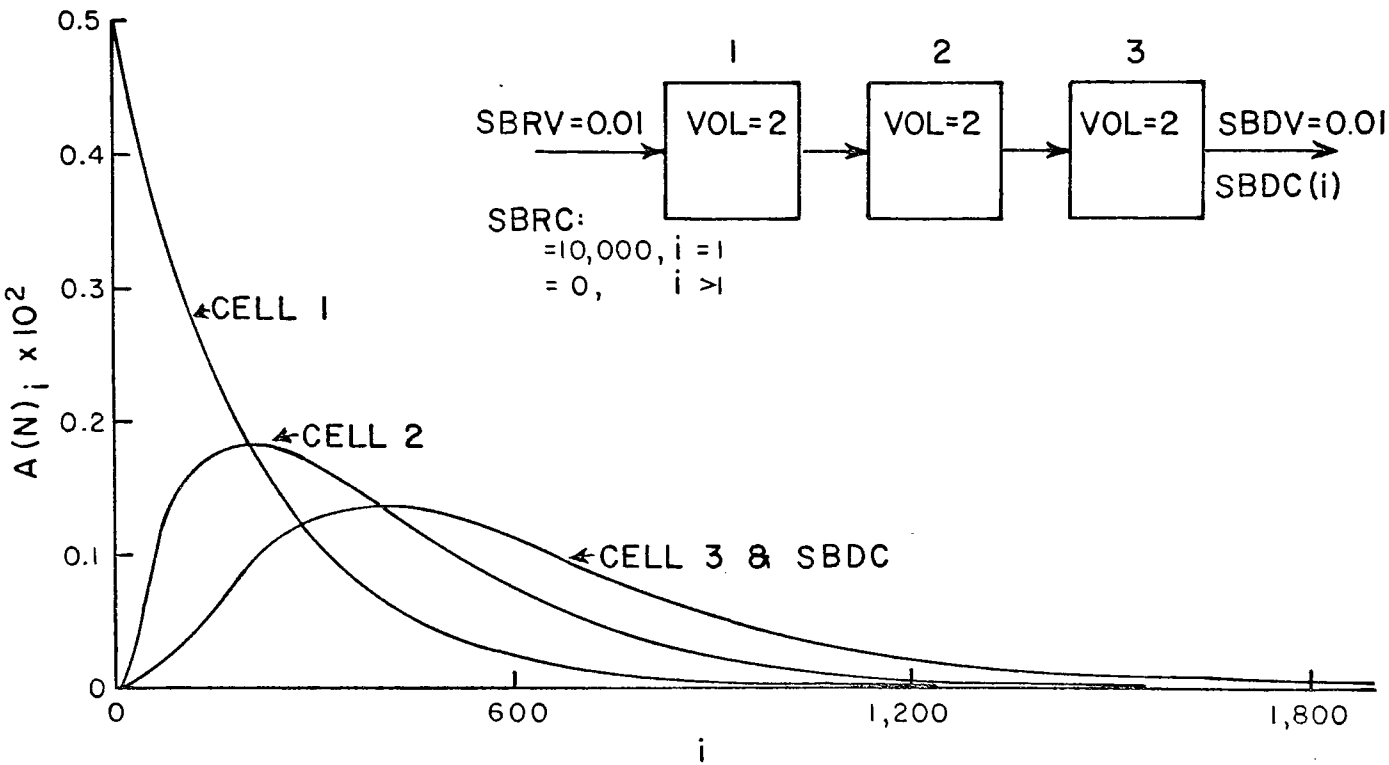

Figure 3. $A(N)_i$ versus i for a FSM composed of three cells in series.

In light of this fact and recalling that $\bar{A}$ is the first moment of A(N), one has (modified from Levenspiel, 1972, p. 261):

$$\bar{A} = \sum_{i=1}^{N'} i \frac{C(N)_i}{SBRC} \tag{30}$$

Since SBRC is constant, Equation (30) can be rewritten as

$$\bar{A} = \frac{\sum_{i=1}^{N'} i\, C(N)_i}{SBRC} \tag{31}$$

Noting that for any cell

$$SBRC = \sum_{i=1}^{N'} C(N)_i \tag{32}$$

one obtains the result

$$\bar{A} = \frac{\sum_{i=1}^{N'} i\, C(N)_i}{\sum_{i=1}^{N'} C(N)_i} \tag{33}$$

$\bar{A}$ can be converted to real-time units as follows:

$$\bar{A} = \frac{\Delta t \sum_{i=1}^{N'} i\, C(N)_i}{\sum_{i=1}^{N'} C(N)_i} \tag{34}$$

where

N' = number of iterations required to remove all tracer from the cell (to the number of significant figures desired);

Δt = real time between iterations, a constant.

The variance of the $C(N)_i$ versus i curve is given by:

$$VAR = \frac{\sum_{i=1}^{N'} (i)^2 C(N)_i}{\sum_{i=1}^{N'} C(N)_i} - (\bar{N})^2 \qquad (35)$$

where

VAR = variance of the $C(N)_i$ versus i (iteration number) curve;

$\bar{N}$ = mean value of the $C(N)_i$ versus i curve.

$\bar{A}$ and the variance of A(N) are equal to $\bar{N}$ and VAR of the $C(N)_i$ versus i curve, but these equalities are valid only for a steady flow, steady volume FSM subjected to an impulse at the first iteration only. If $\bar{N}$ is used in place of $\bar{A}$ in Equation (33), then Equations (33) and (35) can be used to calculate the mean value and variance of the $C(N)_i$ versus iteration number curve for each cell in any FSM. When it is used to calculate the variance VAR' of A(N), Equation (35) can be rewritten as:

$$VAR' = \frac{\sum_{i=1}^{N'} (i)^2 C(N)_i}{\sum_{i=1}^{N'} C(N)_i} - (\bar{A})^2 \qquad (36)$$

To convert VAR' to real-time units, the result of Equation (36) (or Equation [35]) should be multiplied by $(\Delta t)^2$.

Therefore, to obtain $\bar{A}$ and, if desired, VAR', for each cell in a given steady flow, steady volume FSM, one must inject an arbitrary non-zero SBRC into the FSM at the first iteration and a SBRC = 0 for all iterations greater than one. If the FSM has more than one input from outside the system, the same value of SBRC must be used at each of these locations, although this restriction does not apply to SBRVs. After N' iterations, $\bar{A}$ and VAR' will then be calculated for each cell using the proper equations. The specific value used for SBRC does not matter.

4.2.2 Determination of T(N) and $\bar{T}$

T(N) can be determined in a fashion similar to that used to calculate A(N) in section 4.2.1, except that T(N) is computed with respect to the concentration of tracer in the discharging fluid. For a SMC, BDC at any iteration is identical to the cell concentration at that iteration. Consequently, T(N) is identical to A(N) and $\bar{A} = \bar{T}$. In the special case where Equation (29) is valid, one has

$$A(N)_i = C(N)_i = T(N)_i \text{ (numerically)} \tag{37}$$

For a MMC, BDC at any iteration is equal to the concentration in the cell at the previous iteration. Equation (28) thus becomes

$$T(N)_i = \frac{C(N)_{i-1}}{SBRC} \tag{38}$$

where

$C(N)_{i-1}$ = concentration of tracer in the cell at iteration i-1.

From Equation (38), it follows that for a MMC,

$$A(N)_i = T(N)_{i+1} \tag{39}$$

Recall that in the case of a MMC that as BRV becomes small relative to VOL, the MMC approaches the perfect mixing of the SMC. Under these conditions, $\bar{A}$ is a good estimate of $\bar{T}$. One can state that $\bar{A} = \hat{T}$, where $\hat{T}$ is an estimate of $\bar{T}$. In a similar manner A(N) will be a good approximation to T(N).

T(N) and $\bar{T}$ are usually calculated only for those cells discharging some or all of their contents outside the FSM, that is, those cells having SBDCs and SBDVs. By doing this, the transit number distributions and mean transit numbers for the FSM are obtained.

4.2.3 Relationships Among FSM Volumetric Quantities, $\bar{A}$ and $\bar{T}$

Under certain conditions simple relationships exist among the volumetric parameters of the FSM, $\bar{A}$ and $\bar{T}$.

For a steady flow, steady volume FSM with no dead cells (defined in Chapter 5) and with a single SBRV that is distributed throughout all the cells and is discharged as a single SBDV, the following holds for both the SMC and MMC algorithms:

$$\frac{\Sigma VOL + SBDV}{SBDV} = \frac{\Sigma VOL + SBRV}{SBRV} = \bar{T} \tag{40}$$

where

ΣVOL = sum of the effective volumes of all the cells in the FSM, the effective volume of the entire FSM.

Equation (40) may be valid for other types of FSMs, although it has been verified only for the FSMs indicated.

For a steady volume, steady flow FSM consisting of a single SMC, the following is true:

$$\frac{VOL + SBDV}{SBDV} = \frac{VOL + SBRV}{SBRV} = \bar{T} = \bar{A} \tag{41}$$

If the SBRV and SBDV are small compared to VOL, then Equation (41) can be rewritten as:

$$\frac{VOL}{SBDV} = \frac{VOL}{SBRV} \approx \bar{T} \approx \bar{A} \tag{42}$$

For a steady flow, steady volume FSM consisting of a single MMC, the following are true:

$$\frac{VOL}{SBDV} = \frac{VOL}{SBRV} = \bar{A} \tag{43}$$

and

$$\frac{VOL + SBDV}{SBDV} = \frac{VOL + SBRV}{SBRV} = \bar{T} = \bar{A}+1 \tag{44}$$

When the SBRV and SBDV are small compared to VOL, then Equation (43) is a good approximation to $\bar{T}$.

Equations (41) and (43), when multiplied by Δt, are definitions of the average residence times for a SMC and MMC, respectively. The average residence time can be

interpreted as the average amount of time a volumetric input resides in a cell. For cells which are not boundary cells, one must replace SBDV with BDV and SBRV with BRV in Equations (41) and (43) to obtain general expressions for the average residence times of a SMC and MMC, regardless of their locations in a FSM.

4.3 Determination of $\bar{A}$ and $\bar{T}$ from Volumetric Parameters

Based on the materials presented in 4.2.3, it is possible to obtain $\bar{A}$, and thus $\bar{T}$ or $\hat{T}$, but not A(N) and T(N) from the volumetric parameters of the FSM without resorting to the impulse-response method previously discussed. For certain FSMs, this method can be expensive to use, since some or all of the cells may require a large number of iterations (on the order of 10^5 and more) for $C(N)_i$ to reach a steady state value of zero to the number of significant figures used. It was this expense that motivated the author to devise a relatively simple technique to calculate the mean age numbers, based upon the fact that these parameters are dependent only upon the volumetric parameters of the FSM.

For a FSM cell receiving its entire input from outside the system, that is, its BRV is a SBRV, the mean age number of the cell is simply its average residence time, since the SBRV is of age zero until it enters the cell. Thus, for a SMC,

$$\bar{A} = \frac{VOL + SBRV}{SBRV} \tag{45}$$

It is necessary to add the SBRV to the numerator because of the expansion experienced by the SMC.

For a MMC, one has

$$\bar{A} = \frac{VOL}{SBRV} \tag{46}$$

For a cell whose BRV is composed partly of a SBRV and partly of BRVs from other cells, one must consider the fact that inputs from other cells already have ages associated with them, unlike the SBRV. So, in addition to the average residence time of the cell in question, one must add to that the volumetrically-weighted age numbers of the waters from the other cells in order to obtain the mean age number of the cell. Therefore, in the case of a SMC

$$\bar{A} = \frac{VOL + SBRV + \sum_{j=1}^{n} BDV_j * \bar{A}_j}{\Sigma BRV} \tag{47}$$

For a MMC, the following holds:

$$\bar{A} = \frac{VOL + \sum_{j=1}^{n} BDV_j * \bar{A}_j}{\Sigma BRV} \tag{48}$$

In the case of a cell receiving all its inputs from other cells, the mean age number of that cell is simply the average residence time plus the volumetrically-weighted mean age numbers of the cells contributing volumetric inputs to the cell in question:

$$\bar{A} = \frac{VOL + \sum_{j=1}^{n} BDV_j * \bar{A}_j}{\Sigma BRV} \tag{49}$$

where

j = subscript denoting a cell contributing a volumetric input to the cell in question;

n = total number of cells contributing volumetric inputs to the cell in question;

$\bar{A}_j$ = mean age number of a cell contributing a volumetric input to the cell in question;

BDV_j = boundary discharge volume flowing from cell j to the cell in question

ΣBRV = total of all volumetric inputs to the cell in question at a given iteration.

Equation (49) is identical to Equation (48) and is valid for both the SMC and MMC algorithms. It is unnecessary to account for the expansion of the SMC in Equation (49) since the expansion has already been accounted for in the calculations of the mean age numbers of the cells flowing to the cell under consideration.

The SMC mean age of a cell will be exactly one greater than the MMC mean age. This can be seen by writing the equation for the dimensionless residence time $\bar{t}'$ of a SMC:

$$\bar{t}' = \frac{VOL + BRV}{BRV} = \frac{VOL}{BRV} + \frac{BRV}{BRV} \tag{50}$$

or

$$\bar{t}' = \frac{VOL}{BRV} + 1 \qquad (51)$$

Equation (51) is simply the residence time for a MMC plus one, and this factor of one is carried throughout the calculations for the SMC mean age number of a cell.

Once the mean age numbers have been obtained, then for certain FSMs, they can be related to the mean transit numbers using the relationships in 4.2.3. Mean age and transit numbers can be converted to real-time quantities by multiplying them by Δt.

A subroutine incorporating the methods of this section was written for the author's computer model. It is necessary to calculate the mean age numbers sequentially, starting first with boundary cells receiving nothing but SBRVs and proceeding to other cells receiving inputs from these boundary cells until eventually, all cells in the FSM are accounted for. The subroutine will calculate the mean age numbers for any steady flow, steady volume FSM as long as there are no exchanges between cells (see Chapter 5). As was the case with the impulse-response method, Δt must remain constant. The subroutine incorporating the methods of this section need be called but once, unlike the subroutine utilizing the impulse-response method, which must be called at the end of each iteration. Furthermore, the subroutine using the methods of this section does not require a separate computer run as will the impulse-response

subroutine if the FSM is being used to simulate the transport of some real-world quantity in a hydrologic system.

By using the volumetric relationships to calculate mean age numbers, one could calculate these parameters for any FSM, regardless of its regime, simply by calling the subroutine to calculate new mean age numbers whenever the volumetric parameters of at least one cell change. However, at present, A(N), T(N), $\bar{A}$, and $\bar{T}$ are defined only for steady flow, steady volume FSMs. The mean age numbers of the cells in a FSM in a regime other than a steady flow, steady volume regime would probably be the mean age numbers of the cells of a steady volume, steady flow FSM possessing those volumetric parameters present at the iteration at which the mean age numbers were calculated. In other words, with the methods given in this section, it is possible to calculate mean age numbers as a function of iteration number.

The volumetric method to calculate the mean age numbers has been verified for a wide variety of FSMs. When checked against the results of the impulse-response method, the results were identical to the third place to the right of the decimal point, which is the maximum amount of decimal places the author has ever used in calculating mean age numbers.

4.4 Distribution Functions and FSM Regimes

As derived in this chapter, the relationships among $A(N)_i$, $T(N)_i$, and $C(N)_i$ were based upon the assumption of a steady flow, steady volume FSM. This restriction to such a regime follows from consideration of Equation (25) and its simplified special-case form, Equation (29), both of which assume that such a regime is in effect. For other regimes, the calculations of $A(N)_i$, $T(N)_i$, $A(N)$, and $T(N)$, as given here, are not readily applicable. This restriction on the regime of the system is borne out in the field of chemical engineering as well. Two well-known distribution functions in this field are the internal age distribution $I(t)$ of a fluid in a closed vessel and the exit age distribution $E(t)$ of the stream leaving a closed vessel (Himmelblau and Bischoff, 1968, Chapter 4). These distributions may be viewed as the continuous-time analogs of the FSM discrete distributions $A(N)$ and $T(N)$, respectively. In their derivations of $I(t)$ and $E(t)$, Himmelblau and Bischoff (1968, p. 61) assumed that the volume of the system was constant as was the volumetric flow rate through the system. This assumption corresponds to that of a steady flow, steady volume FSM. The aforementioned authors do, however, develop theory which can account for processes that vary in space and time (Himmelblau and Bischoff, 1968, pp. 66-68). Based upon this work, it may be possible to extend the concepts of

A(N) and T(N) to finite-state models in regimes other than the steady flow, steady volume one.

4.5 Concluding Remarks

It should be apparent to the reader that the functions A(N) and T(N) are defined only in terms of a response to an instantaneous pulse of tracer. This is true for I(t) and E(t) as well. Other distribution functions can be defined as responses to other types of inputs, and the chemical engineering literature (Himmelblau and Bischoff, 1968, Chapter 4; Levenspiel, 1972, Chapter 9) goes into detail on the theory and use of these other functions. For example, the F-curve (Himmelblau and Bischoff, 1968, p. 63) has been defined as the dimensionless response to a step input of tracer. Another function, the intensity function $\Lambda(t)$ (Himmelblau and Bischoff, 1968, p. 61) can be related to I(t) and E(t). These distribution functions may have uses in FSM theory, and such potential uses merit investigation. In addition, under certain conditions, there are various relationships existing among all the aforementioned continuous-time distribution functions. Most of these relationships involve derivatives and so they are not directly applicable to the discrete-time realm of finite-state models. Himmelblau and Bischoff (1968, p. 64) summarize the various relationships among these distribution functions.

The author has found the means of A(N) and T(N), $\bar{A}$ and $\bar{T}$, to be more useful than the distributions themselves. $\bar{A}$ is helpful in determining the average amount of time it takes water to move from the boundary of a finite-state hydrologic system to some point within the system. This knowledge will prove to be of great value in studying mass transport and perhaps even energy transport in hydrologic systems.

CHAPTER 5

NON-STEADY REGIMES AND DEAD CELLS

5.1 Introduction

This chapter deals with non-steady flow and/or non-steady volume regimes and the concepts of active and dead cells, and how they might be utilized to model real-world hydrologic systems. Some simple simulation experiments will be performed on hypothetical FSMs to illustrate the applications of the aspects covered. The simulations were performed by the author using his digital computer model.

5.2 Non-Steady Volume, Non-Steady Flow Regimes

Very little has been mentioned regarding non-steady volume, non-steady flow regimes except to say that they do exist. It has been heretofore assumed that the effective volume of each cell was constant (steady volume) and that the BRVs and BDVs of a given cell were also constant with BRV = BDV (steady flow regime). The author will now introduce systems where these constraints are eliminated. It will also be shown that whereas a non-steady volume regime implies non-steady flow, the converse is not necessarily true.

5.2.1 Non-Steady Volume Regime

The effective volume of a cell in a FSM can be changed from one iteration to the next by developing an alogrithm to accomplish this. This algorithm is:

$$VOL(N+1) = VOL(N) + BRV(N+1) - BDV(N+1) \quad (52)$$

where

VOL(N+1) = effective volume of the cell at iteration N+1;

VOL(N) = effective volume of the cell at iteration N;

BRV(N+1) = boundary recharge volume entering the cell during iteration N+1;

BDV(N+1) = boundary discharge volume leaving the cell during iteration N+1.

Equation (52) is entirely analogous to the basic FSM Equation (4), which described the change in the state of the cell. Equation (52) is likewise a recursive equation, although it deals with volumetric quantities, and just as Equation (4) was a discrete form of the continuity equation, Equation (52) is a discrete form of the storage equation which states that the volume in minus the volume out equals the change in volumetric storage. If VOL(N) is subtracted from both sides of Equation (52), the precise form of the storage equation results. Note that Equation (52) reduces to the steady volume case when BRV(N+1) = BDV(N+1).

In order to solve for VOL(N+1), BRV(N+1) and BDV(N+1) must be determined. Since the BRV to a given cell is predetermined as a SBRV and/or BDVs from other cells (though in Chapter 9 the author will present a situation in which the BRV is calculated), an algorithm must be developed for the BDV. Simpson (1974) suggested the following as a possible algorithm:

$$BDV(N+1) = VOL(N)*FAC \tag{53}$$

where

FAC = a constant or function of some quantity such as N or VOL(N).

Since the BDV is now a function of VOL(N), so also will some of the BRVs be functions of VOL(N) and hence the non-steady volume regime implies a non-steady flow regime.

As defined here, the non-steady volume regime will be useful in modeling the transport of hydraulic head (energy) in hydrologic systems. Treatment of this topic will be delayed until Chapter 9, where the author will develop specific algorithms for the movement of hydraulic energy in several different hydrologic systems. For the present, the author will restrict himself to Equation (53), using only constant values of FAC for each cell.

A word of caution is necessary before using Equations (52) and (53) to model non-steady volume regimes. Since negative, and in certain cases, zero effective volumes

are meaningless, one must choose FAC accordingly. If Equation (53) is substituted into Equation (52), the result is:

$$VOL(N+1) = VOL(N) + BRV(N+1) - VOL(N)*FAC \tag{54}$$

By allowing the left-hand side of Equation (54) to vanish and solving for FAC, one obtains

$$FAC = \frac{VOL(N) + BRV(N+1)}{VOL(N)} \tag{55}$$

In order to insure cell effective volumes greater than or equal to zero, one should choose FAC such that the following relationship always holds:

$$FAC \leq \frac{VOL(N) + BRV(N+1)}{VOL(N)} \tag{56}$$

This relationship should be observed regardless of whether FAC is a constant or a function of some quantity.

Since FAC must be specified either as a constant or a function before simulation, it is impossible to know beforehand all values of VOL(N) and BRV(N+1) to be used in (56). However, if one notes that BRV(N+1) will always be equal to or greater than zero, then the following requirement for FAC is obtained:

$$FAC < 1 \tag{57}$$

The relationship expressed by (57), if observed when choosing FAC, will insure that VOL(N+1) will always be greater than zero.

In the case of a functional FAC, the modeler should ascertain that the range of the function should be everywhere less than 1 for all reasonable (in a hydrologic sense) values of the domain. In most real-world cases, FAC is on the order of a few tenths or so.

5.2.2 Non-Steady Flow Regime

In the preceding section it was shown that the non-steady volume implies one of non-steady flow also. But it is possible to have a non-steady flow regime without incorporating one of non-steady volume. By simply making the SBRVs a function of iteration number, a non-steady flow regime FSM will be effected without changing the effective volume of the cells. The model the author developed to model tritium transport in the Edwards Limestone (Chapter 8) is just such a FSM.

5.3 Active and Dead Cells

In the discussion thus far, all the cells of a particular FSM have been visualized as receiving inputs from outside the system and/or upstream cells, and then either before (MMC) or after (SMC) mixing, discharging their contents to downstream cells and/or the outside environment. These cells are "active" cells. In no instance has the author permitted a cell to receive a volumetric quantity from another cell and then discharge an equal volume back to that cell. Such a cell will now be introduced, and if

this cell does nothing but exchange equal volumes of water with another cell or other cells, it will be termed a "dead" cell.

Figure 4 shows a FSM composed of a top layer of three cells, each having an effective volume of 1, and a bottom layer with a single cell of effective volume 3. Cell 1 receives a single SBRV, and cell 3 is the only one discharging its contents outside the FSM. Cell 4 receives an input from each of the top cells and also discharges some of its contents to each of these top cells. There is an exchange of equal volumes between cell 4 and any given cell in the top layer, although the amounts of material in these equal volumes of water are not necessarily the same. In other words, there is no net volumetric flow, but there can be a net flow in terms of mass or energy. In the FSM shown in Figure 4, there are three active cells (1, 2, and 3) and one dead cell, cell 4. Cell 4 is also a dead cell participating in multiple (3) exchanges. It is a dead cell because it is removed from the active flow region of the FSM. A dead cell has the same number of inputs as outputs, and receives material only from active cells or other dead cells, though the latter must ultimately receive material from active cells. Furthermore, a dead cell cannot discharge material to the outside environment nor can it discharge (as opposed to exchange) material to another cell. Since the volume of water entering a dead cell is always equal to the

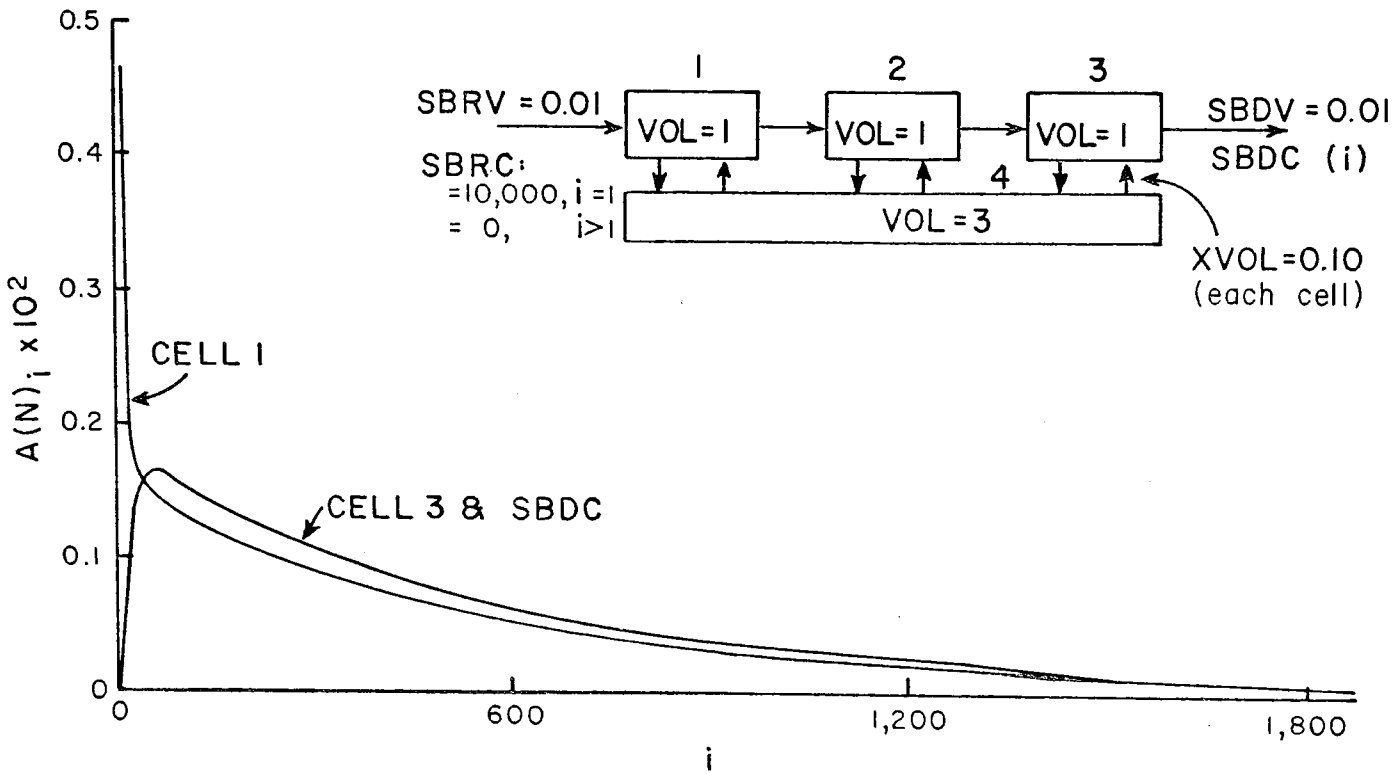

Figure 4. $A(N)_i$ versus i for cells 1 and 3 in a steady volume FSM composed of three active cells and one dead cell.

amount entering, then according to Equation (52), the effective volume of a dead cell remains constant even though the effective volumes of the active cells may change. Exchanges between active cells are permissible, although the writer's computer program requires that there be no net volumetric flow between any pair of exchanging cells. Certain hydrologic situations may be encountered in which this requirement must be relaxed or eliminated entirely.

The volume exchanged between two cells is given as a decimal fraction, termed XVOL, of the effective volume of one of the cells. In the case of an exchange between an active cell and a dead cell, the effective volume of the active cell is used. In other cases, XVOL is taken as the decimal fraction of the effective volume of the cell which the modeler designates as the one discharging its volume first. Thus,

$$EXVOL = XVOL*VOL" \tag{58}$$

where

EXVOL = volume of water exchanged between the two cells;

XVOL = decimal fraction of the effective volume of the cell designated as discharging its volume first;

VOL" = effective volume of the cell designated as discharging its volume first. In the case of exchange between an active cell and a dead cell, VOL" = effective volume of the active cell.

In addition, one must be careful to observe that

$$EXVOL \leq Min(VOL'', VOL''') \quad (59)$$

where

VOL''' = effective volume of the other cell participating in the exchange.

In addition, cells undergoing exchange can be specified as modified mixing cells or simple mixing cells, as long as all cells in the FSM use the same algorithm.

Dead cells and the exchange process might prove useful in modeling those portions of a hydrologic system that are effectively removed from the areas of active flow in the system. These "dead" portions might include the lower parts of aquifers or stagnant or near-stagnant areas of surface water bodies, such as the deep areas in a lake. The exchange process could be used to model the diffusion of mass or energy in a hydrologic system. The zone of diffusion between the salt water-fresh water interface in an aquifer might be modeled using exchange. The exchange of heat in a geothermal reservoir might also be approached using the exchange process described in this chapter.

5.4 FSM Simulation Experiments

5.4.1 Case I: Active and Dead Cells

Figure 4 showed the FSM used in this simulation. A constant SBRV = 0.01 is injected into cell 1 at each iteration, and a SBRC = 10,000 is injected into this cell at

N = 1 only. XVOL = 0.10 for each of the active cells. The FSM is in a steady flow, steady volume regime and all of its cells are simple mixing cells. Table 4 shows the concentration of tracer in each of the cells as a function of iteration number N as well as the mean age numbers of the cells as calculated by the impulse-response method. Figure 4 is a plot of $A(N)_i$ versus i(=N) for cells 1 and 3. Since cell 3 is the only cell in the FSM with a SBDV and a SBDC, its A(N) = T(N) and its mean age number is also the mean transit number of the FSM. Note that the mean transit number as calculated is not obtainable using Equation (40). This equation cannot be applied in this case because of the presence of a dead cell, which permits some fluid elements to circulate through the system twice or more before being discharged from the FSM.

5.4.2 Case II: Active Cells in a Non-Steady Flow, Non-Steady Volume Regime

In this experiment, the three-cell FSM of sections 3.9.1 and 4.2.1 will be used except that a non-steady flow, non-steady volume FSM will be effected, where FAC = 0.005 for each cell. In addition, SBRV = 0.02 for $1 \leq N \leq 500$ and SBRV = 0.01 for N > 500. A SBRC = 10,000 was injected into cell 1 at N = 1 only. Table 5 shows the changes in C(N), VOL(N), and BDV(N) for each cell as well as ΣVOL(N). Figure 5 is a plot of ΣVOL(N), and SBDV(N) and C(N) for cell 3.

Table 4. Cell concentrations and mean age numbers for a FSM composed of three active cells and one dead cell.

Iteration number	Cell concentrations			
	Cell 1	Cell 2	Cell 3	Cell 4
1	89.43	1.12	.34	3.04
10	38.83	10.46	7.87	14.15
50	14.62	16.07	16.57	15.46
100	13.18	14.72	15.31	14.15
200	11.02	12.31	12.81	11.84
300	9.22	10.30	10.71	9.90
400	7.71	8.61	8.96	8.28
500	6.45	7.21	7.50	6.93
600	5.40	6.03	6.27	5.80
700	4.51	5.04	5.25	4.85
800	3.78	4.22	4.39	4.06
900	3.16	3.53	3.70	3.39
1,000	2.64	2.95	3.07	2.84
1,500	1.08	1.21	1.26	1.16
2,000	.44	.50	.52	.48
3,000	.07	.08	.09	.08
5,000	.00	.00	.00	.00
10,000	.00	.00	.00	.00
$\bar{A}$	524.02	569.82	573.76	565.24

Table 5. Concentration C(N), cell effective volume VOL(N), boundary discharge volume BDV(N), and ΣVOL(N) for three cell FSM.

Iteration number N	Cell 1			Cell 2			Cell 3			
	C(N)	VOL(N)	BDV(N)	C(N)	VOL(N)	BDV(N)	C(N)	VOL(N)	BDV(N)	ΣVOL
1	99.010	2.010	0.0100	.493	2.000	0.0100	.002	2.000	0.0100	6.010
10	90.722	2.098	.0104	4.706	2.002	.0100	.129	2.000	.0100	6.100
50	63.851	2.443	.0122	18.828	2.052	.0103	2.443	2.004	.0100	6.499
100	43.629	2.788	.0139	27.665	2.180	.0109	7.456	2.028	.0101	6.995
200	22.639	3.266	.0163	29.019	2.528	.0126	16.946	2.160	.0108	7.954
300	12.635	3.555	.0178	23.195	2.885	.0144	20.991	2.382	.0119	8.822
400	7.314	3.731	.0187	17.004	3.189	.0159	20.400	2.647	.0132	9.567
500	4.330	3.827	.0192	12.019	3.427	.0171	17.595	2.913	.0146	10.167
510	4.218	3.738	.0187	11.605	3.444	.0172	17.265	2.939	.0147	10.121
550	3.772	3.422	.0172	10.185	3.468	.0173	15.935	3.034	.0152	9.924
600	3.236	3.107	.0156	8.779	3.421	.0171	14.347	3.126	.0156	9.654
700	2.285	2.670	.0134	6.652	3.197	.0160	11.594	3.198	.0160	9.065
800	1.539	2.406	.0120	5.037	2.929	.0147	9.363	3.141	.0157	8.476
900	1.001	2.246	.0112	3.751	2.687	.0134	7.521	3.005	.0150	7.938
1,000	.635	2.149	.0108	2.729	2.491	.0125	5.971	2.836	.0142	7.476
1,500	.056	2.012	.0101	.406	2.071	.0104	1.424	2.207	.0110	6.290
2,000	.005	2.001	.0100	.046	2.008	.0100	.227	2.034	.0102	6.043
2,500	.000	2.000	.0100	.005	2.001	.0100	.030	2.005	.0100	6.006
3,000	.000	2.000	.0100	.000	2.000	.0100	.004	2.001	.0100	6.001
4,000	.000	2.000	.0100	.000	2.000	.0100	.000	2.000	.0100	6.000
5,000	.000	2.000	.0100	.000	2.000	.0100	.000	2.000	.0100	6.000

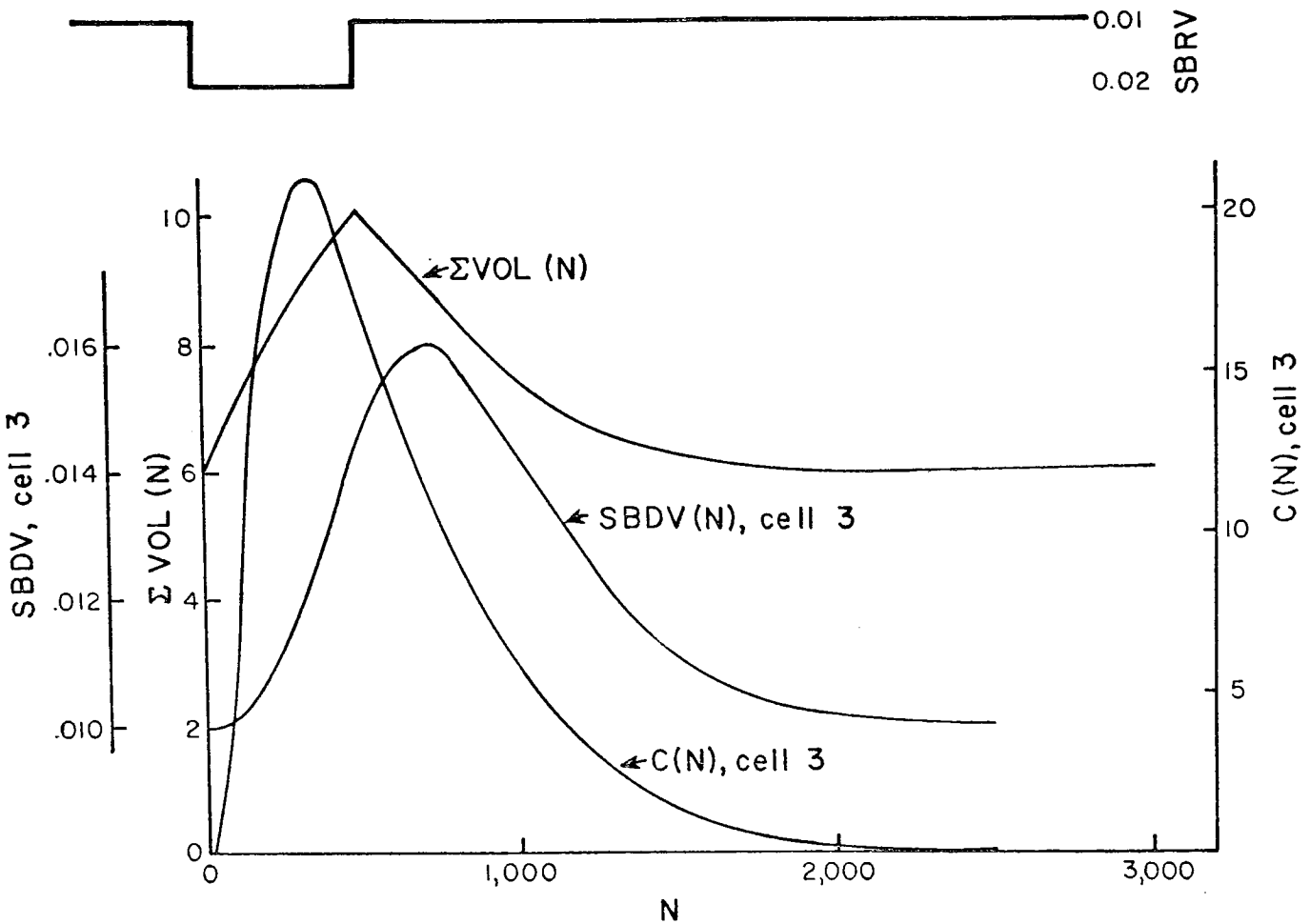

Figure 5. ΣVOL(N) versus N and C(N) and SBDV(N) versus N for cell 3 in a non-steady flow, non-steady volume FSM composed of three cells in series.

5.4.3 Case III: Non-Steady Flow, Non-Steady Volume Regime With Active and Dead Cells

In this experiment, the FSM is identical to that of Case I, except that SBRV and SBRC are identical to those of Case II. FAC = 0.01 for each of the active cells. No FAC was assigned to cell 4, since it is a dead cell whose effective volume remains constant. Table 6 and Figure 6 show the results of this experiment.

5.5 Concluding Remarks

In this chapter, the author introduced the concepts of non-steady flow and non-steady volume FSM regimes. The non-steady volume regime has the potential of modeling the transport of hydraulic energy in hydrologic systems. Active and dead cells, along with the concept of exchange were introduced next with some suggestions as to how they might be used to model processes occurring in hydrologic systems. The chapter concluded with three simple simulation experiments utilizing the various concepts presented earlier. These simulations were given solely to give the reader an idea how the various concepts work in practice. None of the FSMs used in the three simulations purports to represent a real-world hydrologic system. Real-world applications of finite-state models will be detailed in Chapters 7 and 8.

Table 6. Concentration C(N), cell effective volume VOL(N), boundary discharge volume BDV(N) and ΣVOL(N) for four cell FSM composed of three active and one dead cell (Cell 4).

Iteration number N	Cell 1			Cell 2			Cell 3			Cell 4	
	C(N)	VOL(N)	BDV(N)	C(N)	VOL(N)	BDV(N)	C(N)	VOL(N)	BDV(N)	C(N)	ΣVOL
1	88.558	1.010	0.0100	1.115	1.000	0.0100	0.335	1.000	0.0100	3.035	6.010
10	35.881	1.096	.0109	10.386	1.004	.0100	7.841	1.000	.0100	14.008	6.100
50	13.129	1.395	.0139	15.155	1.089	.0109	15.763	1.014	.0101	14.329	6.498
100	11.237	1.634	.0163	12.995	1.264	.0126	13.691	1.079	.0108	12.188	6.977
200	8.435	1.866	.0187	9.713	1.595	.0159	10.315	1.323	.0132	9.046	7.784
300	6.424	1.951	.0195	7.396	1.802	.0180	7.899	1.578	.0158	6.872	8.331
400	4.948	1.982	.0198	5.697	1.910	.0191	6.104	1.763	.0176	5.290	8.655
500	3.854	1.983	.0199	4.418	1.960	.0196	4.741	1.877	.0188	4.103	8.820
510	3.867	1.889	.0190	4.325	1.958	.0196	4.635	1.885	.0188	4.040	8.732
550	3.675	1.595	.0160	4.063	1.881	.0188	4.334	1.898	.0190	3.836	8.374
600	3.408	1.360	.0136	3.774	1.715	.0172	4.007	1.858	.0186	3.589	7.933
700	2.919	1.132	.0113	3.248	1.395	.0140	3.417	1.645	.0165	3.111	7.172
800	2.484	1.048	.0105	2.772	1.193	.0120	2.900	1.406	.0141	2.662	6.647
900	2.102	1.018	.0102	2.347	1.089	.0109	2.448	1.229	.0123	2.256	6.336
1,000	1.769	1.006	.0101	1.976	1.039	.0104	2.058	1.120	.0112	1.900	6.165
1,500	.729	1.000	.0100	.814	1.000	.0100	.847	1.000	.0100	.783	6.003
2,000	.298	1.000	.0100	.333	1.000	.0100	.347	1.000	.0100	.321	6.000
2,500	.122	1.000	.0100	.137	1.000	.0100	.142	1.000	.0100	.131	6.000
3,000	.050	1.000	.0100	.056	1.000	.0100	.058	1.000	.0100	.054	6.000
4,000	.008	1.000	.0100	.009	1.000	.0100	.010	1.000	.0100	.009	6.000
5,000	.001	1.000	.0100	.002	1.000	.0100	.002	1.000	.0100	.002	6.000
10,000	.000	1.000	.0100	.000	1.000	.0100	.000	1.000	.0100	.000	6.000

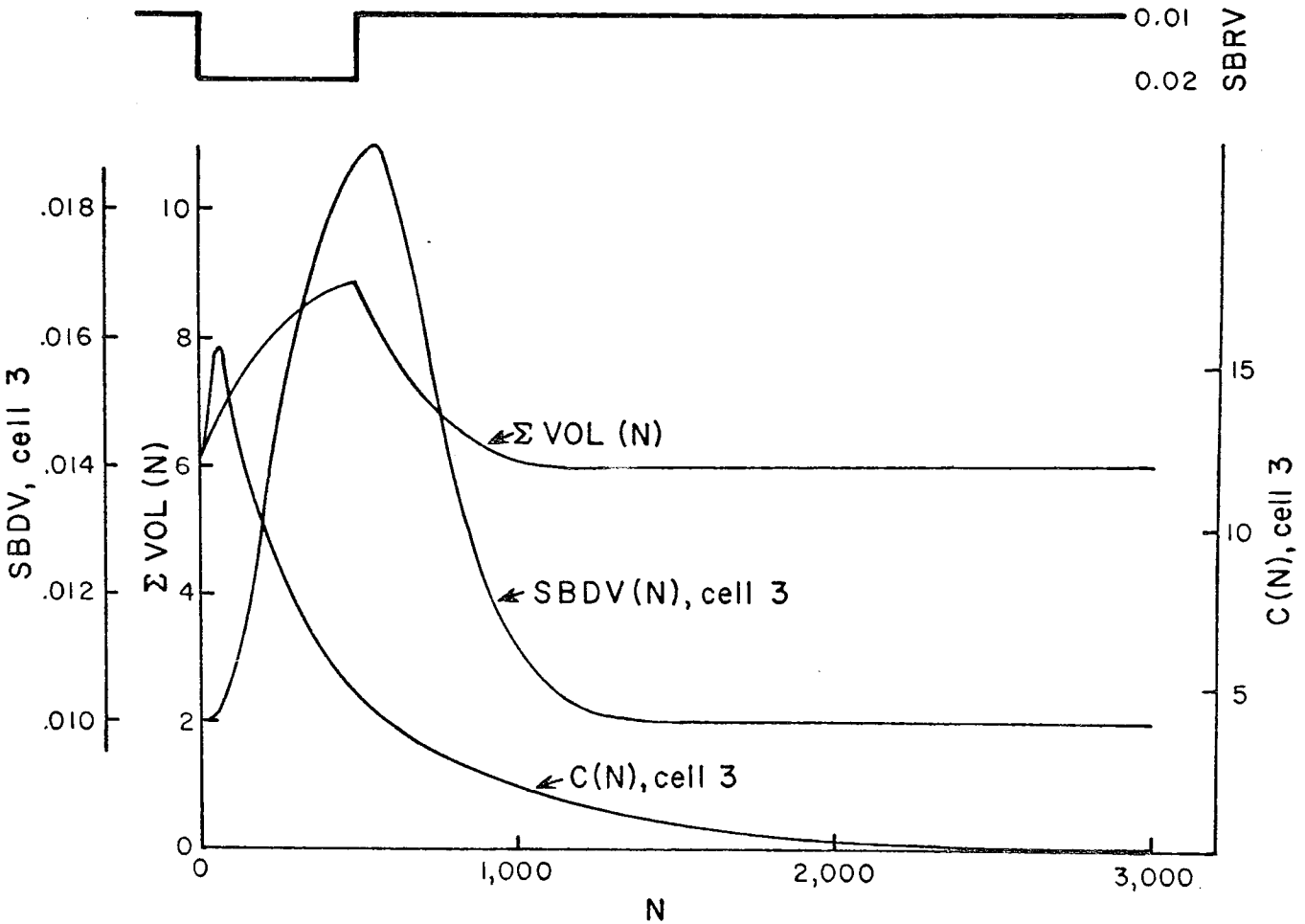

Figure 6. ΣVOL(N) versus N and C(N) and SBDV(N) versus N for cell 3 in a non-steady volume FSM composed of three active cells and one dead cell.

CHAPTER 6

RADIOACTIVE AND STABLE TRACERS IN GROUND-WATER HYDROLOGY

6.1 Introduction

This chapter will treat the subject of radioactive and stable tracers in ground-water hydrology, and particularly the use of two radioactive isotopes, carbon-14 (C-14) and tritium. This chapter will serve as a prelude to Chapters 7 and 8, in which the writer will use FSMs to model the distribution of C-14 ages in a portion of the Tucson Basin Aquifer of southern Arizona and the transient distribution of tritium in the Edwards Limestone Aquifer of south-central Texas. Only the natural introduction of tracers into aquifers will be considered, which is to say that even though the tracers may be in part man-made, they are injected into the aquifer via natural processes only.

Naturally-introduced radioactive tracers can be used to study a wide variety of problems not only in ground-water systems but in other hydrologic systems as well. The interested reader is referred to Payne (1972) and Gaspar and Oncescu (1972) for detailed discussions on the many uses of radioactive tracers in hydrologic systems. In this dissertation, only a few specific applications will be discussed.

6.2 C-14 in the Hydrologic Cycle

C-14 is produced in the atmosphere as the result of both natural and man-made activities. Natural production of C-14 is effected by the collisions of cosmic-ray produced neutrons and nitrogen-14, mainly in the upper atmosphere. The C-14 is then quickly oxidized to carbon dioxide. Munnich and Vogel (1960) stated that the relative concentration of C-14 to C-12 is approximately $1.0 * 10^{-12}$ to 1. Man-made production of C-14 was accomplished by the detonation of atmospheric thermonuclear devices. Payne (1972) stated that in the northern hemisphere these detonations had caused the concentration of atmospheric C-14 to almost double by 1963. Since then it has gradually subsided, though it is still above the natural or pre-bomb level. Increases in the atmospheric C-14 in the southern hemisphere were not as dramatic as those in the northern hemisphere.

The major input of C-14 to the ground-water system is from the carbon dioxide in the soil zone (Payne, 1972). The direct input of C-14 from precipitation is small because the partial pressure of the carbon dioxide is low. The carbon dioxide in the root zone is derived from the respiration of plant roots and the decay of dead plant matter. The soil zone ratio of C-14 to C-12 is usually the same as that of the atmosphere, although in areas where an appreciable fraction is derived from plant decay, this zone may have a slightly lower concentration of C-14 than

atmospheric carbon dioxide (Payne, 1972). The amount of C-14 in the ground water itself is also affected by the time it takes for the recharge water to infiltrate to the ground-water reservoir. The C-14 occurs in the ground water as carbon in the anions HCO_3^- and CO_3^{-2}.

Carbon-14 possesses a half-life of 5730 years, although the original half-life of 5568 years as reported by Libby (1955) is still used in order to reduce the possibility of confusion in published reports. A simple calculation can be used to adjust results based on the 5568 year value to the currently accepted value.

6.3 Tritium in the Hydrologic Cycle

Tritium is one of two isotopes of common hydrogen. The other isotope, deuterium, is not radioactive and differs from common hydrogen in that it has one neutron in its nucleus. Deuterium is given the symbol $_1H^2$ or simply D. On the other hand, tritium is radioactive and differs from common hydrogen in that it has two neutrons in its nucleus and is therefore given the symbol $_1H^3$, or simply T. Tritium possesses a half-life of 12.26 years. As was the case with C-14, tritium is produced in the atmosphere by the interaction between cosmic-ray produced neutrons and nitrogen-14. It is produced primarily in the upper atmosphere although other mechanisms in the hydrosphere and lithosphere produce negligible amounts. The detonation of atmospheric

thermonuclear devices also produces tritium and to a much greater extent than was the case with C-14. Large pulses of tritium were introduced into the atmosphere during the years 1952, 1954, 1958, 1961, and 1962 (Payne, 1972). Since the cessation of most atmospheric nuclear explosions in the early 1960's, these pulses have stopped. Prior to large-scale atmospheric nuclear explosions, Payne (1972) reported that the natural concentrations of tritium were in the range of 5 to 20 tritium units (TU), where one TU is defined as one atom of tritium per 10^{18} atoms of hydrogen. In addition to bomb tritium, Payne (1972) mentioned that industrial nuclear establishments may produce locally significant quantities of man-made tritium.

In hydrologic systems, tritium occurs primarily as tritiated water or water vapor; that is, as molecules consisting of one atom of common hydrogen, one atom of tritium, and one atom of oxygen (HTO). Other combinations of tritium in the water molecule are possible and do occur, but HTO is the most common. HTO is introduced into ground-water reservoirs as recharge from precipitation. Payne (1972) said that in general, the tritium concentrations in ground water do not vary as greatly as in precipitation. The movement of recharge water through the unsaturated zone, diffusion and the effectiveness of certain precipitation events in recharging water to the aquifer all combine to restrict the tritium concentrations in ground water. However, in

karst regions or where rocks are highly fractured, the tritium concentrations in the annual aquifer recharge may be close to the weighted annual mean tritium concentration of precipitation (Payne, 1972). It is always necessary to consider the hydrology of the recharge area whenever attempting to estimate tritium inputs to aquifers.

6.4 Use of C-14 to Date Ground Water

Munnich (1957) was the first to propose a method to obtain the corrected decay age of C-14 in ground water and to use it to obtain an estimate of the residence time of the water in the aquifer. The residence time is interpreted as the time that has elapsed between the time a given volume of water was recharged to the time it is sampled. The corrected decay age of C-14 and the residence time of the water are identical if no mixing occurs between waters of different ages.

Equation (10) of Chapter 3 can be used to obtain the residence time of the water. This equation is repeated here:

$$n = n_o \exp(-\lambda t) \qquad (10)$$

The parameters n and n_o will now be given a slightly different interpretation: n = radioactivity after time t and n_o = initial radioactivity at the time of recharge. By expressing λ in terms of the half-life (Equation [11]) and solving for it, one obtains

$$t = \frac{-t_{1/2} \ln(n/n_o)}{\ln 2} \qquad (60)$$

In this case, t is interpreted as the residence time of the water in the ground-water reservoir. In practice, a different form of Equation (60) is used since the ratio of C-14 to C-12 in the sample is measured, not the absolute amount of C-14.

There are four assumptions made in using the C-14 decay age to obtain the residence time of the water in an aquifer. They are:

1. The initial radioactivity n_o is known or can be estimated.
2. The ratio of C-14 to C-12 has been constant in space and time.
3. Any change in the C-14 to C-12 ratio in the aquifer from causes other than radioactive decay can be corrected by calculation.
4. Flow in the aquifer is piston flow; there is no mixing in the aquifer as a parcel of water retains its integrity from the recharge area to the sampling site.

The first assumption is violated by the production of C-14 by atmospheric thermonuclear detonations. Man-made C-14 might ordinarily make it difficult to estimate n_o. However, since C-14 has a long half-life and is therefore

used to date water on the order of thousands of years old, bomb C-14 does not usually complicate ground-water dating. This is in contrast to the case of tritium, where bomb tritium complicated the use of tritium to date ground water, but is useful when treated as an input pulse.

The second assumption is only approximately valid. The C-14 to C-12 ratio in the atmosphere undoubtedly varied during the past 6000 years (Damon, Long, and Grey, 1966). But the uncertainties in ages caused by this variation are small compared to other sources of error in the C-14 dating of ground water.

The third assumption is more or less valid depending upon the minerals in the aquifer. Some C-14 may be lost via isotopic exchange with any carbonate minerals in the aquifer. This is especially true in limestone or dolomite aquifers. It is also necessary to correct for the dilution of C-14 by the dissolution of carbonate minerals which contain "dead" (non-radioactive) carbon. Various schemes have been devised to account for exchange and dilution of C-14 including a method developed by Wallick (1973) for semi-arid environments. The interested reader is referred to Wallick (1973) for a list of references of previous work.

The fourth assumption is almost always violated. Mixing occurs in all aquifers to a greater or lesser degree, so the C-14 decay age is not identical to the residence time

or mean age of the water; if mixing occurs in the aquifer, the decay age of C-14 or any other radioactive tracer will always be less than the mean age of the water. Nir (1964) discussed the effects of various degrees of mixing on ground-water transit times. He treated three cases: pure piston flow, complete mixing, and the dispersive case, giving equations for each case. However, his results were based on a one-dimensional aquifer. The complete mixing case was derived by assuming that the aquifer could be modeled as a single unit, which in FSM terminology might be represented as a single simple mixing cell. He thus assumed that any tracer introduced into the aquifer is "quickly" mixed throughout the entire system. This assumption may be reasonable for small aquifers or ones in which ground-water flow velocities are very high, but for other instances it is probably unreasonable. Nir's dispersive model requires the evaluation of several parameters, one of which is the dispersivity of the medium. This particular parameter may prove difficult to evaluate. Gaspar and Oncescu (1972, pp. 282-283) also discussed the effects of mixing on age determinations. The age distributions of radioactive isotopes, when modeled by a FSM, can be easily related to the mean age of the water, as will be seen in Chapter 7.

6.5 Use of Tritium to Date Ground Water

Much of what was said in the preceding section regarding C-14 ground-water dating applies to tritium as well. However, because of the relatively short half-life of tritium, the effects of bomb tritium are very important and must be considered. Bomb tritium complicates the task of estimating the input of tritium to ground water through space and time. The problem is mitigated somewhat by the global network of stations reporting the tritium concentrations in precipitation organized by the International Atomic Energy Agency. Payne (1972) claims that the transit time of the ground water may be estimated by calculating the theoretical tritium concentration (the tritium output function) using one of the models of Nir (1964) which best suits the hydrogeology of the area under investigation, having previously estimated the input from precipitation or other data. This assumes that the hydrologist accepts the validity of Nir's (1964) models, the shortcomings of which were discussed in the preceding section. The author will not concern himself with the use of tritium to date ground waters, although the FSM offers a better means to do so than the models of Nir (1964). In his model of the Edwards Limestone Aquifer (Chapter 8), calibration is based on accounting for the distribution of the bomb tritium pulses. Tritium decay age is not calculated, but the mean age of the

water in each cell of the FSM can be calculated for any desired values of average annual recharge to the aquifer.

6.6 Selection of Radioactive Isotopes in Ground-Water Dating

Because of the large difference in their half-lives, C-14 and tritium are suited for different ground-water environments. C-14 can be used to date waters no younger than about a thousand years and no older than about 40,000 years. It can therefore be used only in aquifers where the water moves very slowly and/or aquifers of large size. Tritium, on the other hand, can be used to date or trace waters between the ages of perhaps several years up to a maximum of 50 years (Gaspar and Oncescu, 1972, p. 282). Its use must be restricted to small aquifers or those in which the ground-water velocities are very high such as in karst or certain fractured rock aquifers. There is a gap of nearly a thousand years where neither tritium nor C-14 can be used to date ground waters. Silicon-32 has been suggested recently (Payne, 1972; Gaspar and Oncescu, 1972, p. 285) as a radioactive isotope capable of filling the gap between tritium and C-14. Silicon-32 has a half-life of approximately 500 years and could be used to date waters with ages of between 50 and several thousand years old. Silicon-32 is produced in the atmosphere as a result of cosmic-ray radiation. However, questions involving its artificial production have not

been completely resolved, so its use in dating ground water remains in the developmental stage (Payne, 1972).

In addition to silicon-32, Gaspar and Oncescu (1972, pp. 286-287) also mention the possible uses of three radioactive decay series in dating ground water: the uranium, thorium, and actinium series. However, they state that the use of these series is more difficult than other methods, as many corrections are necessary.

6.7 Finite-State Models and Radioactive Isotope Age Distributions in an Aquifer

Finite-state models will enable a hydrologist to devise a model to account for an observed distribition of radioactive isotope ages in an aquifer and relate this distribution of ages to residence times (mean ages) of the ground water. This can be accomplished without having to assume piston flow in the aquifer, or that the aquifer is one huge perfectly-mixed cell, and without having to estimate aquifer parameters such as the dispersivity. Nor will the aquifer have to be restricted to one spatial dimension. By using a three-dimensional cell network, three-dimensional flow in an aquifer can be modeled, provided that data on such flow are available.

Suppose that a spatial distribution of radioactive isotope decay ages has been obtained for an aquifer by sampling the ground water at different sites. This

distribution, along with other hydrogeological information, can be used to calibrate a FSM. The calibration process would entail adjusting the parameters of the FSM such as the number and arrangement of cells, cell effective volumes, flow paths, etc., until a good agreement was obtained between the observed age distribution and that produced by the FSM. Once a satisfactory agreement is obtained in the case of a steady flow FSM, the mean ages of the individual cells or of the entire FSM immediately follows. Mean age has a well-defined meaning only for the steady flow regime. These mean ages would represent the various residence times of the water. A hypothetical case will illustrate the procedure.

6.8 FSM Simulation of C-14 Decay Ages

Figure 7 depicts a hypothetical alluvial aquifer as modeled by a FSM. The aquifer is composed of 16 simple mixing cells, whose effective volumes are as shown and whose initial states are all arbitrarily zero. Recharge enters the aquifer from two sources: the mountain front bordering cell 1 and the ephemeral stream above cell 6. SBRVs representing the constant average annual recharge were assigned to these two sources. The yearly SBRC at each of these two locations is set equal to 100. This figure of 100 means that the C-14 in the recharge water is 100 per cent of its "normal" atmospheric concentration; its decay age is zero. The recharge water is assumed to reach the aquifer

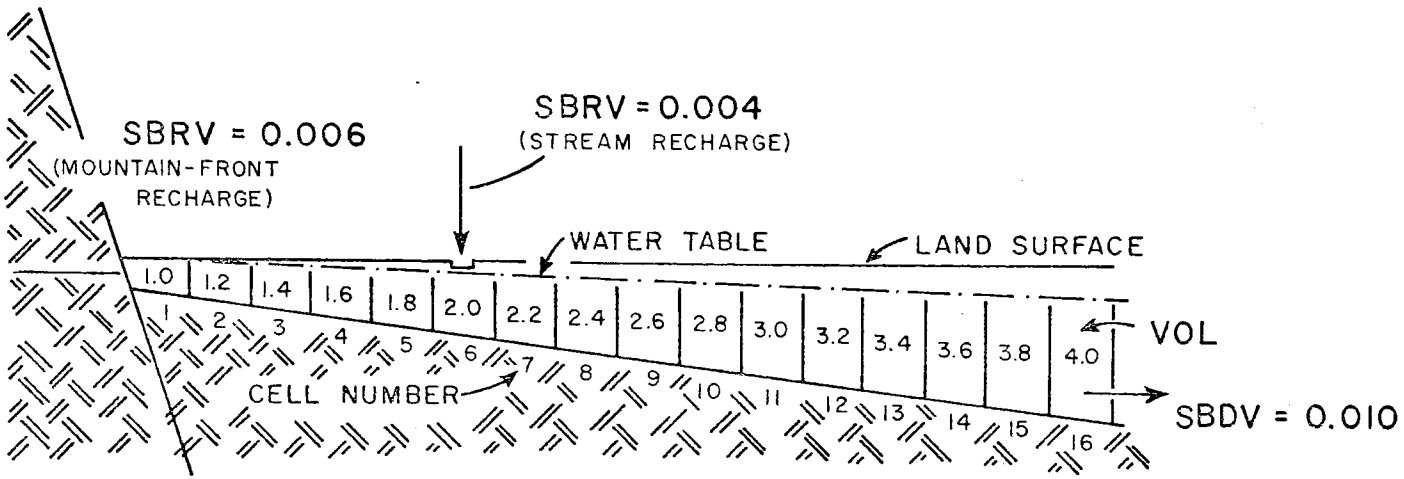

Figure 7. A hypothetical alluvial aquifer.

instantaneously. The time between iterations was chosen as one year, and a C-14 half-life of 5730 years was used. The steady flow, steady volume FSM was then iterated until each cell attained steady state; that is, the amount of C-14 entering each cell equalled the amount leaving plus that lost by radioactive decay. The loss of C-14 was accounted for by multiplying the state of each cell at the end of every iteration by Equation (16). Once steady state was reached, Equation (60) was used to calculate the decay age of each cell. In this equation, n_o = 100 and n = steady state concentration of C-14 in each cell. Table 7 shows the steady state C-14 concentration and the corresponding decay age for each cell. Had this been a real-world system, the modeler would then adjust the parameters of the FSM to obtain a good agreement between the observed and calculated decay ages. Once a satisfactory agreement had been obtained, the mean age numbers of the cells would be calculated, and these quantities are shown in the last column of Table 7. Since all the cells are simple mixing cells, the mean age number of cell 16 is also the mean transit number of the FSM. The reader should note that the mean age of the water is everywhere greater than the C-14 decay age, a result not surprising since the flow in the FSM was not of the piston or zero mixing variety.

In addition to providing the residence times of the ground water in various portions of the aquifer, the FSM

Table 7. Relationship between carbon-14 decay age and the average age of the water in a hypothetical alluvial aquifer.

Cell number	Per cent C-14 at steady state	C-14 decay age (years)	Average age of water (years)
1	98.01	167	168
2	95.70	363	368
3	93.07	591	601
4	90.16	852	868
5	87.01	1151	1168
6	90.02	870	901
7	87.69	1084	1121
8	85.21	1324	1361
9	82.62	1580	1621
10	79.91	1854	1901
11	77.11	2149	2201
12	74.24	2466	2521
13	71.30	2796	2861
14	68.33	3151	3221
15	65.33	3523	3601
16	62.31	3911	4001

also provides estimates of the long-term average annual recharge to the aquifer. This is simply the SBRVs used in the FSM which provided the best agreement between the observed and calculated decay ages. The recharge information would be useful as an input to other models of the aquifer, particularly hydraulic models, whether the models be of the FSM type or other varieties. The knowledge of the long-term average annual recharge would also be useful in water budget studies of the area.

6.9 Stable Tracers and FSMs

Stable tracers and their distributions in an aquifer can be modeled using FSMs. Oxygen-18 and deuterium are two stable isotopes found in water, principally in the forms HDO^{16} and H_2O^{18}. The isotopic ratios D/H and O^{18}/O^{16} are measured and compared to those of a standard, usually the Standard Mean Ocean Water (SMOW), which is a close approximation of the average isotopic composition of the oceans. Tritium can be treated as a stable tracer once radioactive decay is accounted for. Stable isotopes are especially attractive tracers since they are conservative and, because they occur as part of the water molecule, they move at the same velocity as the water. In thermal waters, oxygen-18 is non-conservative since it undergoes isotopic exchange with the aquifer matrix. This exchange may be of interest in certain hydrologic problems.

FSMs can model stable isotope distributions either as steady state distributions in or pulsed inputs to a hydrologic system. The former case would be similar to the FSM simulation of section 6.8 and the real-world example of Chapter 7 in which the steady state distribution of C-14 in an aquifer will be modeled. In Chapter 8, the spatial and temporal distribution of tritium in response to annual tritium pulses will be modeled in order to determine the hydrologic properties of a highly anisotropic and non-homogeneous aquifer.

The FSM modeling of stable isotope distributions in an aquifer has the potential of providing hydrologists with a great deal of information regarding the transport properties of the aquifer without having to wait for years of pollution necessary to calibrate a PDE-based mass transport model. Stable tracers could also be used to obtain information about highly complex aquifer systems such as karst and fractured rock aquifers, which are difficult to analyze using physically-based models. A great deal of research remains to be done in the field of hydrologic applications of stable isotope variations. FSMs could also be used to model distributions of artificially-produced tracers in hydrologic systems, such as fluorocarbons in aquifers (Thompson, Hayes, and Davis, 1974). The principal requirements for tracers are that they be conservative and easy to detect.

6.10 Concluding Remarks

This chapter presented a brief discussion on radioactive and stable tracers, especially C-14 and tritium, in ground-water hydrology. Emphasis was placed on these two isotopes since the author will be using them to model two different ground-water reservoirs.

A simulation depicting how a FSM could be used to model the distribution of C-14 decay ages in an aquifer was presented. Although the aquifer was simple and hypothetical, the concept will be applied to a complex real-world hydrologic system in Chapter 7.

Radioactive tracers are useful in obtaining ground-water residence times, although like stable tracers they can be useful in obtaining information about flow paths in aquifers and other hydrologic systems. In Chapter 8, tritium will be used primarily as a tracer. Stable tracers have great potential in hydrology, although much research remains to be done.

CHAPTER 7

A FINITE-STATE MODEL OF THE C-14 AGE DISTRIBUTION IN A PORTION OF THE TUCSON BASIN AQUIFER

7.1 Introduction

In this chapter, the writer will present a steady flow, steady volume FSM of the C-14 age distribution in a portion of the Tucson Basin Aquifer of southern Arizona. The assumptions and limitations of the model will be analyzed in addition to discussing the usefulness of the model in understanding the hydrology of the area studied. The author will also discuss how the model could be improved. Inherent in the development of a better model is the need for more data. However, the existence of the present model improves the rationale of future data collection.

7.2 Geohydrology of the Tucson Basin

7.2.1 Location

The Tucson Basin, which lies within the Basin and Range Province, is that portion of the Santa Cruz River valley extending for about 50 miles from the Tortolita Mountains on the north to the Pima County-Santa Cruz County County line on the south (see Figure 8). The basin is bounded on the north and northeast by the Tortolita and

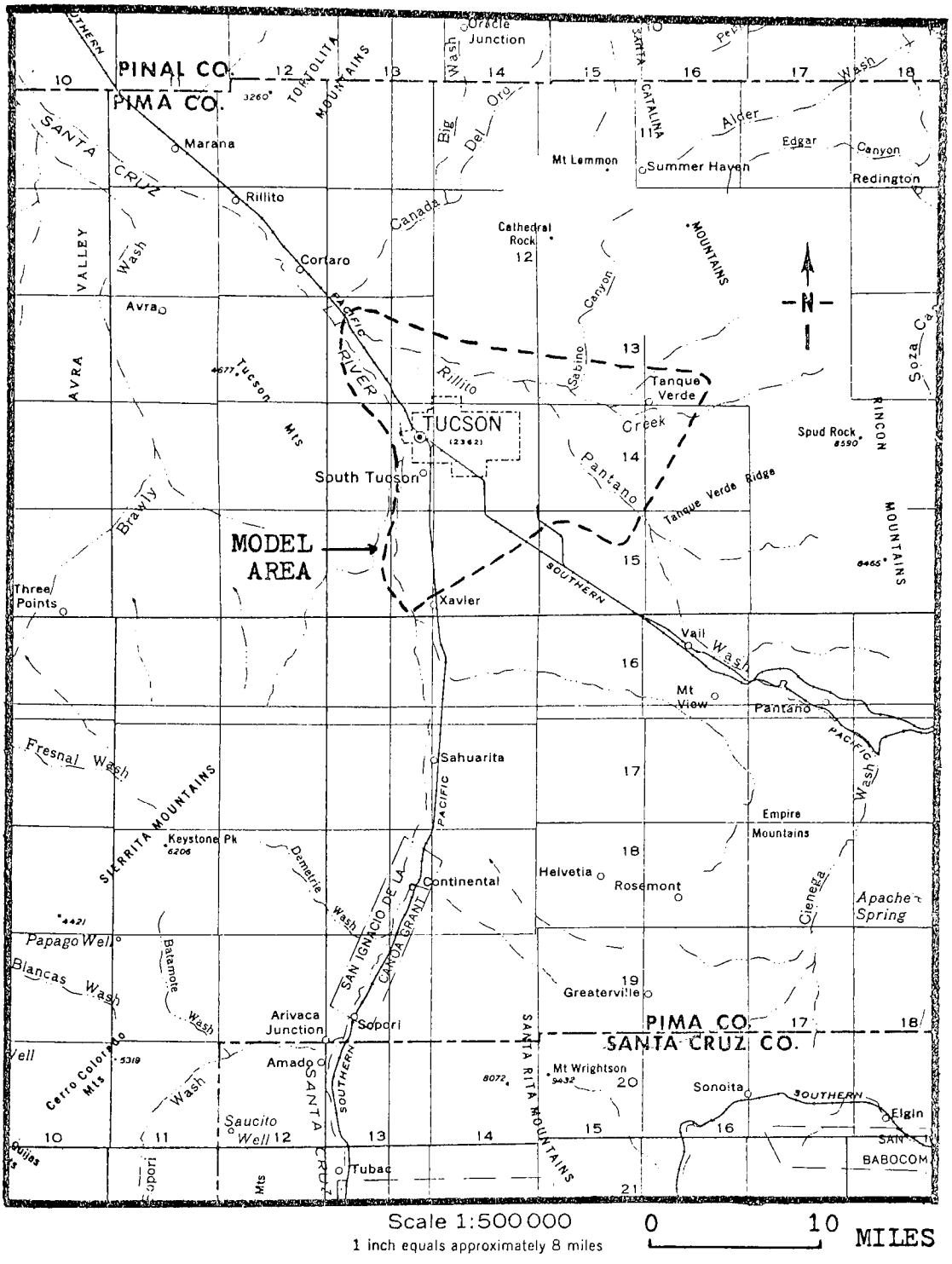

Figure 8. Map of the Tucson Basin and surrounding area.

Santa Catalina Mountains, the Tucson and Sierrita Mountains on the west, the Rincon Mountains and Tanque Verde Ridge on the east, and the Empire and Santa Rita Mountains on the east and southeast. The altitude along the Santa Cruz ranges from about 3000 feet above mean sea level at the Pima County-Santa Cruz County line down to about 2000 feet above mean sea level near the Tortolita Mountains. The entire basin encompasses about 1000 square miles. The city of Tucson occupies about 100 square miles in the north-central part of the basin, and is the only large city in the basin.

7.2.2 Climate

The climate of the Tucson Basin can best be characterized as semi-arid and warm. Precipitation averages about 11 to 12 inches per year in the vicinity of Tucson, increasing to a high of over 25 inches per year in the Santa Catalina Mountains (Green and Sellers, 1964). Approximately 65 per cent of the precipitation falls between May and October, and 50 per cent of the total occurs in July and August (Davidson, 1973). The average monthly temperature ranges from 50°F in January to 86°F in July (Green and Sellers, 1964). Because of the high temperatures and semi-arid climate, the Class A pan evaporation is about 90 inches per year.

7.2.3 Drainage

The main stream in the basin is the Santa Cruz River, which flows north along the western margin of the basin. Its main tributary is Rillito Creek, which joins it northwest of the Tucson city limits. In turn, the Rillito receives most of its water from Canada del Oro, Sabino Canyon Creek, Tanque Verde Creek, and Pantano Wash. All of the aforementioned streams also receive flow from smaller streams running down from the surrounding mountains. All of the major streams in the basin are ephemeral and losing streams; they flow only part of the year, during and immediately following rainfall events.

7.2.4 Geology

The Tucson Basin is an elongated structural valley filled with unconsolidated alluvial deposits and older semi-consolidated and consolidated alluvial sediments (Davidson, 1973). Exploratory drilling by the Humble Oil and Refining Company indicates that these deposits reach a thickness of 12,000 feet, although the average thickness is on the order of several thousand feet. The deposits include the Pantano Formation and Tinaja beds of Tertiary age and the Fort Lowell Formation of Quaternary age, and form a single aquifer (Davidson, 1973).

The mountains surrounding the basin are composed primarily of intrusive and extrusive igneous rocks,

metamorphic rocks, and to a lesser degree, consolidated sedimentary rocks. The entire basin has been downfaulted with respect to the mountains, a necessary condition for the filling of the basin with sediments. Faulting also continued during the depositional episodes, as evidenced by the offset in some of the Tertiary and Quaternary beds.

7.2.5 Ground-Water Reservoir

The aquifer system in the Tucson Basin is essentially a single unconfined aquifer, though it is partly confined at some of the present depths of development (Davidson, 1973). Transmissivities in the aquifer range from about 1000 to 500,000 gallons per day per foot (Anderson, 1972) though in most places they are less than 50,000 gallons per day per foot (Davidson, 1973). The depth to the water table is currently between 100 and 250 feet in most places; during the past half-century, increasing withdrawals from wells for farm, municipal, and industrial use resulted in a continual lowering of the water table. Along the major streams the depth to the water table is the least, whereas in the southeastern part of the basin the depths to water are the greatest. The average porosity of the aquifer is about 28 per cent (Davidson, 1973).

Recharge to the aquifer comes primarily from two sources: infiltration from streams during flow events and seepage through fractures along the mountain fronts.

Davidson (1973) estimated that the average annual recharge to the aquifer is about 100,000 acre-feet, a figure about evenly divided between the two sources listed above. In addition, the aquifer receives about 10,000 and 8000 acre-feet per year of underflow across its southern and northern boundaries respectively, and discharges about 7800 acre-feet per year of underflow across its northwestern boundary (Davidson, 1973).

The Tucson Basin Aquifer is essential to the well-being of the area. The city of Tucson and its surrounding area are totally dependent upon ground water for their water supply, and Tucson is perhaps the largest city in the nation that is 100 per cent dependent upon ground water. This complete dependence arises from the fact that the streamflow in the area is too erratic to serve as a major water supply. The Santa Cruz River and Rillito Creek are dry for about 320-335 days per year (Davidson, 1973). The mean annual streamflow past gaging stations on the major streams is about 10,000 to 20,000 acre-feet and the mean annual streamflow out of the basin is about 17,000 acre-feet (Davidson, 1973).

For more information on the geohydrology of the Tucson Basin, the interested reader is referred to Davidson (1973). Specialized reports include an electric analog analysis by Anderson (1972), depletion of streamflow by infiltration (Burkham, 1970), the chemical quality of the

water in the basin (Laney, 1972), and a study of streamflow in the upper Santa Cruz River basin by Condes de la Torre (1970).

7.3 The Area Modeled

The FSM of the author does not model the entire Tucson Basin Aquifer. The model area is the area enclosed by the dashed line on Figure 8. Since the available C-14 age data were confined to this area the writer felt it best to restrict his model to the same region. The author initially attempted to model the entire aquifer, but abandoned the attempt because of the calibration difficulties imposed by the sparse data. When and if the C-14 age data are extended to encompass a greater areal extent, the present model should be expanded, re-calibrated and validated to include these data.

7.4 C-14 Ages

The author used the adjusted C-14 ages calculated by Wallick (1973) from the raw ages measured by Bennett (1965). Bennett took water samples from wells penetrating to approximately the same depth in the aquifer, after allowing the wells to flow for several minutes in order to make certain that all standing water in the wells had been purged. Such a procedure was necessary, because if the ground water is in contact with the atmosphere for a long enough time, an isotopic exchange will occur between the

atmospheric carbon dioxide and the dissolved bicarbonate ion (HCO_3^-), a mechanism which will increase the C-14 content of the water (Vogel, 1967). In addition, since temperature changes will affect the C-14 content of the water (Wendt et al., 1967) samples were not taken from the well water until its temperature stabilized (Bennett, 1965).

7.5 Cell Locations and Effective Volumes

The study area was modeled using a steady flow, steady volume FSM of 26 simple mixing cells arranged in a three-dimensional network. Earlier FSMs attempted a two-dimensional network; however, the writer found it essential to consider the three-dimensional flow of ground water in order to obtain a reasonable agreement between the observed and calculated ages. The FSM is composed of an upper tier and lower tier of cells.

The upper tier of cells consists of 17 cells (Figure 9), assigned the numbers 10 through 26. The locations of these cells were chosen primarily on the basis of the available C-14 age distribution and the hydrogeology of the area, particularly the distribution of the faults. All the age data were taken from the cells in the upper tier, although not all cells in this tier were represented by an observed age.

Each cell in the upper tier was assumed to extend to a depth of approximately 500 feet below the water table.

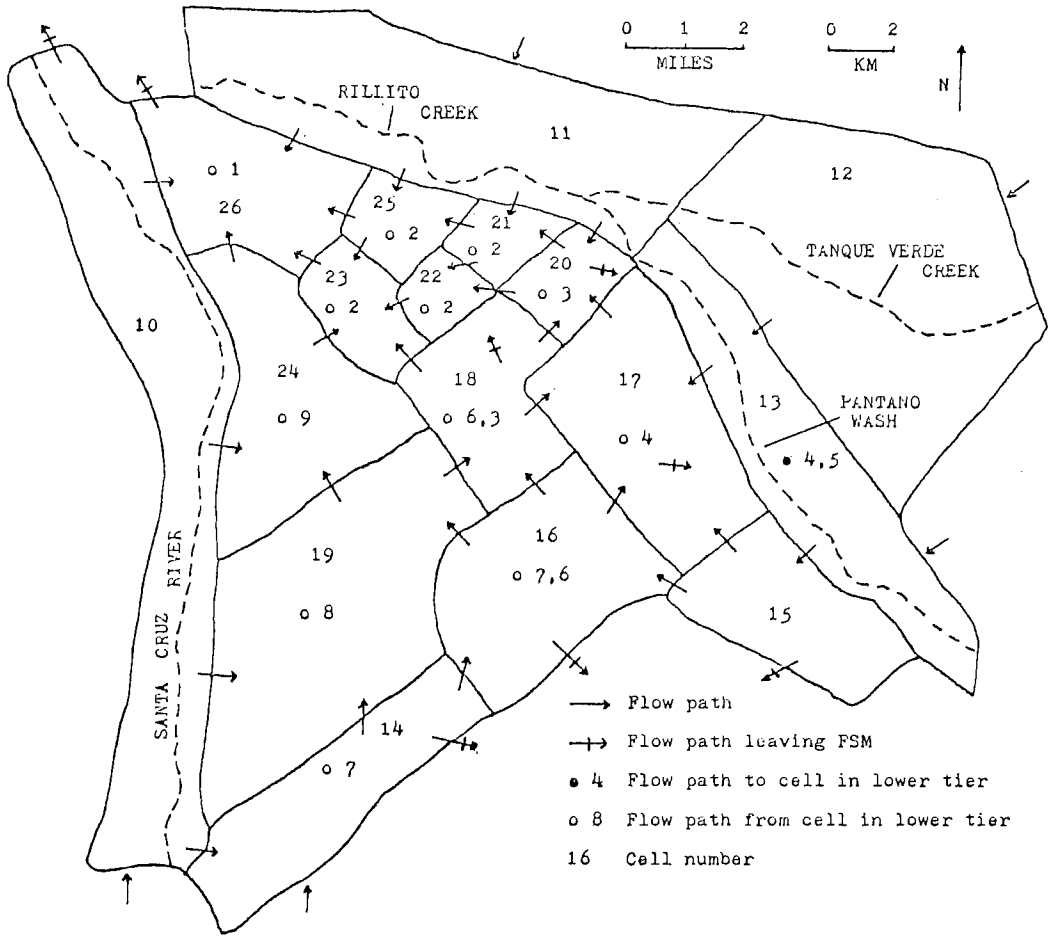

Figure 9. Upper tier of cells in the Tucson Basin FSM.

Effective volumes were calculated by assuming an effective porosity of about 25 per cent. Some of these effective volumes were changed as a result of the calibration process. A suitable choice for the URV was found to be 10^6 acre-feet (a-f), and so all volumetric quantities will be expressed as multiples of this figure. Table 8 shows the final effective volumes of the upper tier cells, as well as their BRVs and the ratios BRV/VOL.

The cells in the lower tier (Figure 10), numbered 1 through 9, were assumed to be approximately 1500 feet thick, extending from about 500 feet below the water table to about 2000 feet below it. Effective volumes were calculated on the basis of an effective porosity of about 20 per cent. The arrangement of these cells was dictated by hydrogeological considerations, relationships between the upper tier of cells, and a healthy dose of intuition. Calibration of the model also played a substantial role in determining not only the cell locations but also their final effective volumes. Table 9 shows the final effective volumes of the cells in the lower tier, as well as their BRVs and the ratios BRV/VOL.

7.6 Flow Distribution

Once an initial arrangement of cells had been determined, it was necessary to specify the flow distribution among the cells in the network. One might use the

Table 8. VOL, BRV, and BRV/VOL for each cell in the upper tier of the Tucson Basin FSM.

Cell number	VOL (10^6 a-f)	BRV (10^6 a-f)	BRV/VOL (%)
10	1.20	.0070	.58
11	1.52	.0160	1.05
12	1.62	.0092	.57
13	1.10	.0142	1.29
14	.75	.0006	.08
15	.85	.0099	1.17
16	1.15	.0020	.17
17	1.10	.0059	.54
18	.65	.0011	.17
19	1.70	.0012	.07
20	.19	.0056	2.95
21	.10	.0102	10.20
22	.10	.0090	9.00
23	.24	.0190	7.92
24	1.15	.0012	.10
25	.18	.0097	5.39
26	.80	.0218	2.73
Total	14.40		

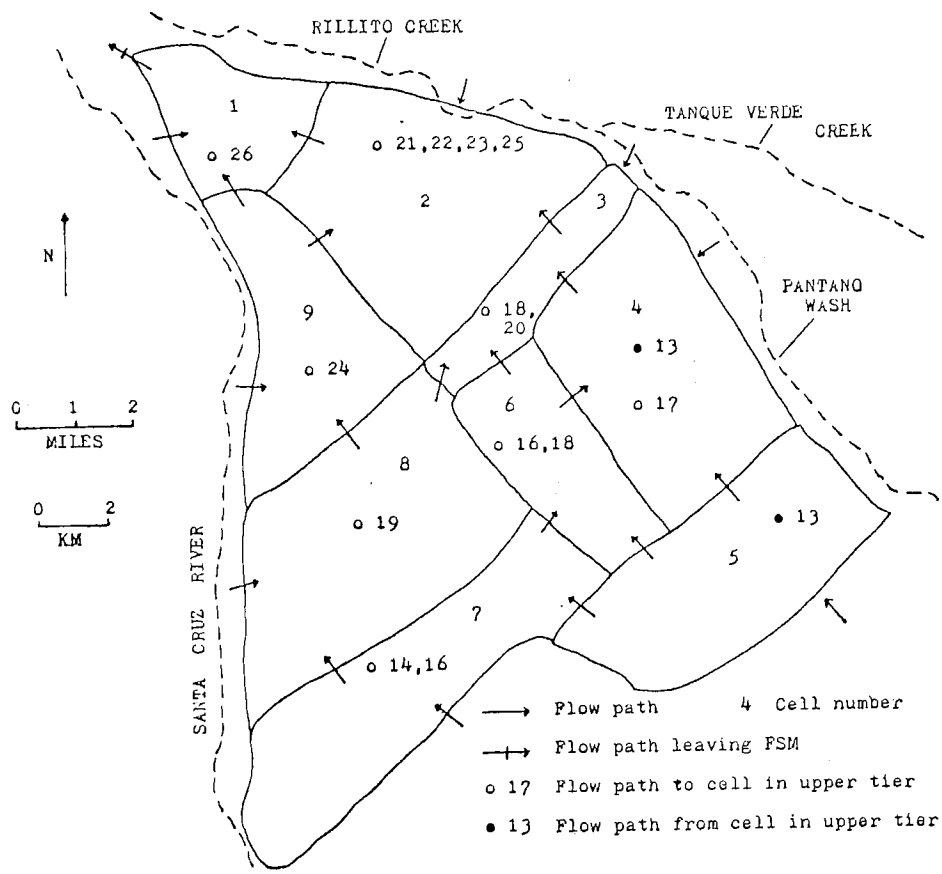

Figure 10. Lower tier of cells in the Tucson Basin FSM.

Table 9. VOL, BRV, and BRV/VOL for each cell in the lower tier of the Tucson Basin FSM.

Cell number	VOL (10^6 a-f)	BRV (10^6 a-f)	BRV/VOL (%)
1	1.00	.0015	.15
2	2.47	.0011	.04
3	.77	.0003	.04
4	2.00	.0011	.06
5	2.21	.0008	.04
6	1.00	.0004	.04
7	2.20	.0004	.02
8	2.15	.0003	.01
9	1.50	.0002	.01
Total	15.30		

output of a hydraulic model to determine the flow distribution, if such a model is available. A finite-difference hydraulic model of the Tucson Basin exists (Supkow, 1973), however the writer concluded that this model was not suited to the requirements of his FSM. The author resorted to information contained in Davidson (1973), and especially the geohydrologic map contained in this report (Davidson, 1973, plate 1) to designate the initial flow distribution in the model, or at least in the upper tier of cells. But since the map is limited to two spatial dimensions and since data pertaining to the vertical flow of water and of water movement at great depths in the aquifer are scarce, the author had a difficult time assigning flow distributions within the lower tier of cells and between the upper and lower tiers. Data from a few deep test wells indicate that the hydraulic head generally increases with depth where the aquifer includes thick sequences of silt and clayey silt and generally decreases with depth where the aquifer is mainly sand or gravel (Davidson, 1973). The former condition implies upward movement of ground water and this condition exists generally in the downfaulted central portion of the basin (Davidson, 1973) where much of the author's model lies. The latter condition implies downward flow of water. Most of the vertical flow in the author's model is directed upward from the lower tier of cells to the upper tier, although there is some downward movement from

the upper tier to the lower tier. The upward movement of water occurs mainly in the central part of the model, and the downward movement occurs mainly along the model boundaries. In any event, the rate of flow in the vertical direction is a relatively small fraction of the horizontal flow; however, this vertical flow, small though it may be, is quite critical to the model. The final vertical flow distribution was obtained almost entirely through the calibration process. The good agreement between the observed ages and calculated ages perhaps indicates that the author's estimate of vertical flow distribution is not unreasonable. Until a three-dimensional hydraulic model of the aquifer is constructed or until there is extensive deep-well drilling, the author's vertical flow distribution will be difficult to verify but even more difficult to refute.

The assignment of the flow distribution among the cells of the lower tier also presented a problem. As previously mentioned, little information is available on the flow of ground water at great depths in the aquifer. The initial flow distribution in the lower tier to some extent mirrored that of the upper tier. The final flow distribution was determined largely through the calibration process.

Table 10 lists the flow distribution for the entire FSM.

Table 10. Flow distribution within the Tucson Basin FSM.

Output cell	Input cell	Flow as fraction of total BDV of output cell[a]
10	19	.020
12	13	1.000
13	5	.050
13	4	.050
13	15	.700
13	17	.200
10	14	.050
5	6	.400
5	4	.250
5	7	.350
10	24	.020
7	6	.200
7	8	.400
7	14	.200
6	4	.150
6	3	.150
6	16	.350
6	18	.350
7	16	.200
4	17	.850
4	3	.150
8	3	.020
3	20	.200
3	18	.350
3	2	.450
8	9	.230
8	19	.750
9	24	.750
9	2	.100
9	1	.150
2	1	.960
2	21	.010
2	22	.010
2	23	.010
2	25	.010
1	26	.750
15	17	.100
15	16	.170
14	16	.180
14	19	.650
16	17	.350
16	18	.270
16	19	.250
19	18	.250

Table 10.--Continued

Output cell	Input cell	Flow as fraction of total BDV of output cell[a]
19	24	.750
18	20	.100
18	17	.400
17	20	.650
11	20	.100
11	21	.475
11	25	.415
11	26	.010
20	21	.470
20	22	.330
18	23	.200
24	23	.150
24	26	.850
21	22	.700
21	25	.300
25	26	.020
25	23	.980
22	23	1.000
23	26	1.000
10	26	.040

[a]The sum of all fractions from a given output cell equals unity, except where that cell discharges to the FSM boundary, in which case the difference is accounted for by such discharge. For example, in the case of cell 13, .050 + .050 + .700 + .200 = 1.000. In the case of cell 10, .020 + .050 + .020 + .040 = .130, and .870 is discharged to the boundary.

7.7 Inputs and Outputs

Information regarding volumetric inputs to the model (SBRVs) was taken mainly from Davidson (1973, plate 7), although some adjustments were made in the SBRVs during the calibration phase. Table 11 is a list of all cells receiving SBRVs, the final SBRVs and the real-world sources of these inputs. Input data are given on an annual basis, and therefore a choice of Δt = 1 year was made. All SBRVs were maintained constant throughout the operation of the model. The SBRVs due to underflow (see Table 10) represent educated guesses by the writer, as do the sources and values of the SBRVs to cells 1, 2, 3, 4, 5, and 9.

For each SBRV, a SBRC of 100 was assigned. The reasoning behind this was discussed in Section 6.8. The assignment of SBRCs with a value of 100 to the underflow SBRVs may be subject to question. The underflow SBRVs have been in the ground-water reservoir for some time, and therefore have some age greater than zero assigned to them. However, the underflow SBRVs represent a small fraction of the total recharge to the model, so their uncertainties probably do not affect the model to a great degree. The underflow SBRVs are those obtained in the calibration process.

Specification of those cells discharging some or all of their contents to the outside environment was determined in large part in the calibration process.

Table 11. SBRVs and their sources for the Tucson Basin FSM.

Cell number	Source	Amount (10^6 a-f)
1	Infiltration from Rillito Creek (?)	.0005
2	Infiltration from Rillito Creek (?)	.0009
3	Infiltration from Rillito Creek (?)	.0001
4	Infiltration from Pantano Wash (?)	.0001
5	Infiltration from Pantano Wash (?)	.0001
7	Underflow	.0001
8	Underflow	.0001
9	Infiltration from Santa Cruz River (?)	.0001
10	Infiltration from Santa Cruz River	.0070
11	Infiltration from Rillito Creek and mountain front recharge	.0160
12	Infiltration from Tanque Verde Creek and mountain front recharge	.0092
13	Infiltration from Pantano Wash and mountain front recharge	.0050
14	Underflow	.0002
	Total	.0394

Table 12 shows those cells discharging to the outside environment and the volumetric amount discharged. The SBDVs from cells 1, 10, and 26 are envisioned as underflow from the system and are not unreasonable in light of the present knowledge of the system (Davidson, 1973). The SBDVs from cells 14, 15, 16, 17, 18, and 20 were determined almost entirely by the calibration process, more so than the SBDVs from cells 1, 10, and 26. The former SBDVs could represent flow of water out of the system by evapotranspiration. Since the present-day water table is too deep to allow this, it might appear quite unreasonable at first glance. However, since the time span of the model covers many thousands of years, such loss of water could have occurred in the past when the water table was much closer to the surface of the land. Indeed, before the onset of large-scale pumping in the Tucson Basin, springs were found in the area and the aquifer also discharged to streams (Smith, 1910, p. 98). The SBDV emanating from cell 15 may represent either evapotranspiration losses or downward flow of water outside the system.

No effort was made to relate the model outflow to withdrawals from the aquifer represented by current pumping. These withdrawals are greater than the recharge to the aquifer, with the result that the water table is dropping. When viewed against the long period of time represented by the model, the period of time occupied by large-scale

Table 12. SBDVs from the Tucson Basin FSM.

Cell number	SBDV as a fraction of the total BDV from the cell	Amount (10^6 a-f)
1	.250	.0004
10	.870	.0061
14	.170	.0001
15	.730	.0072
16	.130	.0003
17	.350	.0021
18	.300	.0003
20	.200	.0011
26	1.000	.0218
Total		.0394

pumpage of the aquifer is almost infinitesimal and for this reason the author neglected these withdrawals when formulating his model. In the FSM, volumetric inputs were perfectly balanced by volumetric outputs.

7.8 Operation and Results

Once the initial parameters of the FSM are specified, the model is ready for operation. All cell initial states are arbitrarily zeroed, and the same set of SBRVs and SBRCs is injected into the model at the beginning of each iteration, until each cell in the FSM

reaches steady state. The steady state concentrations of C-14 were converted to decay ages using Equation (60). A C-14 half-life of 5568 years was used, in keeping with Wallick's (1973) use of this figure to calculate his adjusted ages. The agreement between observed and calculated ages is checked, and if poor, adjustments are made in the FSM parameters and the model run again. All the different types of parameters of the FSM required adjustment at one time or another. In the process of calibration, the author found it necessary to add, delete, or consolidate cells. And since the writer's initial models were two-dimensional network FSMs, at one point it was necessary to reconstruct the model into its present three-dimensional network form.

Once the author obtained what he felt was the best possible agreement between the observed and calculated ages, the mean ages and transit times of the cells were obtained. Throughout the modeling procedure, the author used the simple mixing cell algorithm. However, once the best agreement was effected, the author operated the FSM using the modified mixing cell algorithm in order to observe the differences between the ages using the two different algorithms. The mean ages and transit time approximations were also determined using the MMC algorithm. Table 13 contains all the results of the simulation, including information on approximately how long it took for each cell

Table 13. Observed decay ages and simulation results for the Tucson Basin FSM.

Cell number	Observed decay age[a] (years)	Calculated decay age (years)		Mean age of water (years)		Approximate time to reach steady state (years)
		SMC	MMC	SMC	MMC	
1	-	2336	2335	3018	3017	38000
2	-	2588	2587	3253	3252	42000
3	-	4163	4162	5166	5165	36000
4	-	2463	2462	2895	2894	32000
5	-	2516	2515	2897	2896	26000
6	-	5263	5263	6346	6345	37000
7	-	6109	6109	7879	7878	42000
8	-	8918	8917	13255	13254	50000
9	-	8538	8537	14358	14357	50000
10	-	171	170	172	171	2000
11	0	95	95	96	95	2000
12	-	175	175	177	176	3000
13	-	191	190	193	192	3000
14	1848	1759	1758	2258	2257	33000
15	161	276	275	278	277	3000
16	-	1333	1332	1668	1667	39000
17	1281	1035	1034	1282	1281	42000
18	3018	3131	3130	4090	4089	42000
19	3598,3680	3379	3378	4834	4833	42000
20	639	854	853	1078	1077	30000
21	0	296	295	362	361	25000
22	0	421	420	523	522	26000
23	0	367	366	471	470	37000
24	4176	4208	4207	6201	6200	45000
25	0	179	178	202	201	21000
26	1841	635	634	900	899	40000

[a]Raw decay age obtained by Bennett (1965) and adjusted by Wallick (1973). Adjusted age given.

to attain steady state. The C-14 ages can be interpreted as the ages as of 1950, in keeping with the convention Wallick (1973) used to report his adjusted ages.

7.9 Discussion

7.9.1 Observed and Calculated Decay Ages

With the exception of cell 26, the agreements between the observed and calculated decay ages are very good. The excellent agreement between the decay ages in cells 11, 15, 21, 22, 23, and 25 is not apparent until one considers that because of cumulative sampling, analytical and computational errors, any C-14 decay age of 500 years or less can be considered to be of age zero (Long, 1975). Wallick (1973) suspected that the zero decay ages in cells 21, 22, 23, and 25 indicated that the waters from which these samples were taken were recharged after 1954, and suggested that the samples be analyzed for the presence of bomb tritium. The presence of bomb tritium in these samples would confirm the post-1954 recharge hypothesis. The poor agreement between the ages in cell 26 may indicate that this cell should receive direct recharge from outside the FSM.

In addition to bomb tritium, sampling should also be done for silicon-32 in the cells with decay ages on the order of 1000 years or less. Those cells with very young decay ages might also be sampled for the presence of

fluorocarbons (Thompson et al., 1974), which might aid in determining the age of the water in these cells. More C-14 ages should also be obtained, especially for the cells in the lower tier of the FSM, although observed ages should be obtained for all cells which are not presently represented by an observed C-14 decay age.

7.9.2 Mean Age Numbers

With the exception of cell 11, the calculated decay age in each cell is less than the mean age of the water, regardless of the mixing algorithm. This was expected, since each cell in the FSM is relatively well-mixed, even in the case of the MMC. In the upper tier boundary cells the differences between the mean ages and calculated decay ages are generally slight, and in cell 11 the decay age is greater than the mean age by one year in the SMC case and equal to it in the MMC case. This could indicate a lesser degree of mixing in this cell, or it may be an anomalous result. The difference of one year in the case of the SMC is so small as to be insignificant.

7.9.3 SMC and MMC Algorithms

Table 13 indicates that there is very little difference between the two algorithms. This was to be expected in the case of the mean age numbers. The SMC mean age number of each cell is exactly one year greater than its MMC counterpart. Such a uniform difference can be

predicted by noting the expansion effect of the SMC algorithm, which increases the average residence time of the cell by a factor of one over the MMC average residence time (see Equations [50] and [51]). This increase in the average residence times is reflected in the mean age numbers.

The remarkable agreement between the SMC and MMC decay ages in each cell is perhaps more surprising. In 23 cells, the SMC decay age is exactly one year greater than the MMC decay age, whereas in cells 6, 7, and 11 the two ages are identical. Several reasons may be responsible for this. The first reason may have to do with the expansion effect of the SMC as discussed in the preceding paragraph. The second reason may be the fact that the cell BRVs are generally small compared to the cell effective volumes (see Table 8). In Section 3.5.2 it was stated that as the BRV becomes small relative to the effective volume of the cell, the MMC algorithm approaches the perfect mixing regime of the SMC. This effect is undoubtedly occurring here, although the agreement between the two algorithms is just as good in cell 21, where the BRV is greater than 10 per cent of VOL. Agreement is also excellent in cells 22, 23, and 25 where the BRVs range between 5.39 and 9 per cent of VOL. The third factor may be the fact that in a steady state FSM such as this, in which a great number of iterations are required to attain steady state, the steady state

concentrations are virtually independent of the algorithm used. The author believes that all three factors are involved in the exceptional agreements between the SMC and MMC calculated decay ages for the cells. The first two factors are perhaps the most important. It would appear that a quantitative investigation is warranted into the conditions under which the MMC algorithm approaches the SMC algorithm. For example, it would be useful to know just how small BRV/VOL must be before the MMC behaves in the same manner as the SMC.

7.10 Interpretations of the Model

If one starts on the north, east, or south sides of the FSM and moves toward the center of the model, there is a general tendency for the ages, both decay ages and mean ages, to increase. This is especially true for the mean ages of the water. The increases in age are logical, since the recharge areas are located mainly around the model periphery and the recharge water must travel farther to reach the central parts of the FSM. This pattern of increasing age as one moves toward the center of the model is disrupted somewhat if one starts on the west side of the area at cell 10 (the Santa Cruz River) and moves toward the center. The ages increase sharply in cells 19 and 24, then decrease slightly as one moves past these cells. In fact, the oldest ages in the upper tier of cells are found

in cells 19 and 24, both of which border cell 10. From this observation, one would suspect that the Santa Cruz River is not effective in recharging the aquifer in the interior of the study area. The FSM was designed to minimize recharge from the Santa Cruz River to this portion of the aquifer, and the rationale behind this were the very old observed decay ages in cells 19 and 24. Only 2 per cent of cell 10's BDV goes to cell 19, and the same amount is discharged to cell 24. Fully 87 per cent of cell 10's BDV is discharged outside the system. The current Santa Cruz River may recharge more water to the aquifer in the central portion of the study area than is depicted by the FSM, so one might question the author's logic in assigning such a small amount of recharge to this part of the aquifer from cell 10. However, ground-water flow in cell 10 appears to have paralleled the bed of the Santa Cruz (Anderson, 1972, Plate 3; Davidson, 1973, Plate 1). It is possible that the author assigned too much aquifer recharge to cell 10, since as recently as 90 years ago, the Santa Cruz River in the area was essentially a perennial stream (Hastings and Turner, 1965, p. 1), and therefore recharged little, if any, of its water to the aquifer. The aquifer may have contributed base flow to the river, although this base flow was not specifically included in the model. Conceivably, the SBDV from cell 14 could be construed as base flow to the Santa Cruz River, as could part of the SBDV from

cell 26. The question of whether or not the Santa Cruz River is recharging the aquifer in the central part of the study area might be resolved by sampling for tritium and perhaps silicon-32 and fluorocarbons in the cells bordering cell 10. If one accepts the FSM as a valid representation of the system, then averaged over the lifetime of the model, about 50,000 years, the Santa Cruz River at Tucson has not contributed a large amount of recharge to the aquifer in the interior of the study area. Unlike the Santa Cruz River, the FSM indicates that Rillito Creek (cell 11), Tanque Verde Creek (cell 12) and Pantano Wash (cell 13) are reasonably effective in recharging the interior regions of the aquifer in the study area.

The FSM also provides an estimate of the long-term average annual recharge to the portion of the aquifer modeled. This is simply the sum of the SBRVs recharging the model at each iteration, or slightly less than 40,000 acre-feet.

The FSM also provides some insight into the vertical movement of ground water in the study area. At each iteration (year), a total of 3100 acre-feet of water is moving from the lower tier of cells to the upper tier, an amount that is less than 8 per cent of the total flow moving among the cell network during each year. The total amount of water moving down from the upper tier of cells to the lower tier of cells is about 1400 acre-feet per year, so

only about 11 per cent of the total flow during a given year is moving in the vertical plane. As previously mentioned, without incorporating this three-dimensional flow, the author was unable to obtain an acceptable agreement between the calculated and observed decay ages.

7.11 Assumptions

The author made numerous assumptions in the Tucson Basin FSM. For example, he assumed that within a given cell, the hydrologic properties were constant and identical throughout the entire cell. The SMC algorithm assumed that perfect mixing occurred in each cell during an iteration, which was equal to a period of one year. The MMC mixing algorithm assumed that piston flow occurred in each cell, although in almost all cells, the piston flow process approached one of perfect mixing. The author also assumed that the FSM flow distribution was a good approximation of the real-world distribution. The vertical flow distribution and the flow distribution among the cells of the lower tier represent the most tenuous portions of the flow distribution assumption. However, the major assumption of the model is that the hydrologic conditions represented by the model have been constant for the lifetime of the model, about 50,000 years. The hydrologic regime of the Tucson Basin has probably changed during the past 50,000 years. Yet despite this fact, the Tucson Basin FSM seems to work

quite well, perhaps because it is representative of the "average" hydrologic conditions during the past 50,000 years. In light of the good performance of the FSM, the assumption of long-term hydrologic constancy, as well as all other assumptions which the author has mentioned or not, appear to have some validity.

7.12 Concluding Remarks

The FSM presented in this chapter is not an end, but a beginning. The author believes that his model demonstrates the capability of finite-state models to account for age distributions of a radioactive tracer in an aquifer, and in doing so, provide useful information on the aquifer. Age distributions reflect amounts of substances, and a FSM can model the transport of any kind of mass, radioactive or not. But the FSM seems particularly well-suited to modeling the distribution of radioactive tracers, and it can do so in three dimensions, something most other models may find difficult to do.

The model should be validated by collecting C-14 ages from those cells not represented by C-14 ages. Information on the distributions of other substances such as tritium, silicon-32 and fluorocarbons could prove useful in validating the model or serving as cross-checks on some of the younger C-14 decay ages.

Investigation into three-dimensional flow in the study area is also required, so that the FSM's portrayal of vertical flow in the area can be verified or refuted. The FSM could be used as a guide in identifying those areas in which the investigations should be conducted. Information regarding the three-dimensional nature of the flow in the study area as well as the nature of the flow at great depths would also be useful in efficiently managing and exploiting the ground-water resources of the area. Consideration might also be given to constructing a three-dimensional flow model of the area. Since existing PDE-based three-dimensional flow models require very large computers and can be expensive to run when a large enough computer is found, a FSM hydraulic model might be built. Such a hydraulic model would provide the modeler with an output which could be readily adapted to serve as the input to a FSM mass transport model.

CHAPTER 8

A FINITE-STATE MODEL OF TRITIUM MOVEMENT IN THE EDWARDS LIMESTONE AQUIFER

8.1 Introduction

In this chapter, the author will describe a finite-state model depicting the movement of tritium pulses through the Edwards Limestone Aquifer of south-central Texas. Unlike the FSM described in Chapter 7, this model is a two-dimensional non-steady flow FSM. Both models, however, are steady volume FSMs. The "initial guess" for this model was a 29-cell, steady flow FSM provided by Pearson (1974), who also provided the initial and boundary conditions for the model. In the course of his work, the author found it necessary to change the regime to non-steady flow, as well as to alter the cell network and the accompanying initial and boundary conditions.

8.2 Geohydrology of the Edwards Limestone Aquifer

The Edwards Limestone Aquifer, located in south-central Texas, lies within two physiographic sections: the Edwards Plateau to the north and northwest and the West Gulf Coastal Plain to the south and southwest (see Figure 11). The Balcones Escarpment, a fault scarp in the Balcones fault zone, separates these two sections.

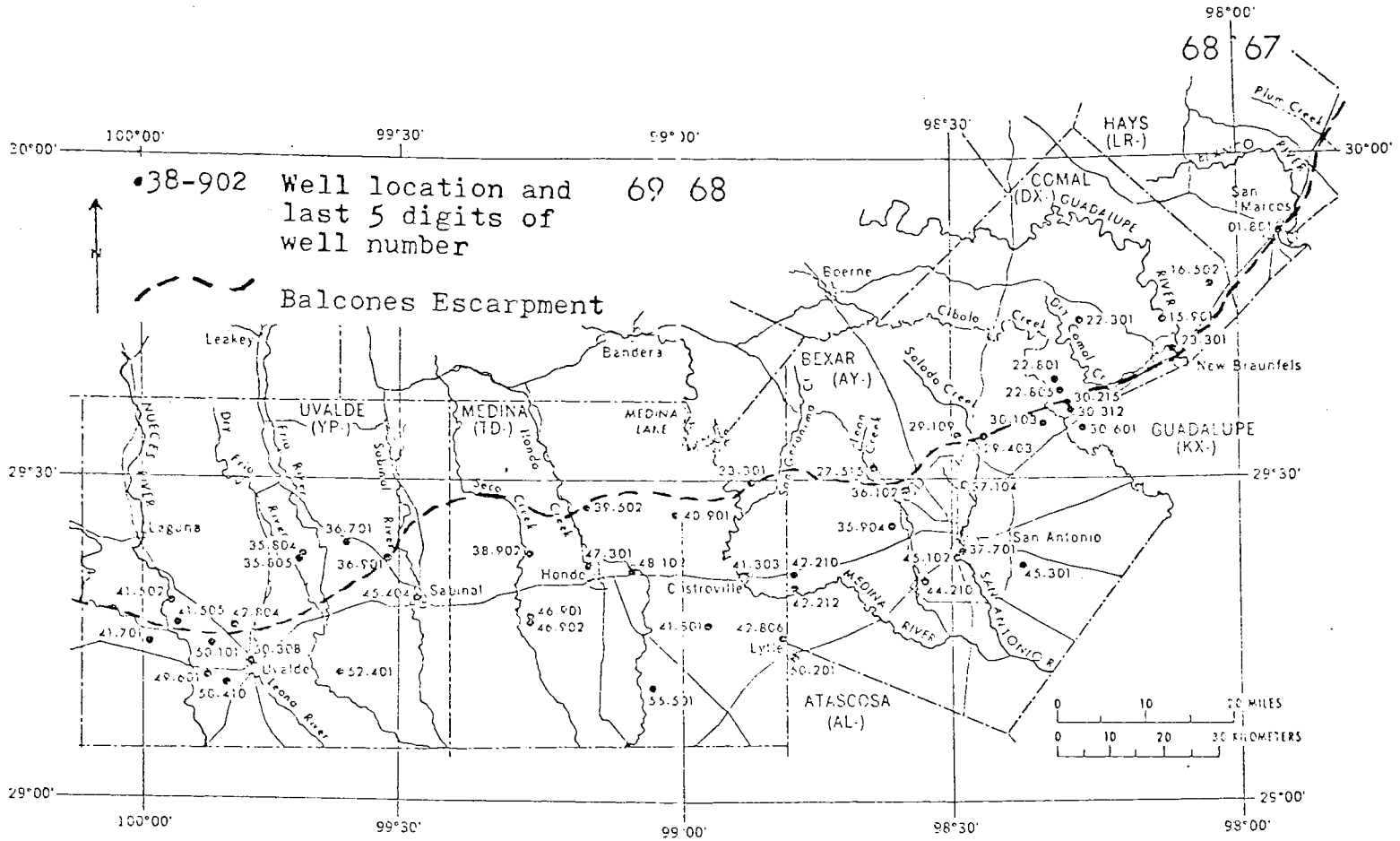

Figure 11. Map of the Edwards Aquifer area.

In the study area, the Edwards Aquifer is actually composed of the Edwards Limestone and several other limestone formations. Since all these limestones behave as a single aquifer, the entire unit is referred to as the Edwards and associated limestones or simply, the Edwards Aquifer.

In outcrop, the rocks of the Edwards Aquifer are dense, hard, crystalline limestones, though upon weathering they become extensively honeycombed and cavernous (Garza, 1968). As is typical of karst aquifers, most of the water in the Edwards Aquifer is transmitted via solution channels and open fractures. The quantitative analysis of the flow in the Edwards Aquifer is complicated by its high degree of anisotropy and inhomogeneity and the fact that in some of the large cavities and fractures, the flow of ground water may approach turbulent or at least nonlinear laminar flow, both of which can be termed non-Darcian flow. Therefore, the use of the usual linear transport equations, which demand Darcian flow, may prove fruitless in the case of the Edwards Aquifer.

Recharge to the Edwards Aquifer is accomplished partly by direct infiltration of precipitation on the outcrop of the aquifer at the Balcones fault zone (Garza, 1968), and partly by seepage losses from streams as they cross the fault zone. These streams are fed by base flow from the aquifer on the Edwards Plateau (Pearson, Rettman,

and Wyerman, 1974). Infiltration to the aquifer in the Balcones fault zone is relatively quick because of the highly fractured nature of the aquifer.

The thickness of the Edwards Aquifer is not everywhere known, though it appears to have an average thickness of about 500 feet (Garza, 1968). South of the Balcones Escarpment, the Edwards Aquifer is confined, whereas north of the escarpment, on the Edwards Plateau, the Edwards Aquifer is unconfined.

For more detailed descriptions of the hydrology of the Edwards Aquifer, the reader is referred to Pettit and George (1956), Garza (1962, 1966, 1968), and Abbott (1975).

8.3 Tritium Data

The tritium data were provided to the author by Pearson (1974). The data are in the form of time series of tritium concentrations in selected wells in the area. The time series themselves consist of annual or semi-annual measurements from as early as 1963 in some cases to as late as 1971. The author was also provided information as to which wells represented which cells in the FSM, and the initial states of tritium in the cells prior to the introduction of thermonuclear bomb tritium in 1954. Pearson (1974) also provided the author with the tritium inputs to the model, and these will be discussed in more detail in a later section.

8.4 Cell Locations and Effective Volumes

Pearson (1974) provided the writer with his estimate of cell locations, effective porosities and effective volumes. The writer found it necessary to increase the number of cells from 29 to 31 and to alter the effective volumes of the cells by adjusting the effective porosities. Figure 12 shows the cell network of the author, and Table 14 shows the effective volumes and porosities, all obtained by the author in the calibration process.

Cells 1 through 9 are located in the unconfined portion of the aquifer, and with the exception of cell 9, these cells receive inputs from outside the system. Cells 10 through 31 are located in the confined part of the aquifer. The thicknesses of cells 1 through 9 ranged from a low of about 200 feet to a high of about 400 feet, while the thicknesses of the remaining cells averaged approximately 500 feet. A suitable URV was found to be one cubic kilometer.

8.5 Flow Distribution

The original flow distribution was obtained from Pearson (1974) and was subsequently modified by the author during the process of calibration. How this flow distribution was obtained will be explained in more detail in a later section. Table 15 lists the flow distribution obtained by the author.

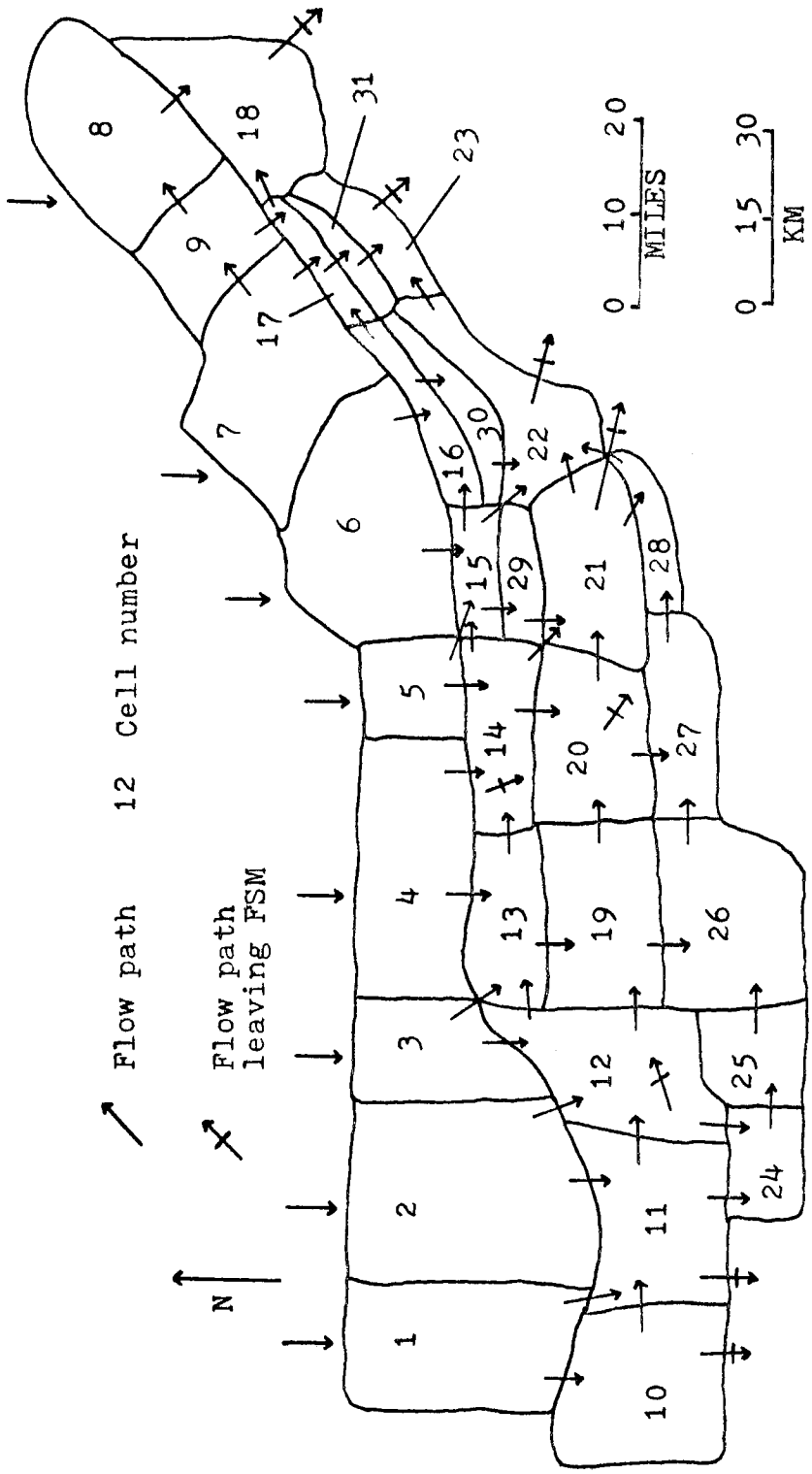

Figure 12. The Edwards Aquifer FSM.

Table 14. Effective volumes (VOL) and effective porosities (EP) of the cells in the Edwards Aquifer FSM.

Cell number	VOL (km^3)	EP
1	2.000	.024
2	3.250	.051
3	1.000	.069
4	3.100	.053
5	.375	.084
6	1.173	.040
7	.850	.043
8	.977	.050
9	.300	.040
10	2.080	.024
11	3.250	.086
12	3.400	.064
13	1.650	.048
14	3.600	.075
15	1.070	.040
16	.878	.050
17	.400	.070
18	1.150	.083
19	2.100	.048
20	2.000	.045
21	2.000	.055
22	2.250	.061
23	.780	.093
24	.828	.040
25	1.754	.040
26	3.507	.040
27	1.094	.040
28	.691	.050
29	.950	.036
30	.800	.046
31	.280	.070
Total	49.537	

Table 15. Flow distribution within the Edwards Aquifer FSM.

Output cell	Input cell	Flow as fraction of total BDV of output cell[a]
1	10	.650
1	11	.350
10	11	.910
2	11	.500
2	12	.500
11	12	.600
11	24	.280
3	12	.500
3	13	.500
12	24	.453
12	13	.100
12	19	.360
24	25	1.000
4	13	.500
4	14	.500
13	14	.300
13	19	.700
19	20	.900
19	26	.100
25	26	1.000
5	15	.650
5	14	.350
14	15	.200
14	20	.330
14	21	.450
20	27	.093
26	27	1.000
20	21	.870
6	15	.500
6	16	.500
15	16	.450
15	29	.350
29	21	1.000
15	22	.200
21	22	.700
21	28	.100
27	28	1.000
16	17	.550
16	30	.450
30	22	1.000
28	22	1.000
7	17	.450
7	9	.550
9	17	.500

Table 15.--Continued

Output cell	Input cell	Flow as fraction of total BDV of output cell[a]
17	31	.400
22	23	.500
9	8	.500
8	18	1.000
17	18	.600
31	23	1.000

[a]The sum of all fractions from a given output cell equals unity, except where that cell discharges to the FSM boundary, in which case the difference is accounted for by such discharge. For example, in the case of cell 4, .500 + .500 = 1.000. In the case of cell 14, .200 + .330 + .450 = .980, and .020 is discharged to the boundary.

8.6 Inputs and Outputs

8.6.1 Volumetric Inputs

Cells 1 through 8 are the only cells receiving inputs from outside the FSM. Each of these cells corresponds to a river basin located on the Edwards Plateau, and Table 16 shows these basins along with the 1934-1970 and 1934-1952 average annual recharge to the aquifer from these basins.

The SBRVs to each of the eight recharge cells were assigned using information from Garza (1966, Table 3). Pearson (1974) suggested using the 1934-1970 average annual recharge data and injecting the average value into the appropriate recharge cell at each iteration, thus producing a steady flow FSM. However, the author found this approach unfeasible and thus resorted to a non-steady flow FSM by using the yearly recharge values instead of the 1934-1970 average values. Table 17 shows the yearly SBRVs to each of the eight recharge cells for the years 1953 through 1971, and the total recharge for each year.

8.6.2 Tritium Inputs

The SBRCs for each of the eight recharge cells were provided by Pearson (1974). In any given year, the same SBRC was injected into each of the recharge cells, although the values of these SBRCs changed from year to year (Table 18). The yearly SBRCs are the average concentration of tritium in the precipitation for a particular year. Since

Table 16. Cells receiving SBRVs, the river basins represented by the cells, and the 1934-1952 and 1934-1970 average annual recharge for the Edwards Aquifer FSM.

Cell number	River basin	Average annual recharge (km^3)	
		1934-1952	1934-1970
1	Nueces and West Nueces Rivers	.1139	.1190
2	Frio and Dry Frio Rivers	.0903	.1080
3	Sabinal River	.0296	.0400
4	Seco and Hondo Creeks	.0789	.0900
5	Medina River	.0585	.0630
6	San Geronimo, Salado and Leon Creeks	.0693	.0700
7	Cibolo and Dry Comal Creeks	.1047	.1120
8	Blanco River and Plum Creek	.0348	.0400
	Annual totals	.5800	.6420

Table 17. 1953-1971 SBRVs in cubic kilometers for the Edwards Aquifer FSM.

Year	Cell 1	2	3	4	5	6	7	8	Total
1953	.0264	.0186	.0039	.0054	.0446	.0248	.0522	.0307	.2066
1954	.0756	.0390	.0088	.0147	.0312	.0052	.0109	.0132	.1986
1955	.1580	.0273	.0007	.0095	.0204	.0053	.0041	.0117	.2370
1956	.0193	.0052	.0020	.0044	.0078	.0025	.0027	.0101	.0540
1957	.1340	.1650	.0817	.1598	.0686	.2165	.4920	.0943	1.4119
1958	.3290	.3700	.2760	.3640	.1178	.2350	.3320	.0872	2.1110
1959	.1354	.1960	.0760	.1193	.1168	.0708	.0960	.0415	.8518
1960	.1095	.1580	.0810	.1568	.1284	.1105	.1975	.0770	1.0187
1961	.1050	.1868	.0708	.1300	.1090	.0855	.1370	.0610	.8851
1962	.0585	.0575	.0053	.0290	.0707	.0206	.0305	.0357	.3078
1963	.0490	.0333	.0062	.0127	.0517	.0115	.0263	.0200	.2107
1964	.1555	.0680	.0201	.0756	.0535	.0442	.0630	.0274	.5073
1965	.1210	.1025	.0286	.1283	.0674	.0972	.1425	.0823	.7698
1966	.2090	.1652	.0465	.0965	.0623	.0500	.0820	.0427	.7542
1967	.1015	.1700	.0375	.0802	.0551	.0373	.0707	.0234	.5757
1968	.1610	.2170	.0820	.2450	.0740	.1025	.1485	.0608	1.0908
1969	.1480	.1400	.0379	.1038	.0671	.0742	.1232	.0575	.7517
1970	.1390	.1750	.0437	.1005	.0840	.0850	.1400	.0487	.8159
1971	.3250	.2620	.0484	.1920	.0848	.1003	.1018	.0274	1.1417

Table 18. 1953-1971 SBRCs for the Edwards Aquifer FSM.

Year	SBRC (TU)
1953	10.440
1954	100.580
1955	20.700
1956	55.070
1957	48.230
1958	160.140
1959	165.090
1960	56.490
1961	108.910
1962	472.670
1963	864.920
1964	386.670
1965	227.960
1966	156.470
1967	76.810
1968	75.550
1969	86.140
1970	68.690
1971	50.170

part of the aquifer recharge is from stream infiltration, the tacit assumption was made that the average tritium concentration of the streamflow in any given year equalled the concentration of tritium in the precipitation of that year. This assumption was necessary since the tritium concentration of the streamflow crossing the Edwards Plateau is not well known. However, there is reason to believe that the tritium concentrations of these streams approximate the tritium in the precipitation, suggesting that there is no lengthy delay from the time the tritium enters the unconfined portion of the aquifer on the Edwards Plateau to the time it appears in the baseflow of streams and is recharged to the confined portion of the aquifer as the streams cross the Balcones fault zone (Pearson et al., 1974).

The tritium SBRCs are those of the precipitation at Waco, Texas, located about 170 miles northeast of San Antonio, the only major city in the study area. There are no records of tritium concentrations in precipitation at San Antonio or anywhere else in the study area. The SBRCs for 1961 and later years are direct measurements, while those prior to 1961 were obtained by correlating the existing Waco data with those of Ottawa, Ontario, Canada, the location with the longest record in North America (Pearson et al., 1974). No measurements had been made at Waco prior to 1961.

8.6.3 Volumetric Outputs

The author had virtually no leeway in designating which cells discharged SBDVs and the amounts discharged. Since the model covered such a short period of time and during this time there were large withdrawals from the aquifer, it was necessary to have the model account for the distribution of these withdrawals in space. Some of these withdrawals were in the form of springflow, and others were in the form of pumpage, mainly by the City of San Antonio and other governmental organizations. Pearson (1974) supplied the author with a list of discharging cells, and the amount each of these cells should discharge in order to match the 1934-1970 average annual withdrawals from the Edwards Aquifer. The proper flow distribution was obtained by adjusting the author's FSM until it reproduced the observed average annual 1934-1970 withdrawals from the aquifer. The FSM in this case was a steady flow FSM, since the recharge inputs to the model were the 1934-1970 average annual recharge quantities to the eight recharge cells (see Table 16). This 1934-1970 average annual recharge-discharge model will be henceforth referred to as the AARDIM. Table 19 shows the results of the AARDIM along with the observed 1934-1970 average annual discharges. The AARDIM reproduces the observed data to a good degree of accuracy, though it does not accurately duplicate the yearly discharges from the Edwards Aquifer, given the yearly

Table 19. Major areas of discharge from the Edwards Aquifer, the cells representing these areas, and the observed and AARDIM 1934-1970 average annual discharges from these areas.

Cell number	Area of discharge	1934-1970 average annual discharge (km^3)	
		Observed	AARDIM
10,11,12	Uvalde County	.042	.042
14,20	Medina County	.007	.007
21,22	Bexar County	.227	.219
23	Comal County	.238	.229
18	Hays County	.128	.145
Annual totals		.642	.642

recharge to the aquifer. The AARDIM is just what its name implies: an average model.

8.7 Operation and Results

8.7.1 Calibration and Validation

The model was programmed to start with the year 1953 and continue through the year 1971, a total of 19 iterations, since Δt was set at one year. The selection of Δt was governed by the annual nature of the data. The observed tritium concentrations from 1963 through 1969 were

used to calibrate the model, and the years 1970 and 1971 were utilized for validation purposes.

The calibration process consisted of two phases. In the first phase, the AARDIM was formulated by calibrating the FSM against the flow distribution only. Once the best possible flow distribution was obtained with the AARDIM, the second phase of the calibration process started, that of trying to get the model to reproduce the observed tritium concentrations. In this latter phase, the flow distribution of the AARDIM was altered very little so as not to disturb the excellent agreement between the observed and calculated 1934-1970 average annual discharges. The parameters varied in the second phase of calibration were primarily the effective volumes of the cells. Adjustments in the effective volumes of the cells represented changes in their effective porosities. These changes did not affect the flow distribution of the AARDIM, since in the particular FSMs used the effective volumes did not affect the flow distribution.

8.7.2 Initial Concentrations of the Cells

The initial (pre-1953) tritium concentrations of the cells in the Edwards Aquifer FSM were calculated by assuming that the system had been in a condition of steady state with respect to tritium prior to the introduction of bomb tritium in 1954. According to Pearson (1974), the natural

tritium concentration of the precipitation in the area was about 8 TU. This value was used as a SBRC for each of the eight recharge cells, and the 1934-1952 average annual recharge figures were used as SBRVs to these same cells. These quantities were injected into the model at each iteration, thus effecting a steady flow, steady volume FSM which eventually reached steady state after 350 iterations (years). The steady state tritium concentrations calculated in this manner were then used as the initial tritium concentrations of the cells at the start of 1953. The FSM was then operated for the remaining 19 years (1953-1971) using the SBRVs and SBRCs given in Tables 17 and 18. Each time the author made changes in the model, new initial tritium concentrations had to be determined, but this presented no problem. The model was programmed to run for 350 iterations as a steady flow, steady volume FSM which eventually reached steady state, and then at the 351st iteration the FSM changed to a non-steady flow, steady volume model and remained this way until the last (369th) iteration. Table 20 shows the calculated steady state or initial tritium concentrations for both the MMC and SMC algorithms.

Throughout the operation of the Edwards FSM, the author used the SMC algorithm. Once he obtained what he felt to be good agreement between the observed and calculated tritium concentrations, the author then operated the

Table 20. Calculated SMC and MMC initial (pre-1953) or steady state tritium concentrations of each cell in the Edwards Aquifer FSM.

Cell number	Calculated steady state concentrations (TU)	
	SMC	MMC
1	3.847	3.958
2	2.538	2.586
3	2.646	2.698
4	2.393	2.435
5	5.590	5.827
6	3.916	4.031
7	5.227	5.434
8	3.241	3.309
9	4.064	4.170
10	1.512	1.502
11	1.117	1.101
12	.757	.737
13	.906	.890
14	.817	.806
15	2.448	2.478
16	1.901	1.899
17	3.176	3.238
18	2.178	2.181
19	.390	.370
20	.253	.237
21	.300	.284
22	.273	.261
23	.622	.610
24	.635	.612
25	.340	.319
26	.133	.121
27	.099	.088
28	.097	.087
29	.914	.892
30	.823	.796
31	2.390	2.402

FSM once more using the MMC algorithm. Table 21 shows the observed and calculated (MMC and SMC) tritium concentrations in certain cells for the years 1963 through 1971. Only those cells for which observed tritium data were available are shown. None of these cells had observations for the entire 9 years of record. Figures 13 through 18 are graphs of tritium concentrations (observed, SMC and MMC) versus time for cells 2, 10, 12, 14, 21, and 23. Table 22 contains the cell tritium concentrations for the years prior to the start of sampling in 1963, and Table 23 contains the same information through 1971 for those cells not included in the sampling program.

8.8 Discussion

8.8.1 SMC and MMC Initial Tritium Concentrations

Based on the remarkable agreements he obtained between the SMC and MMC steady state concentrations as reflected in the decay ages of the Tucson Basin C-14 FSM, the author suggested in Section 7.9.3 that perhaps the steady state concentrations for such an FSM might be virtually independent of the mixing algorithm. This suggestion was based upon the observation that even in cells in which the BRV was 9 or 10 per cent of VOL, the SMC and MMC decay ages were still within one year of each other. This hypothesis can be tested in another model, the present

Table 21. Observed and calculated tritium concentrations in selected cells of the Edwards Aquifer FSM, 1963-1971.

Cell		Tritium concentration (TU)								
		1963	1964	1965	1966	1967	1968	1969	1970	1971
2	Obs.	-	-	-	-	53.2	48.0	45.4	89.6	30.1
	SMC	40.9	45.3	48.1	50.4	48.9	47.8	46.7	45.2	43.0
	MMC	42.8	47.3	50.1	52.4	50.7	49.5	48.3	46.7	44.4
4	Obs.	-	-	-	-	-	-	40.4	40.7	-
	SMC	29.9	36.3	41.5	45.5	41.0	41.1	40.3	38.9	37.4
	MMC	31.6	38.0	43.4	44.3	42.7	42.8	41.8	40.3	38.7
10	Obs.	10.2	18.9	-	-	22.1	18.0	19.8	20.1	21.0
	SMC	7.5	10.5	12.6	16.5	17.6	19.4	20.8	21.7	24.3
	MMC	5.9	8.3	10.6	14.8	16.3	18.7	20.3	21.5	25.1
11	Obs.	-	-	-	-	16.6	13.7	11.1	15.2	9.3
	SMC	6.0	7.4	8.6	11.1	12.3	14.0	14.9	15.8	17.9
	MMC	4.7	5.8	7.1	9.6	11.1	13.1	14.2	15.3	17.9
12	Obs.	4.3	6.5	-	-	8.5	8.0	12.3	13.0	11.5
	SMC	5.4	5.7	6.3	7.5	8.4	9.9	10.4	11.1	12.4
	MMC	4.1	4.4	5.0	6.2	7.3	9.0	9.6	10.5	11.8
14	Obs.	5.6	6.7	-	-	8.5	10.3	9.9	11.2	-
	SMC	6.6	7.6	9.0	10.1	10.7	12.0	12.5	13.0	13.6
	MMC	5.1	6.2	7.8	9.1	9.9	11.5	12.2	12.8	13.5
15	Obs.	-	-	-	-	45.8	-	44.4	42.8	-
	SMC	27.2	31.8	37.7	41.2	42.8	44.4	45.1	45.6	44.9
	MMC	23.1	28.6	36.2	41.2	44.0	46.9	48.1	49.1	48.6

Table 21.--Continued Observed and calculated tritium concentrations in selected cells of the Edwards Aquifer FSM, 1963-1971.

Cell		Tritium concentration (TU)								
		1963	1964	1965	1966	1967	1968	1969	1970	1971
17	Obs.	-	-	-	-	39.3	60.0	-	54.2	-
	SMC	27.8	30.8	39.8	42.9	44.5	47.7	49.2	49.8	47.8
	MMC	29.7	32.0	41.6	45.6	47.9	53.0	54.7	55.4	52.3
18	Obs.	-	34.2	-	-	33.5	30.7	32.5	32.6	26.1
	SMC	14.8	16.3	22.0	24.2	25.2	28.5	30.6	32.3	32.7
	MMC	11.6	13.4	19.0	21.9	23.3	27.8	30.7	33.1	34.0
20	Obs.	-	-	-	-	1.7	2.7	2.0	1.9	2.4
	SMC	.9	1.0	1.1	1.3	1.4	1.9	2.1	2.3	2.8
	MMC	.4	.5	.6	.7	.8	1.2	1.4	1.6	2.0
21	Obs.	1.2	1.6	-	-	1.7	1.3	2.2	1.9	1.9
	SMC	.9	1.0	1.2	1.4	1.6	2.1	2.3	2.6	3.0
	MMC	.5	.6	.7	.9	1.0	1.4	1.6	1.9	2.3
22	Obs.	.6	.5	-	-	2.9	4.6	.5	.6	5.4
	SMC	1.0	1.1	1.3	1.4	1.5	1.9	2.1	2.3	2.5
	MMC	.6	.7	.9	1.0	1.1	1.5	1.7	1.9	2.1
23	Obs.	2.0	2.6	-	-	6.2	6.3	4.4	5.3	6.7
	SMC	2.6	2.7	3.4	3.5	3.6	4.3	5.0	5.7	5.7
	MMC	1.4	1.6	2.2	2.4	2.6	3.4	4.2	5.1	5.2
29	Obs.	-	-	-	-	-	-	-	-	13.9
	SMC	3.9	4.4	5.5	6.3	6.9	8.4	9.3	10.3	11.5
	MMC	2.5	2.9	3.8	4.5	5.2	6.8	7.8	9.1	10.5

Table 21.--Continued Observed and calculated tritium concentrations in selected cells of the Edwards Aquifer FSM, 1963-1971.

Cell		Tritium concentration (TU)								
		1963	1964	1965	1966	1967	1968	1969	1970	1971
30	Obs.	-	-	-	-	-	-	6.1	5.4	-
	SMC	2.6	2.7	3.3	3.6	3.8	4.7	5.3	6.0	6.9
	MMC	1.5	1.6	2.0	2.2	2.5	3.2	3.7	4.5	5.4

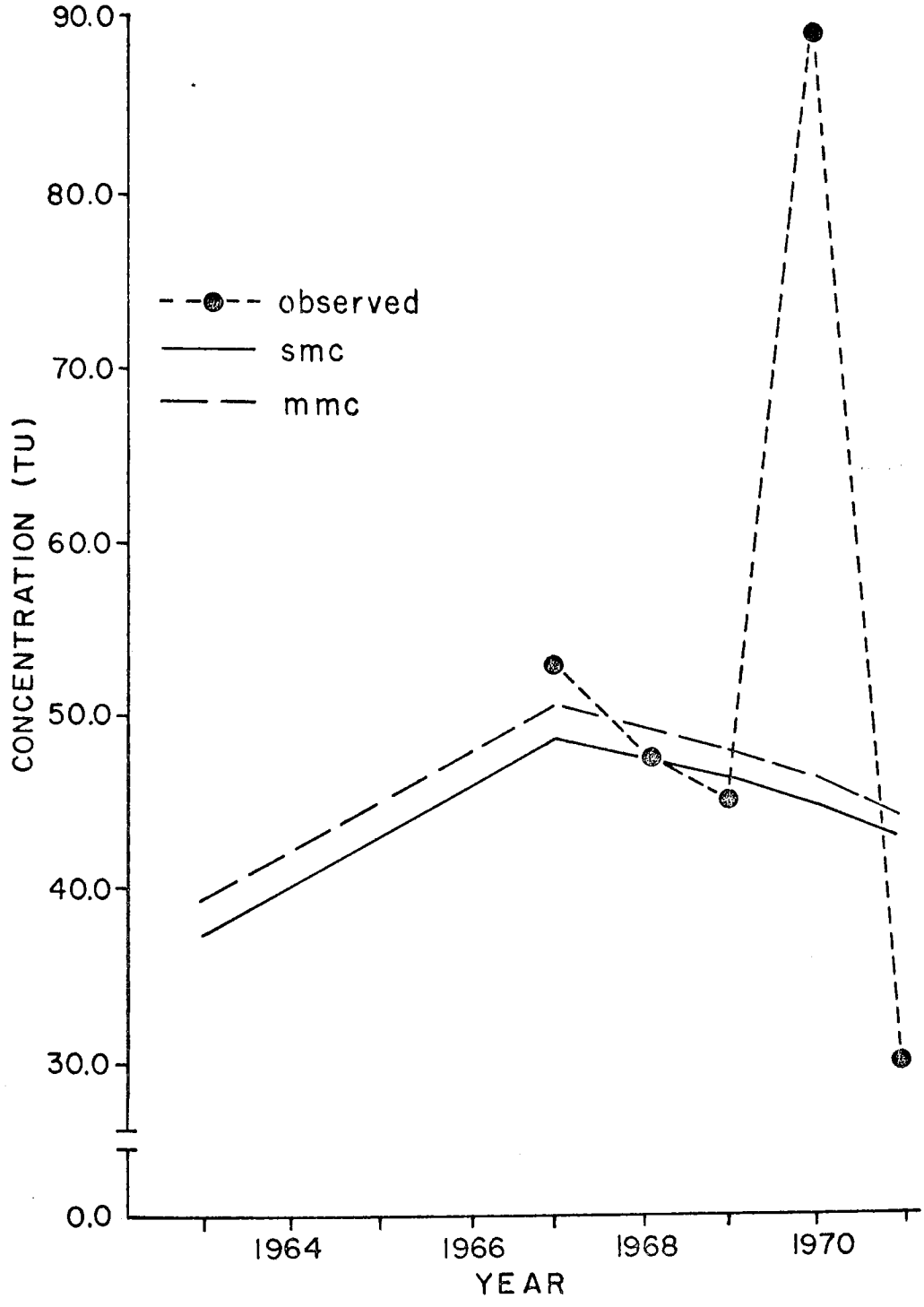

Figure 13. 1963-1971 tritium concentrations in cell 2 of the Edwards Aquifer FSM.

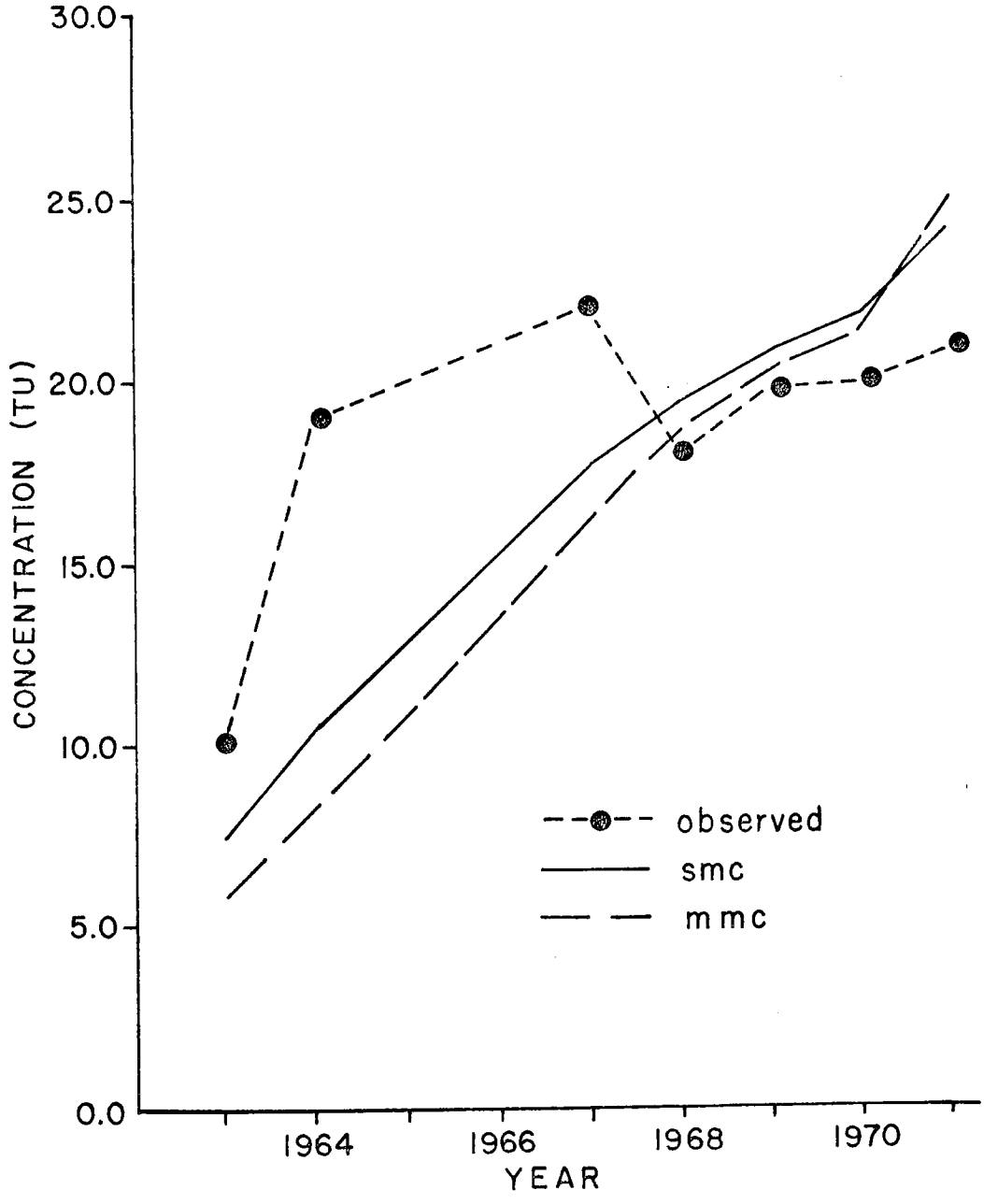

Figure 14. 1963-1971 tritium concentrations in cell 10 of the Edwards Aquifer FSM.

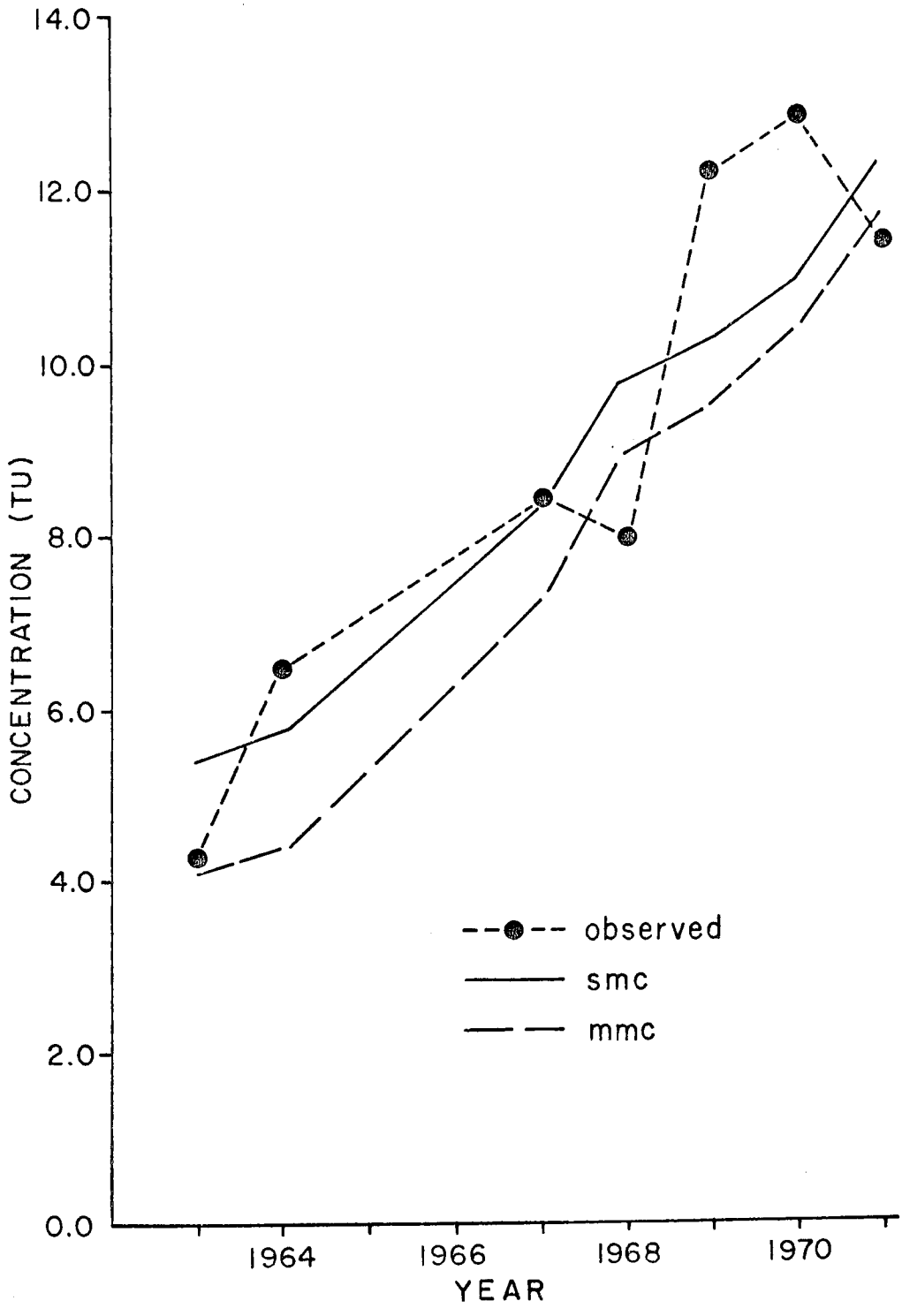

Figure 15. 1963-1971 tritium concentrations in cell 12 of the Edwards Aquifer FSM.

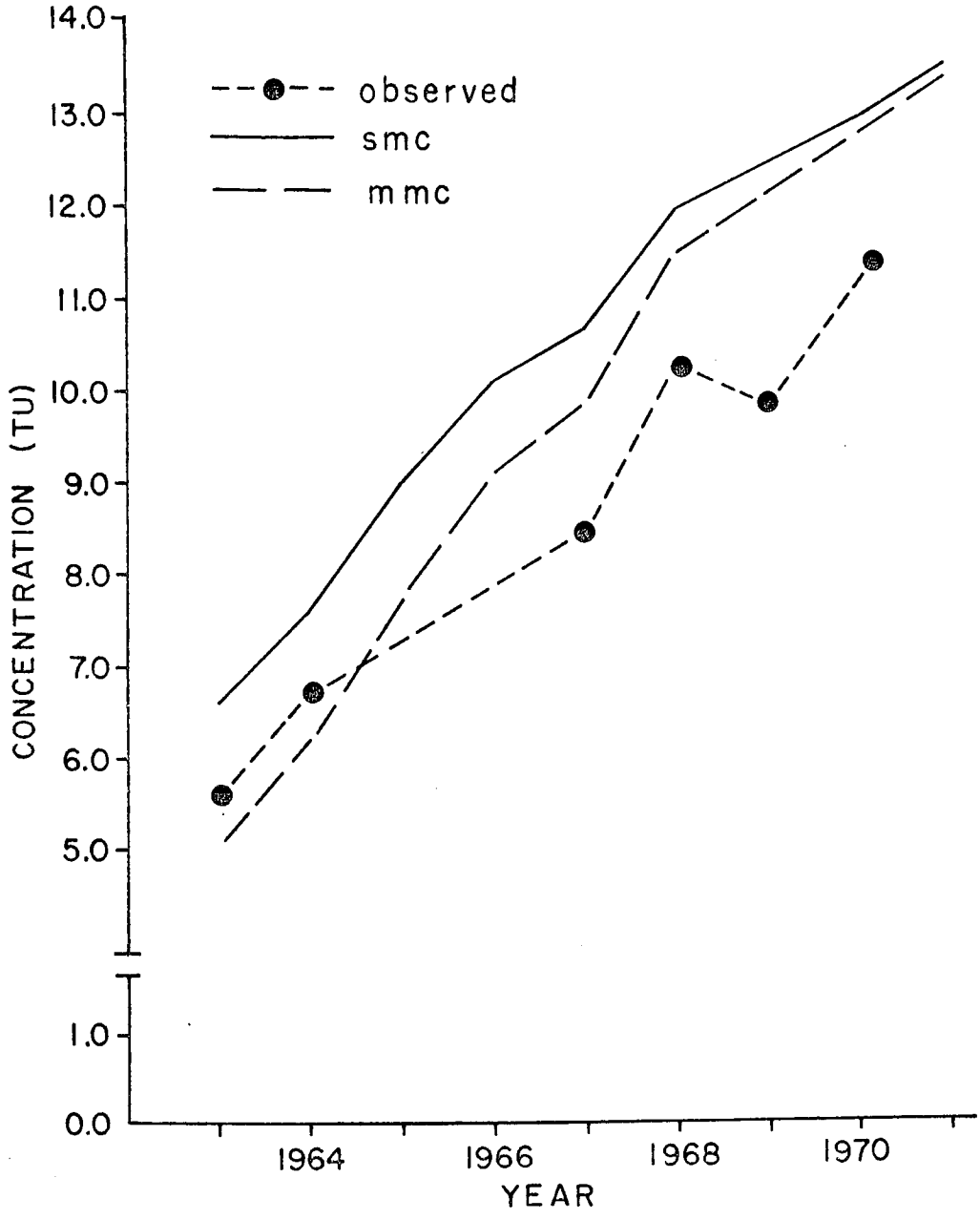

Figure 16. 1963-1971 tritium concentrations in cell 14 of the Edwards Aquifer FSM.

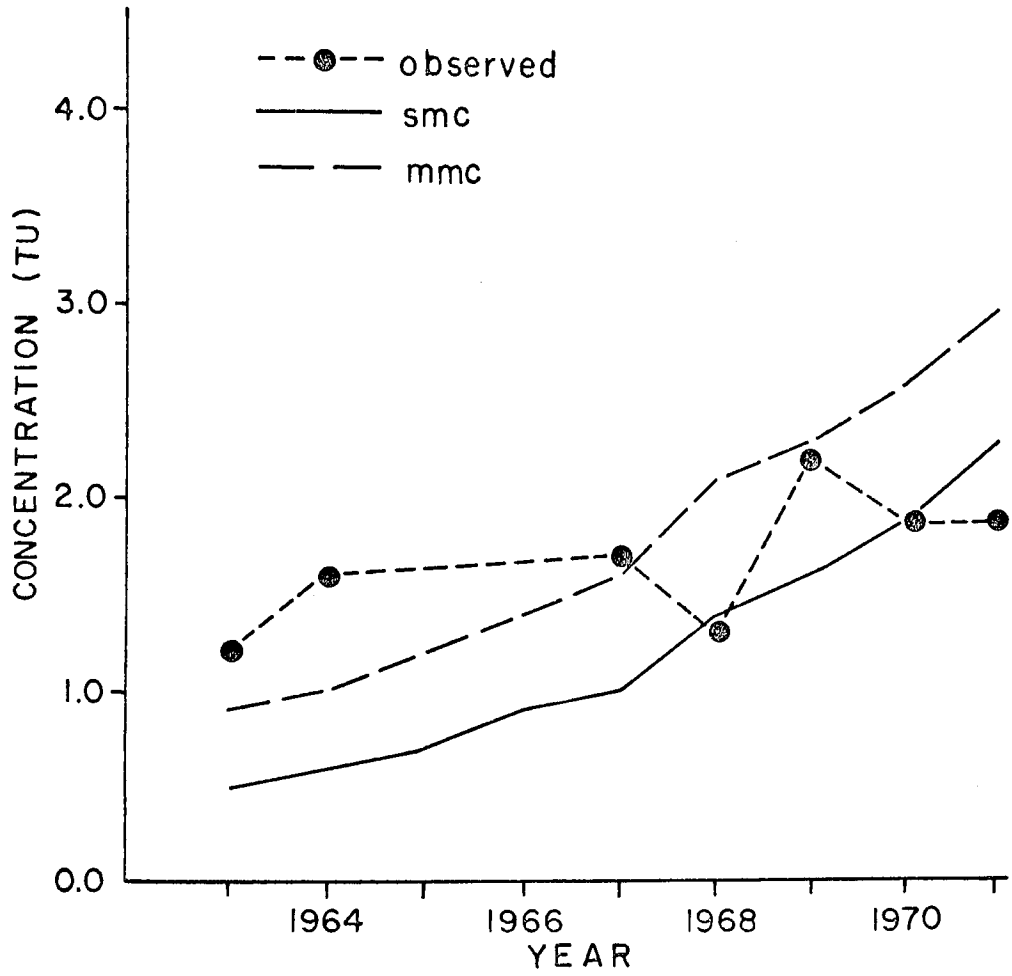

Figure 17, 1963-1971 tritium concentrations in cell 21 of the Edwards Aquifer FSM.

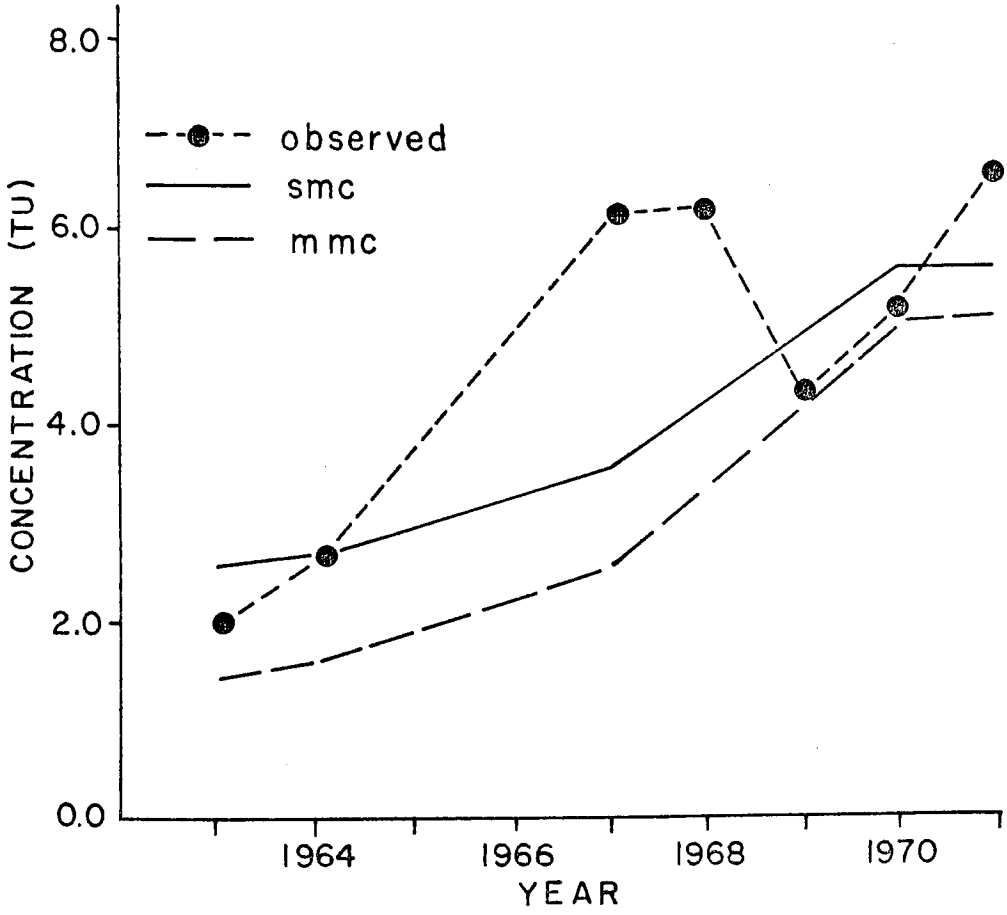

Figure 18. 1963-1971 tritium concentrations in cell 23 of the Edwards Aquifer FSM.

Table 22. 1953-1962 SMC tritium concentrations for those cells in the Edwards Aquifer FSM that were sampled during the period 1963-1971.

	Tritium concentration (TU)									
Cell	1953	1954	1955	1956	1957	1958	1959	1960	1961	1962
2	2.4	3.4	3.4	3.2	5.1	19.8	26.5	26.4	29.2	34.9
4	2.3	2.6	2.5	2.4	4.4	19.6	23.7	23.8	25.8	28.3
10	1.4	1.5	1.7	1.6	1.9	4.3	5.4	6.0	6.7	7.0
11	1.1	1.1	1.2	1.1	1.3	3.1	4.1	4.8	5.6	5.8
12	.7	.7	.7	.7	.8	3.1	4.0	4.7	5.5	5.5
14	.8	.8	.8	.7	.9	2.3	3.3	4.4	5.2	5.9
15	2.4	2.5	2.4	2.4	3.4	8.4	12.7	16.5	19.4	22.9
17	3.1	3.0	2.8	2.6	8.4	19.4	21.6	26.2	28.5	27.8
18	2.1	2.1	2.0	1.9	3.8	7.8	9.1	11.8	13.8	14.4
20	.2	.2	.2	.2	.2	.5	.6	.7	.9	.9
21	.3	.3	.3	.3	.3	.5	.6	.7	.9	.9
22	.3	.3	.2	.2	.3	.4	.5	.7	.9	.9
23	.6	.6	.5	.5	.6	1.5	1.7	2.3	2.7	2.6
29	.9	.9	.8	.8	.9	1.5	2.0	2.7	3.4	3.7
30	.8	.8	.7	.7	.8	1.4	1.7	2.1	2.5	2.6

Table 23. 1953-1971 SMC tritium concentrations for those cells of the Edwards Aquifer FSM not sampled during the period 1963-1971.

	Tritium concentration (TU)																		
Cell	1953	1954	1955	1956	1957	1958	1959	1960	1961	1962	1963	1964	1965	1966	1967	1968	1969	1970	1971
1	3.7	6.8	7.4	7.5	9.5	29.1	35.6	34.7	36.3	46.0	62.0	80.7	84.2	86.0	80.9	76.1	72.5	68.3	62.2
3	2.5	3.2	3.0	3.0	6.0	37.2	43.7	42.2	44.0	43.8	46.1	49.9	51.9	53.4	51.3	50.2	48.7	46.8	44.4
5	5.8	12.3	12.1	12.2	16.8	48.3	71.8	64.2	70.2	126.7	204.2	214.5	204.7	186.9	163.3	140.7	125.1	108.5	92.4
6	3.8	4.0	3.9	3.8	10.1	33.2	38.5	37.8	40.3	45.2	50.2	59.0	68.0	67.6	64.2	61.5	59.5	56.8	53.2
7	5.2	6.1	5.8	5.6	20.1	56.2	63.5	58.8	62.1	72.1	90.7	105.0	115.9	112.9	104.1	94.3	88.2	80.7	73.2
8	3.3	4.3	4.3	4.5	8.3	20.2	24.9	26.3	29.8	42.9	56.0	61.2	69.7	69.1	65.5	62.6	60.7	58.1	55.0
9	4.0	3.8	3.6	3.4	11.2	27.8	31.9	37.7	41.0	40.5	40.7	45.3	58.0	62.4	64.1	67.8	68.5	68.0	65.7
13	.9	.8	.8	.7	1.0	3.1	6.3	7.5	8.5	8.3	8.0	8.4	9.5	10.5	11.1	13.4	13.8	14.2	15.1
16	1.8	1.8	1.7	1.6	2.5	6.3	7.5	9.5	11.0	11.2	11.2	12.5	16.0	17.6	18.4	21.4	22.9	24.5	26.1
19	.4	.4	.3	.3	.4	1.1	1.3	1.7	2.0	2.0	1.9	2.1	2.3	2.6	2.9	3.7	4.0	4.4	5.2
24	.6	.6	.6	.6	.6	1.4	1.8	2.2	2.7	2.7	2.7	3.1	3.4	4.4	5.0	6.0	6.7	7.5	9.1
25	.3	.3	.3	.3	.3	.5	.6	.7	.8	.9	.9	1.0	1.1	1.4	1.6	2.0	2.3	2.6	3.5
26	.1	.1	.1	.1	.1	.2	.2	.2	.2	.2	.2	.2	.3	.3	.4	.5	.5	.6	.8
27	.1	.1	.1	.1	.1	.1	.1	.1	.2	.2	.2	.2	.2	.2	.2	.3	.3	.4	.5
28	.1	.1	.1	.1	.1	.1	.1	.1	.2	.2	.2	.2	.2	.2	.2	.3	.4	.4	.5
31	2.3	2.2	2.1	2.0	4.5	9.5	10.8	14.0	16.1	15.9	15.6	16.3	19.9	21.7	22.9	26.8	29.2	31.6	32.8

Edwards Aquifer FSM, by comparing the steady state tritium concentrations as calculated by the MMC and SMC mixing algorithms (Table 20). Table 24 shows the percentage change of the MMC steady state tritium concentration relative to the SMC concentration and the percentage of VOL represented by the BRV for each of the 31 cells of the Edwards FSM. Table 23 illustrates that whereas the agreement between the figures calculated by the two different algorithms is generally good in each cell, the agreement is not nearly as good as that of the Tucson Basin C-14 FSM. One might expect that agreement is better in cells where the BRV is a relatively small percentage of VOL and worse in those cells in which the BRV is an appreciable percentage of VOL. These expectations are not necessarily borne out by the data. In cell 31, in which the BRV is over 16 per cent of VOL, the percentage change is just .50 per cent. In cells 17 and 23, in which the BRVs are 29.23 and 26.58 per cent of their respective volumes, the per cent differences are just 1.95 and -1.93 per cent. Cases similar to cells 17, 23, and 31 are also found in cells 9 and 18. Cells 19, 20, 25, and 26 have relatively small percentages of BRV/VOL, yet relatively large per cent changes between the two algorithms. The expected patterns of small per cent changes and low percentages of BRV/VOL are seen in cells 2, 3, 4, 10, 11, 12, 13, and 14, and of large per cent differences and large percentages of BRV/VOL are observed in cells 27 and 28. All

Table 24. Per cent change in the MMC steady state concentration relative to that of the SMC and BRV/VOL for the steady state portion of the Edwards Aquifer FSM.

Cell	Per cent change in MMC (%)	BRV/VOL (%)
1	2.89	5.70
2	1.89	2.78
3	1.97	2.96
4	1.76	2.55
5	4.24	15.60
6	2.94	5.91
7	3.96	12.32
8	2.10	6.51
9	2.61	19.20
10	-.66	3.56
11	-1.43	4.69
12	-2.64	4.45
13	-1.77	4.21
14	-1.35	2.24
15	1.23	8.30
16	-.11	8.50
17	1.95	29.23
18	.14	11.63
19	-5.13	4.91
20	-6.32	5.97
21	-5.33	8.57
22	-4.40	14.27
23	-1.93	26.58
24	-3.62	13.43
25	-6.18	6.34
26	-9.02	3.47
27	-11.11	12.13
28	-10.31	21.68
29	-2.41	3.27
30	-3.28	4.20
31	.50	16.71

these data seem somewhat equivocal, though they perhaps lend weak support to the hypothesis that steady state concentrations or states are somewhat independent of the mixing algorithm. It might be less controversial to say that the steady state concentrations or states are only mildly dependent upon the mixing algorithm used.

8.8.2 Observed and Calculated Tritium Concentrations

By inspection of Figures 13 through 18 and Table 21, the reader can compare the observed tritium concentrations with the calculated ones. The calculated tritium concentrations illustrate two trends. For a given cell, both the calculated values monotonically increase throughout the period of record, or else they monotonically increase to maximums and then monotonically decrease. The observed data do not necessarily show these trends wherever the calculated data do. Apparently, the FSM is not as sensitive as the real-world system, and there are several reasons for this.

The first reason is the fact that the FSM does not sample the system at the same times as do the real-world measurements. The FSM gives the tritium concentrations of the cells at the end of a given iteration; thus the calculated concentrations for a given year are those at the end of the year. The observed data were not necessarily taken at the end of a particular year; they were scattered throughout the year. In other words, the observed tritium

concentrations and the calculated ones are non-contemporaneous. A possible way to rectify this problem is to make Δt smaller for the FSM so that the FSM outputs correspond temporally to the observed system outputs. The choice of Δt = 1 year was more or less dictated to the author by the annual nature of his volumetric recharge data.

The second reason deals with the constraint on Δt expressed in Section 3.8.2. This constraint required that Δt be less than .01 of the half-life of the radioactive tracer. This requirement is clearly violated in the Edwards FSM, and it is again apparent that Δt is too large.

The final reason for the insensitivity of the FSM is also related to the choice of Δt. By its very nature, the FSM "lumps" all inputs; that is, all inputs to the FSM are injected into the model at the beginning of each iteration. The FSM makes no provision for the temporal variations in input quantities within a given Δt. The real-world recharge to the Edwards Aquifer is not "lumped" in this manner. It is distributed throughout the year, and it is not distributed evenly as there are distinct wet and dry seasons. Therefore, one is again forced to conclude that Δt = 1 year is too large. Nevertheless, overall results are good.

Aside from examining the overall trends of the data, one can examine the data on a year-by-year basis. If this is done, the reader will discover that agreements between

the observed and calculated concentrations are not very good in many cases. In cells 12, 14, 18, and 20, both algorithms agree reasonably well with the observed data throughout the period of record. In the other cells, the agreement may be good for part of the record and poor in the other part. The very high observed tritium concentration in cell 2 in 1970 is believed by the author to be anomalous. If this value is discarded, the agreement in cell 2 improves considerably. The data also indicate that in general, the SMC and MMC algorithms are about equal when it comes to modeling the observed tritium concentrations. This is a bit surprising, since the model was calibrated and validated using the SMC algorithm. The good agreement between the two algorithms may indicate that in these cells the mixing regime may be a combination of perfect mixing and piston flow. It is possible that once a more refined model of the Edwards Aquifer is constructed, one of the mixing algorithms will yield better results.

8.9 Interpretation of the Model

8.9.1 Tritium Concentrations

In general, as one moves farther away from the recharge areas, cell tritium concentrations decrease. This is quite logical, since if the water must travel a greater distance to reach a cell, much of its tritium may decay away. The highest tritium concentrations are found in cells 1

through 8, the recharge cells, and cell 9, which receives its entire input directly from a recharge cell. As one moves away from this top row of cells, in any given year the tritium concentrations generally decline.

The tritium concentrations in cells 26, 27, and 28 show very little change for the entire period of record, implying that bomb tritium has not yet reached these cells. This same implication would also seem to be the case in cells 19 through 23 and 25. Cell 24 represents somewhat of an exception, since it receives a great deal of its input from cells 11 and 12, both of which receive flow directly from recharge cells.

The discharge concentrations from cell 23 also represent those of Comal Springs, and the relatively low concentrations from this spring indicate that it is discharging water of relatively long residence time, a conclusion also reached by others (Pearson et al., 1974). In contrast, the discharge concentrations from cell 18, representing San Marcos Springs, indicate that this spring is discharging water of relatively short residence time in the system. Pearson et al. (1974) also reached this conclusion.

The tritium concentrations in cells 13 and 14 seem rather low when compared to those in cells 15, 16, and 17. This may suggest that the ground-water flow is somewhat restricted in the vicinity of these two cells. This is

indeed found to be the case upon examination of the flow distribution in Table 15. These data show that most of the flow from cell 12 is diverted around cell 13, and that a good deal of the flow from cell 13 is diverted around cell 14. Cell 30 may also indicate an area of restricted ground water movement.

It is also interesting to note the response of the recharge cells and of the entire system to the tritium inputs. Table 18 showed the yearly SBRCs to each of the recharge cells. The reader can see that the 1962 SBRC was over four times greater than that of 1961. Yet nowhere in any of the eight recharge cells do the tritium concentrations show an increase even approaching four times as great from 1961 to 1962. In some cells, even a slight decrease occurred. This illustrates a simple but nevertheless important consideration: in relating the response of the recharge cells and ultimately of the entire system to the tritium SBRCs, it is insufficient to consider the SBRCs alone but is essential to consider the volume of recharge associated with the SBRCs. Table 17 shows that there was much less recharge to the system in 1962 than in 1961. Thus, the great increase in the tritium SBRC for 1962 was offset by the relatively small amount of volumetric recharge. Table 25 shows the amount of tritium (equal to SBRC*SBRV) introduced annually into each of the eight recharge cells as well as the total amount introduced into

Table 25. Amounts of tritium in TU*km^3 introduced annually into the eight recharge cells of the Edwards Aquifer FSM and the total annual amounts.

Year	Cell 1	2	3	4	5	6	7	8	Total
1953	.276	.194	.041	.056	.466	.259	.545	.320	2.157
1954	7.604	3.923	.885	1.479	3.138	.523	1.096	1.328	19.976
1955	3.271	.565	.014	.197	.422	.110	.085	.243	4.907
1956	1.063	.286	.110	.242	.430	.138	.149	.556	2.974
1957	6.463	7.958	3.940	7.707	3.309	10.442	23.729	4.548	68.096
1958	52.686	59.252	44.199	58.291	18.864	37.633	53.166	13.964	338.055
1959	22.353	32.358	12.547	19.695	19.283	11.688	15.849	6.849	140.622
1960	6.186	8.925	4.576	8.858	7.253	6.242	11.157	4.350	57.547
1961	11.436	20.344	7.711	14.158	11.871	9.312	14.921	6.643	96.396
1962	27.651	27.179	2.505	13.707	33.418	9.737	14.416	16.877	145.490
1963	42.381	28.802	5.363	10.984	44.716	9.947	22.747	17.298	182.238
1964	60.127	26.294	7.772	29.232	20.687	17.091	24.360	10.595	196.158
1965	27.583	23.366	6.520	29.247	15.365	22.158	32.484	18.761	175.484
1966	32.702	25.849	7.276	15.099	9.748	7.824	12.831	6.681	118.010
1967	7.796	13.058	2.880	6.160	4.232	2.865	5.430	1.797	44.218
1968	12.164	16.394	6.195	18.510	5.591	7.744	11.219	4.593	82.410
1969	12.749	12.060	3.265	8.941	5.780	6.392	10.612	4.953	64.752
1970	9.548	12.021	3.002	6.903	5.770	5.839	9.617	3.345	56.045
1971	16.305	13.145	2.428	9.633	4.254	5.032	5.107	1.374	57.278

the entire system each year. This table shows that in terms of the total amount of tritium introduced into the system, 1958 was the most effective year, although the SBRC for 1958 was less than 20 per cent of the peak SBRC in 1963. However, the 1958 SBRV was about ten times that in 1963. Referring back to Tables 22 and 23, it is seen that the greatest percentage increases in the tritium concentrations of the recharge cells occurred in 1958. Unfortunately, there are no field data against which the FSM values may be compared.

The calibration of the Edwards Aquifer FSM also provided estimates of the effective porosities of the cells. These values were shown in Table 14 along with the effective volumes of the cells. Most of the cell effective porosities obtained by calibration are higher than those estimated by Pearson (1974), most of whose estimates fell between 0.03 and 0.05. All of the effective porosities obtained by calibrating the Edwards Aquifer FSM are equal to or greater than Pearson's estimates; most are greater. In 13 of the 31 cells, the effective porosities are greater than Pearson's upper limit of 0.05. In four cells, 5, 11, 18, and 23, the FSM effective porosities are greater than 0.08. More research is needed before the differences between the FSM effective porosities and those estimated by Pearson can be resolved. The effective porosities of the Edwards Limestone

might be useful in constructing a hydraulic model of the aquifer.

8.9.2 Mixing Properties of the Edwards Aquifer

Some indication of the mixing properties of the Edwards Aquifer can be obtained from the FSM. To do so it is necessary to look at the flow distribution during each year of the non-steady flow (1953-1971) FSM, although to simplify matters the author will examine two extreme flow distributions: the distribution for 1956, the year of the least volumetric recharge to the system, and that of 1957, the year of the second highest volumetric recharge. The volume of recharge was over 26 times greater in 1957 than in 1956. In 1958, the year of highest volumetric recharge, the amount was 50 per cent greater than that of 1957, but 1957 was chosen since it directly follows 1956 and could thus afford a more meaningful comparison. Table 26 shows for 1956 the per cent changes in the MMC concentrations relative to those of the SMC and the percentage BRV/VOL for all 31 cells. Table 27 shows the same information for 1957.

The 1956 data indicate that only nine cells, 5, 8, 17, 18, 22, 23, 24, 27, and 28, have BRVs greater than one per cent of their effective volumes. The highest percentage, 2.37 per cent, is found in cell 28. As might be expected, Table 26 shows that there is little difference in

Table 26. Per cent change in the MMC tritium concentration relative to that of the SMC and BRV/VOL for each cell in the Edwards Aquifer FSM in 1956.

Cell	Per cent change in MMC (%)	BRV/VOL (%)
1	3.42	.97
2	1.54	.76
3	1.58	.20
4	1.48	.14
5	5.67	2.08
6	2.47	.21
7	3.19	.32
8	1.83	1.11
9	1.82	.50
10	-5.56	.60
11	-5.08	.64
12	-3.95	.47
13	-2.14	.29
14	-3.79	.18
15	-3.48	.71
16	-.38	.54
17	1.33	1.13
18	-.90	1.18
19	-5.14	.43
20	-6.10	.52
21	-5.53	.73
22	-4.85	1.34
23	-2.46	2.17
24	-4.57	1.58
25	-6.33	.75
26	-9.40	.40
27	-10.47	1.37
28	-9.76	2.37
29	-2.56	.28
30	-3.05	.26
31	.60	.64

Table 27. Per cent change in the MMC tritium concentration relative to that of the SMC and BRV/VOL for each cell in the Edwards Aquifer FSM in 1957.

Cell	Per cent change in MMC (%)	BRV/VOL (%)
1	4.09	6.70
2	2.90	5.08
3	5.05	8.17
4	3.19	5.15
5	8.91	18.29
6	12.67	18.46
7	42.88	57.88
8	-1.17	23.50
9	-52.92	90.20
10	-8.58	4.19
11	-9.98	6.42
12	-13.14	7.31
13	-17.32	8.82
14	-11.09	4.10
15	-21.10	17.05
16	-27.70	21.67
17	-50.44	115.40
18	-34.89	44.03
19	-9.12	9.11
20	-8.30	11.05
21	-8.00	16.13
22	-10.82	26.26
23	-30.44	61.54
24	-8.51	20.65
25	-7.05	9.75
26	-9.92	5.42
27	-10.11	19.26
28	-10.34	35.17
29	-9.94	6.72
30	-13.00	10.70
31	-48.30	65.89

the two algorithms for each cell. The per cent differences are based upon tritium concentrations calculated to three decimal places, even though tritium concentrations can be measured to just one decimal place, since the author is interested in numerical results as calculated by two different algorithms. The 1956 data suggest that the Edwards Aquifer as modeled by a FSM was well-mixed during this year, regardless of the mixing algorithm.

The 1957 data in Table 27 indicate that the agreement between the two algorithms is generally poorer than in 1956. It is not unusual that in the cells in which the BRV is greater than 40 per cent of VOL (cells 7, 9, 17, 18, 23, and 31), the per cent differences in the MMC concentrations relative to those of the SMC are the greatest. In 29 of the 31 cells, the per cent differences in the MMC values relative to those of the SMC are greater in 1957 than in 1956. In only two cells, 8 and 27, are the per cent differences less in 1957 than in 1956.

These data suggest that the differences between the two algorithms become noticeable once the cell BRVs become more than a few per cent of the effective volumes. This may seem contrary to the conclusion reached in Section 8.8.1, and perhaps it is. However, the two models are not strictly analogous, since the model of Section 8.8.1 is a steady flow FSM that was iterated until steady state was reached. The FSM in this section is a non-steady flow, non-steady

state model. The data also imply that the Edwards Aquifer as modeled by a MMC-FSM exhibited more piston flow in 1957 than in 1956. One cannot help but wonder whether this was actually the case in the real-world aquifer.

The reader may have noticed that in Table 27, the BRV of cell 17 is greater than the effective volume of the cell. Strictly speaking, this condition is not permissible with the MMC algorithm, and it was the only instance where it occurred. It is perhaps fortuitous that no negative concentrations resulted. Its existence constitutes a flaw in this model which does not seem serious.

The data in Table 27 also point out something with regard to the SMC mixing algorithm. Since this algorithm requires that the effective volume of the cell expand by an amount equal to the BRV, when the BRV becomes large relative to VOL or even exceeds VOL, one would be justified in questioning the validity of the SMC in modeling mixing in a real-world system, especially one modeled with a steady volume FSM. In a non-steady volume SMC-FSM, the size of the BRV and the expansion of the cell are not as critical since the effective volume of the cell is allowed to change. But in other cases, one must wonder about the physical reality of a large degree of cell expansion. However, the SMC never purported to be an exact duplication of real-world systems, but only a method to account for perfect mixing which may occur in some of these systems. In light of this,

one should judge the performance of the SMC algorithm primarily by the results it gives.

8.9.3 The AARDIM

The AARDIM can be examined to obtain some insight into the properties of the Edwards Aquifer. Table 28 summarizes all the information on the AARDIM. It should be remembered that the AARDIM is the averaged steady flow model of the Edwards Aquifer during the period 1934-1970.

The AARDIM suggests that perhaps more flow in the Edwards Aquifer occurs in a southerly direction than was previously thought (Pearson, 1974). Cells 12 and 13 divert a good deal of their flow to the two rows of cells represented by cells 19 through 23 and cells 24 through 28. Cells 14 through 17 also divert a lot of their flow to the cells in the lower parts of the FSM. The results of the AARDIM run somewhat counter to the hypothesis that most of the flow in the Edwards Aquifer is easterly and northeasterly, approximately paralleling the Balcones fault zone (Pearson et al., 1974).

The AARDIM also illustrates the interdependence between the mean age or residence time of the water in a cell and the tritium concentrations in the cell. The high mean ages correspond to cells with low tritium concentrations, such as cells 19 through 23 and 25 through 28. These high residence times indicate that much of the

Table 28. BRV, BRV/VOL, and the SMC mean age for each cell in the Edwards Aquifer AARDIM.

Cell	BRV (km^3)	BRV/VOL (%)	SMC mean age (years)
1	.1190	5.95	17.807
2	.1080	3.32	31.093
3	.0400	4.00	26.000
4	.0900	2.90	35.444
5	.0630	16.80	6.952
6	.0700	5.97	17.757
7	.1120	13.18	8.589
8	.0708	7.25	20.220
9	.0616	20.53	13.459
10	.0774	3.72	44.697
11	.1660	5.11	53.101
12	.1736	5.11	62.717
13	.0824	4.99	58.934
14	.0918	2.55	74.156
15	.0943	8.81	35.387
16	.0774	8.82	38.757
17	.1238	30.95	23.412
18	.1451	12.62	29.781
19	.1202	5.72	78.379
20	.1384	6.92	91.903
21	.1947	9.74	93.710
22	.3595	15.98	103.101
23	.2293	29.40	90.514
24	.1251	15.11	65.761
25	.1251	7.13	79.777
26	.1372	3.91	105.224
27	.1500	13.71	111.373
28	.1695	24.53	113.420
29	.0330	3.47	64.170
30	.0348	4.35	61.715
31	.0495	17.68	29.066

tritium recharged to the aquifer decayed by the time it reached these cells. In contrast, the low residence times correspond to those cells with the highest tritium concentrations, primarily the recharge cells but some other cells as well. This interdependence is illustrated despite the fact that the AARDIM is a steady flow model and the tritium transport FSM is not. The relatively high mean ages in cells 13, 14, and 12 may indicate a restriction in groundwater flow in these cells.

The percentages BRV/VOL indicate that some of the cells exhibit piston flow while others approach a more well-mixed regime. Piston flow should be particularly strong in cells 17, 23, and 28, whereas well-mixed conditions should be found in cells 3, 4, 10, 14, 26, and 29. The other cells may display types between the extremes of piston flow and well-mixed flow.

The author is reluctant to speculate further regarding the nature of the flow in Edwards Aquifer on the basis of the AARDIM. This model is partly physically-based and partly black-box, though it is perhaps more of the latter than the former. It was obtained by adjusting the flow distribution until it matched the observed volumetric outputs from the aquifer. It also represents average flow conditions in the Edwards Aquifer during the period 1934-1970, and as was noted, the Edwards Aquifer received great extremes of recharge in that period, and also experienced

great variations in withdrawals. Interpretation of the AARDIM must be done with great care and should be tempered by the results of other investigations.

8.10 Refinement of the Edwards FSM

The author believes that the tritium transport FSM can be much improved by choosing a Δt of less than one year, preferably using a value of one month or thereabouts. The reasons were discussed in Section 8.8.2, and the author will not mention them again. A Δt of one or two months might be best; however, a Δt of three or four months or even iterating on a wet season-dry season basis should improve the performance of the Edwards Aquifer FSM. In addition, the tritium transport FSM would be aided by the construction, calibration and validation of a hydraulic model of the Edwards Aquifer. The output from such a model could be used as the flow distribution input to the mass transport model.

8.11 Concluding Remarks

Although the Edwards Aquifer FSM is not as good as it might be, it does provide a quantitative estimation of what is occurring in a highly complex hydrologic system. The complex nature of the Edwards Aquifer should not be underestimated when judging the performance of the FSM. The Edwards Aquifer FSM is significant in that it is perhaps unique in attempting to model mass transport in a karst aquifer using principles that have some physical

basis. The author is aware of only one other physically-based model capable of modeling transport in karst systems, and this is a hydraulic model (Thrailkill, 1972).

Previous models of karst systems were input-output (black box) models such as time series analysis or linear regression models. Time series analysis such as one performed by Knisel (1972) usually require detailed information, whereas linear regression models are difficult to justify on physical grounds (Simpson and Duckstein, 1975). The Edwards Aquifer FSM demonstrated that it is possible to model highly complex karst systems without treating the system entirely as a black box. If one must indeed classify a FSM, it should probably be termed a "grey box" model.

FSMs will be useful in modeling mass transport in karst and fractured rock aquifers because they make no assumptions regarding the nature of the flow, whether it be laminar, nonlinear laminar, or turbulent flow. This ability is particularly important in modeling the aforementioned aquifers, since flow in these systems may be mixtures of the three types of flow mentioned. For such systems and flow types, it would be extremely difficult to write and solve the partial differential equations governing the flow, yet a black box approach would tell the modeler little if anything about the physicochemical processes occurring in

these systems. The FSM takes a middle ground between the two approaches.

CHAPTER 9

FINITE-STATE MODELS OF ENERGY TRANSPORT IN HYDROLOGIC SYSTEMS

9.1 Introduction

Until now, the author emphasized the ability of FSMs to model mass transport in hydrologic systems. In this chapter, he will discuss briefly how FSMs might model the transport of energy, especially hydraulic energy or head, in hydrologic systems. Hydraulic energy content can be related to the effective volumes of the cells of the FSM. Changes in cell effective volumes can be described with Equation (52), the FSM storage equation, first introduced in Chapter 5 as:

$$VOL(N+1) = VOL(N) + BRV(N+1) - BDV(N+1) \qquad (52)$$

To use Equation (52) to model changes in effective volumes, and hence, changes in hydraulic energy content, algorithms for computing BDV(N+1) must be specified. This is similar to the case of the FSM continuity equation, Equation (4), in which it was necessary to specify algorithms for BDC(N+1) before solution of the equation could be effected. In general, the algorithm for BDV(N+1) will depend upon the type of system being modeled. This

chapter will be devoted to the development of these algorithms.

In using Equation (52) to model the transport of hydraulic energy, one is free to use Equation (4) to model mass transport, thus providing the potential of simultaneously modeling the transport of mass and hydraulic energy.

9.2 Saturated Flow

9.2.1 The Saturated Medium as a Linear Reservoir

In modeling flow in an aquifer or other saturated porous medium, it is advantageous wherever possible to treat the system as a linear system. Although saturated media in the real world may not behave as linear systems, this approach has met with some success, particularly in modeling ground-water reservoirs (Kraijenhoff van de Leur, 1958; Dooge, 1960; Eliasson, 1971; Eliasson et al., 1973; Gelhar and Wilson, 1974). Despite the fact that linear systems theory and specifically, the theory of linear reservoirs, has been used for some time in surface water hydrology, Dooge (1973, p. 49) stated that this approach has not been applied to ground-water hydrology until recently, and then to a very limited extent. The main advantage in using linear systems theory is that the mathematics is a great deal more tractable than that of nonlinear systems theory.

If, for example, one assumes that the outflow from a ground-water reservoir is proportional to the storage in the reservoir, then (Dooge, 1960)

$$S = KQ \tag{61}$$

where

S = storage above or below the basic storage at which the outflow is zero;

K = storage delay time of the element;

Q = volume rate of outflow from the element.

Using Equation (61), the author can define a finite-state linear storage element as one with the property

$$VOL(N) = K*BDV(N) \tag{62}$$

Unlike Equation (61), Equation (62) does not account for the presence of thresholds in the system. If K is held constant for all N, then the system described by either of the above equations is a linear, time-invariant system; if K is a function of time or iteration number, then the system is said to be a linear, time-variant system (Mandeville and O'Donnell, 1973).

If Equation (62) is rewritten for iteration N+1 and substituted into Equation (52), the result is

$$VOL(N+1) = VOL(N) + BRV(N+1) - \frac{VOL(N+1)}{K} \tag{63}$$

Equation (63) simplifies to

$$VOL(N+1) = \frac{K}{K+1} * (VOL(N) + BRV(N+1)) \quad (64)$$

At iteration N+1, all quantities on the right-hand side of Equation (64) are known, so VOL(N+1) can be calculated. Once this has been accomplished, then BDV(N+1) can be calculated using the following:

$$BDV(N+1) = \frac{VOL(N+1)}{K} \quad (65)$$

The equations developed in this chapter were applied to a single-cell FSM possessing an initial volume of 1.00. A SBRV of 0.25 was injected into the cell for the first 10 iterations and zeroed thereafter. Figure 19 is a plot of VOL and SBDV versus N for K = 6. The exponential natures of the recession curves are illustrated on Figure 20, a semi-logarithmic plot of the SBDV and VOL versus N. The exponential decay of the recession curves from a linear storage element is a characteristic of this element (Dooge, 1960).

There has been little mention of the meaning of K in a physical sense. If one solves Equation (62) for K, the following is obtained:

$$K = \frac{VOL(N)}{BDV(N)} \quad (66)$$

Since the BDV(N) has the units of a volume of water per iteration or per Δt, K will have the units of iterations

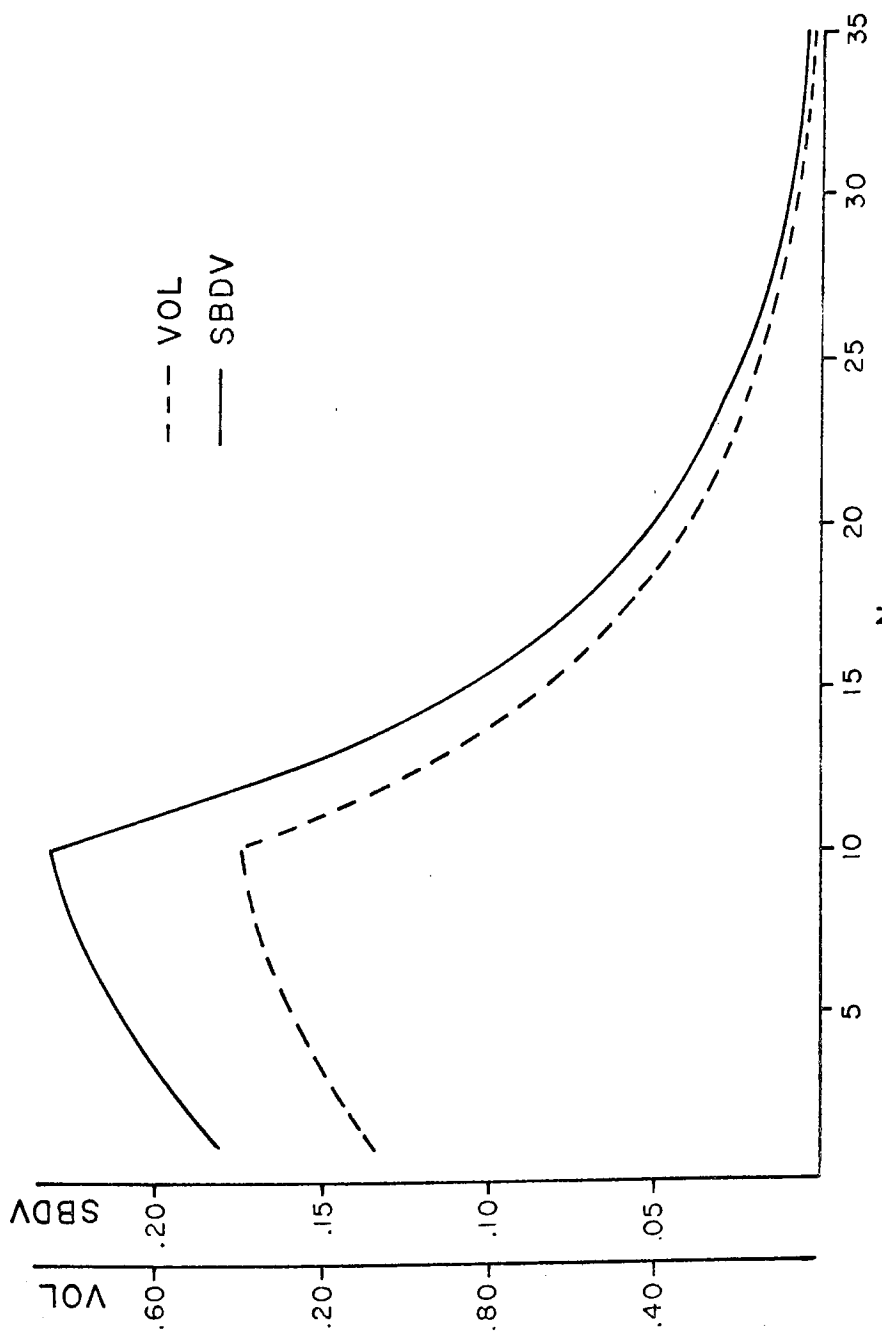

Figure 19. Dimensionless VOL and SBDV versus N for a single finite-state linear storage element.

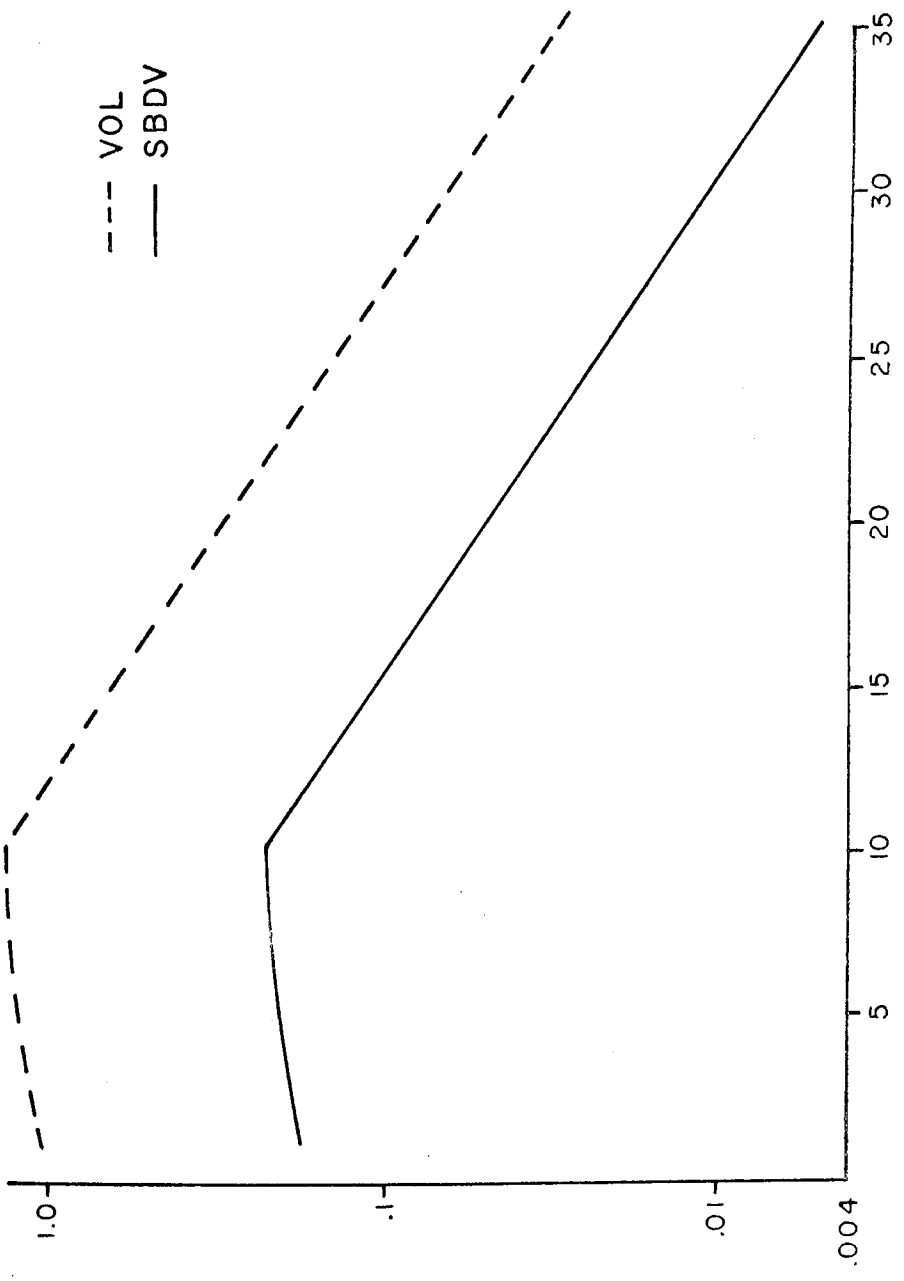

Figure 20. Semilogarithmic plot of dimensionless VOL and SBDV versus N for a single finite-state linear storage element.

or in real time, the same units assigned to Δt. In light of this and following the example of Dooge (1960), a possible interpretation of K is the average number of iterations or the average amount of time BDV(N) resides in VOL(N). Other workers who have used linear reservoir theory to model flow in ground-water reservoirs also showed that their equivalents of K possessed the dimensions of time. These equivalent parameters include the reservoir coefficient of Kraijenhoff van de Leur (1958) and the linear reservoir parameters of Gelhar and Wilson (1974). The former related his reservoir coefficient to the geometry of the aquifer as well as its transmissive and storage properties. The linear reservoir parameters of Gelhar and Wilson (1974) were found to be functions of the geometry of the aquifer, the storage and transmissive properties of the aquifer as well as the nature of the flow in the aquifer, steady or unsteady.

The calibration of a linear reservoir FSM will consist of finding suitable values of K for each cell which yield the best results, as well as determining the initial effective volumes of the cells, the flow distribution and other quantities.

As mentioned previously, a linear time-variant system may be introduced by specifying K as a function of time or iteration number. For a linear time-variant FSM storage element, Equation (62) becomes

$$VOL(N) = K(N)*BDV(N) \tag{67}$$

At iteration N+1, one will have

$$VOL(N+1) = K(N+1)*BDV(N+1) \quad (68)$$

and

$$VOL(N+1) = VOL(N) + BRV(N+1) - BDV(N+1) \quad (52)$$

Equations (68) and (52) form a system of two equations in three unknowns: VOL(N+1), K(N+1), and BDV(N+1). In order to solve this system, one of the unknowns must be specified, and a logical choice for specification is K(N+1). It is apparent that in the time-variant case, K will be a function of iteration number or time. Different ground-water reservoirs will probably require different functional relationships between K and N, and a great deal of research is required before these relationships can be identified. The use of linear time-variant systems may prove useful in modeling ground-water reservoirs; however, a comprehensive treatment of this topic is beyond the scope of this dissertation. In mentioning the topic here, the author intended merely to show that FSMs possess the potential of modeling linear time-variant ground-water systems.

9.2.2 Concluding Remarks on Saturated Flow

In the preceding section, the author briefly described how FSMs in conjunction with linear reservoir theory could be used to model flow in saturated porous

media. Although flow in ground-water reservoirs was emphasized, the theory presented could be applied to any saturated medium, such as a saturated soil. The author neglected the effects of translation and considered only the effects of storage. Translational effects will be discussed in the section on surface water flow, and the results of that section will be applicable to flow in saturated porous media in which translational effects cannot be neglected, such as might be the case in certain karst or fractured rock aquifers.

In an aquifer, the changes in the effective volumes of the cells can represent changes in the hydraulic head in the cell by requiring that any changes in cell effective volumes are the results of changes in the vertical dimensions (heights of water) of the cells. This does not mean that the modeler is restricted to unconfined aquifers only. Confined and semi-confined aquifers can be considered by defining the height of water in a cell as a consequence of the hydrostatic pressure in the cell by using the equation

$$h = \frac{p}{\rho g} + z \tag{69}$$

where

h = hydraulic head in the cell;

p = hydrostatic pressure;

ρ = density of water, assumed constant;

g = acceleration due to gravity, assumed constant;

z = elevation relative to a datum.

Equation (69) ignores the effect of velocity on hydraulic head, an effect that is negligible in most ground-water reservoirs. Equation (69) is also applicable to unconfined aquifers.

One difficulty may arise if one attempts to simultaneously model mass transport and fluid flow in a semi-confined or confined aquifer. Cell effective volumes with heights based on Equation (69) and cell effective volumes based on water content alone will not necessarily be identical. Therefore, it will undoubtedly be necessary to define two volumes for each cell, one for flow and one for mass transport. This task does not seem overly difficult to the author. It may also be necessary to do this in cases not involving mass transport, especially in situations involving semi-confined aquifers or aquifers modeled with a three-dimensional cell network. In the former case, careful track must be kept of the difference between the two cell effective volumes, while in the latter case the modeler must keep track of the relationships between the effective volume of a given cell and the effective volumes of cells directly above or below it.

One can also model flow in a saturated medium using nonlinear systems theory although in doing so one loses the

mathematical tractability of linear systems theory. Non-linear reservoirs will be discussed in a later section.

9.3 Surface Water Flow

9.3.1 Translation Effects

The development of algorithms to relate storage to discharge in surface water systems is complicated by the fact that one must usually consider the effects of translation in addition to those of storage. This is the case in considering flow in natural perennial streams, around which most of the following discussion will center.

In order to modify a linear reservoir so that it can account for the effects of translation, the concept of lag time must be introduced. The linear reservoir equation then becomes (Dooge, 1973, p. 255)

$$S(t) = KQ(t+\tau) \tag{70}$$

where

τ = lag time.

In words, Equation (70) states that the storage at time t is directly proportional to the discharge at time $t+\tau$. In FSM notation, Equation (70) is

$$VOL(N) = K*BDV(N+\tau) \tag{71}$$

Since the BDV is now a function of some previous value of VOL, all quantities on the right-hand side of the storage equation

$$VOL(N+1) = VOL(N) + BRV(N+1) - BDV(N+1) \quad (52)$$

are known at iteration N+1. As an example, if $\tau = 1$, then by Equation (71) one has:

$$BDV(N+1) = \frac{VOL(N)}{K} \quad (72)$$

and in general,

$$BDV(N+1) = \frac{VOL(N+1-\tau)}{K} \quad (73)$$

Equation (52) can then be rewritten as:

$$VOL(N+1) = VOL(N) + BRV(N+1) - \frac{VOL(N+1-\tau)}{K} \quad (74)$$

Difficulties arise if $N+1-\tau$ is less than zero, since effective volumes are undefined for iterations less than zero. This problem could be overcome by operating the FSM in a steady flow, steady volume regime (i.e., BRV = BDV) for $\tau-1$ iterations and then switching over to Equation (74). Another difficulty arises over the specification of τ. The nature of the FSM demands that τ assume integer values only, since the parameters of the FSM do not exist for noninteger iteration values. Dooge (1973, p. 255) gave an equation for calculating τ, an equation which does not necessarily yield integer values of τ. Dooge also mentioned that for short stream reaches, τ may be negative, which is mathematically optimal but physically unrealistic. For this reason, it may be best to determine τ by calibration.

The concept of time variance can also be introduced into Equation (71) by introducing K(N) and identifying a functional relationship between K and N. In addition, the concept of translation as given here is directly applicable to flow in saturated systems in which translation cannot be neglected.

9.3.2 Effect of Wedge Storage

Whereas Equation (70) included the effects of translation, it neglected the fact that in natural river channels, wedge storage (Linsley, Kohler, and Paulhus, 1958, p. 227) is important. During rising stages, a considerable volume of wedge storage may exist before large increases in outflow occur. The Muskingum method (Linsley et al., 1958, p. 228) is one method to account for the wedge storage in a stream reach. The equation for storage is:

$$S = K'(XI + (1-X)O) \tag{75}$$

where

S = storage in the reach;

K' = storage constant, the ratio of storage to discharge and approximately equal to the travel time through the reach;

I = inflow to the reach;

O = outflow from the reach;

X = a constant ($0 \leq X \leq 1$) expressing the relative importance of inflow and outflow in determining storage.

In FSM notation, Equation (75) can be expressed as:

$$VOL(N) = K' * (X*BRV(N) + (1-X)*BDV(N)) \quad (76)$$

If Equation (76) is solved simultaneously with Equation (52) for iteration N+1, the following expression for BDV(N+1) is obtained:

$$BDV(N+1) = \frac{VOL(N) + (1-K'X)*BRV(N+1)}{K' - K'X + 1} \quad (77)$$

If Equation (77) is substituted back into Equation (52), the result is

$$VOL(N+1) = VOL(N) + BRV(N+1) - \frac{VOL(N) + (1-K'X)*BRV(N+1)}{K' - K'X + 1} \quad (78)$$

which simplifies to

$$VOL(N+1) = \frac{K'*[(1-X)*VOL(N) + BRV(N+1)]}{K' - K'X + 1} \quad (79)$$

Equation (79) is valid only when its right-hand side is finite and greater than zero. Note that when X = 0, Equation (79) reduces to that of a simple linear reservoir in which the wedge storage is neglected.

It is possible to determine K' and X from previous data, if they are available. Linsley et al. (1958, p. 228) stated that X is between 0.0 and 0.3 for most streams, with a mean around 0.2. Dooge (1973, p. 254) presented an

algorithm for calculating X, but warned that negative values of X may result, particularly when the stream reach is short. If X cannot be obtained from data or other means, it could be obtained along with K' during calibration of the model. It is possible to introduce time variance into Equation (76) by introducing K'(N) and deriving the appropriate expressions.

9.3.3 Concluding Remarks on Surface Water Flow

The algorithms presented in the preceding sections are applicable to modeling flow in natural perennial streams. In a FSM, each cell could be used to model a definite stream reach, and then the appropriate algorithm applied to each cell. The algorithms presented may have shortcomings, but all are based on current methodology. Extension to nonlinear models should be simpler in a FSM framework as opposed to seeking solutions to the governing partial differential equations. Time did not permit the exploration of this interesting possibility.

The author mentioned nothing regarding other surface water systems besides perennial streams. Surface water systems are many and varied, including such systems as ephemeral streams, lakes, estuaries, reservoirs, oceans, and of course the perennial streams to which the writer devoted most of his attention. As an example, modeling of flow in ephemeral streams will undoubtedly require a

nonlinear relationship between storage and discharge such as

$$S = KQ^n \tag{80}$$

where n is not equal to 1 and is usually greater than 1.

Clearly, because of the wide diversity among surface water systems, there remains a great deal of research to be done in developing suitable algorithms for each system.

9.4 Unsaturated Flow

9.4.1 Introduction

Unsaturated flow is of prime importance in considering the movement of water through a soil. Unsaturated flow is an extremely complex process, and for this reason it is perhaps the most difficult hydrologic process to treat quantitatively. The modeling of unsaturated flow will provide the greatest challenge to FSMs.

Many factors play roles in the phenomenon of unsaturated flow: the infiltration of water into the soil and the redistribution of this moisture, evapotranspiration, capillary rise, vapor movement, osmotic effects, thermally-induced flow and the presence of hysteresis in the soil moisture characteristic curve. Any attempt to rigorously model unsaturated flow should account for all these factors.

The soil-water system is the subsystem of the hydrologic cycle in which the least systems work has been

done (Dooge, 1973, p. 267). One of the reasons for the lack of systems work in soil hydrology may relate to the difficulty in accounting for all the processes mentioned in the preceding paragraph, but it would seem to the author that a systems approach to soil hydrology and unsaturated flow in particular would be no more difficult than the current approach. This consists of formulating a partial differential equation governing flow in an unsaturated soil and then seeking either analytical or numerical solutions to this equation (see Kirkham and Powers, 1972). The partial differential equations used in unsaturated flow do not always take into account all the factors affecting the movement of water in an unsaturated soil; if all factors were considered, the solution to the particular PDE might be difficult to obtain, and the calibration and validation of such a model might be so difficult as to be impossible.

In the following sections, the author will treat primarily the problem of infiltration, though some treatment of moisture redistribution will also occur. Infiltration is perhaps the most important process occurring in a soil, since it determines how much water will be available for other soil processes.

9.4.2 The Soil as a Linear Absorber

Dooge (1973, p. 283) stated that the formulation of the infiltration as a relationship between a rate of

infiltration and a volume of actual or potential infiltration would be useful in the formulation and computation of conceptual models of the soil-moisture system. If the rate of infiltration is related to potential infiltration volume, the simplest equation is (Dooge, 1973, p. 282)

$$f = AF_p \tag{81}$$

where

f = rate of infiltration capacity, the maximum rate at which the soil in a given condition can absorb water applied to its surface;

A = a constant;

F_p = volume of potential infiltration.

If the actual rate of application y of water to the surface of the soil is less than f, then the actual infiltration rate will equal y. If y is greater than or equal to f, then the actual rate of infiltration will be f as calculated from Equation (81).

In the section on saturated flow, the linear reservoir or storage element was introduced as a conceptual element in which the outflow from the element was directly proportional to the storage in the element. Dooge (1973, p. 283) stated that Equation (81) represents a conceptual element known as a linear absorber or one in which the inflow is proportional to the storage deficit in the element. In the context of FSM theory, such an element

may require that inputs to a cell modeled by Equation (81) be calculated and then compared with the specified input before determining the BRV to the cell.

The volume of potential infiltration F_p can be expressed as (Dooge, 1973, p. 273)

$$F_p = F_c - F \tag{82}$$

where

F_c = ultimate volume of infiltration;

F = volume of infiltration = volume of water present minus the amount present at the start of the infiltration event.

For the sake of simplicity, the author will assume that F_c is equal to the amount of water present at total saturation minus the amount present at the start of the infiltration event. This assumption implies that sufficient water infiltrates to saturate the soil or some subdivision of the soil.

In FSM notation, for a given cell Equation (82) becomes

$$FP(N) = FC - VOL(N) \tag{83}$$

where

FP(N) = F_p at iteration N.

FC = the effective volume of the cell at total saturation.

In FSM notation, Equation (81) is

$$BRV(N) = B*FP(N) \tag{84}$$

where

B = constant.

If BRV(N) as determined from Equation (84) is greater than the volumetric application rate Y(N), then the results of Equation (84) should be discarded and BRV(N) should be set equal to Y(N).

When FP(N) equals zero, then by Equation (84) BRV(N) equals zero. Physically, this means that the cell is completely saturated and cannot store any more infiltrating water. However, the cell will be allowed to accept infiltrating water in an amount equal to that which it can discharge to other cells or across the FSM boundaries.

Rules can now be formulated regarding the calculation of cell effective volumes. For the sake of simplicity, the writer will assume that no cell can discharge water until it has been completely saturated by infiltrating water, i.e., when VOL(N) equals FC. With this assumption in mind, then for a cell saturating with infiltration water the effective volume algorithm becomes

$$VOL(N+1) = VOL(N) + BRV(N+1) \tag{85}$$

or

$$VOL(N+1) = VOL(N) + B*(FC - VOL(N+1)) \tag{86}$$

which simplifies to

$$VOL(N+1) = \frac{VOL(N) + B*FC}{1 + B} \tag{87}$$

In no case will the effective volume of the cell be allowed to exceed FC. If this should occur, then the effective volume will be set equal to FC.

Once the cell is completely saturated, it will be allowed to discharge a BDV equal to the amount of water it will be allowed to absorb. If it is discharging some of its BDV to other cells not completely saturated, the BRVs of these unsaturated cells must be calculated in accord with the principles set forth so far. The calculated BRVs to these cells will then determine the amount of water the saturated cell will be allowed to absorb at its surface via infiltration. The relationship between the volumetric application rate Y(N) and the actual volumetric rate of infiltration must also be kept in mind. In any event, once a cell is saturated it will assume a steady flow, steady volume regime provided that infiltration has not ceased. In this regime the effective volume of the saturated cell will be determined by Equation (52).

Once the application rate ceases, the cells will begin to desaturate, so it will be necessary to specify an algorithm for the BDV from a desaturating cell. The simplest possible algorithm is that of a linear reservoir, given

earlier as

$$VOL(N) = K*BDV(N) \qquad (62)$$

Equation (62) predicts that the BDV from a cell will be zero when the effective volume is zero, which corresponds to a condition of total desaturation.

Once Equation (62) has been specified for a desaturating cell, Equations (64) and (65) can be utilized to calculate the effective volume of the cell and its BDV at iteration N+1. Some care must be used here. The BDV from a desaturating cell as calculated in accord with linear reservoir theory may be too large to be disposed of if the desaturating cell is discharging to saturating cells. These saturating cells, whose inputs must be calculated by Equation (84) may be unable to accept all of the BDV from the desaturating cell. If this is the case, then the BDV from the desaturating cell must be specified according to how much of it can be accepted by the locations to which it is flowing. One may have to discard the BDV as calculated by Equation (65).

9.4.3 Concluding Remarks on Unsaturated Flow

The simple algorithms presented in the preceding section represent a first step in modeling moisture movement in soils with FSMs. The algorithms were based upon the theory of linear time-invariant systems, although time-variance could be introduced as it has been in previous

sections. The author's treatment also neglected such factors as evapotranspiration, capillary rise, thermal gradients and their effect on fluid flow, vapor movement, and others. The problem of hysteresis was avoided by assuming that infiltration continues long enough so that all cells saturate, and then once the cells reach the saturated state, they desaturate monotonically. In theory algorithms could be introduced to account for hysteresis, although these algorithms would invariably require that one consider nonlinearity.

The author also required that cells reach total saturation before discharging BDVs. The undesirable effects of this assumption might be minimized by reducing the total volumes of the cells, that is, requiring that the cells encompass a relatively small volume of soil, and that the vertical dimensions of the cells be small compared to the other two dimensions. If one desired, an algorithm for the BDV could be specified to allow the cell to discharge before reaching complete saturation. Such an algorithm might be a nonlinear one similar to Equation (80).

Nonlinearity might also demand consideration in the case of infiltration to a cell. For example, Holtan (1961) proposed the relationship

$$f = AF_p^n + f_c \tag{88}$$

where

f_c = ultimate rate of infiltration capacity;

n = exponent not equal to 1.

Another relationship proposed by Dooge (1973, p. 281) is

$$f = \frac{A}{F} \tag{89}$$

Dooge (1973, p. 283) referred to this equation as one representing a conceptual element known as a linear inverse absorber. The uses of such an element in modeling unsaturated flow (infiltration) should be investigated.

In considering a volumetric sink such as evapotranspiration, one could add a sink term to the FSM storage equation to account for this, or volumetric sources as well. Equation (52) would become:

$$VOL(N+1) = VOL(N) + BRV(N+1) - BDV(N+1) \pm RVOL(N+1) \tag{90}$$

where

RVOL(N+1) = volumetric source and/or sink term.

This term could also be added to the other effective volume algorithms given in Section 9.4.2. One could also use such a term to model volumetric sources and sinks in other hydrologic systems as well.

In conclusion, the reader should regard the author's treatment of unsaturated flow as simply a preliminary step in modeling this phenomenon with a FSM. A

rigorous treatment of unsaturated flow modeling with FSMs is beyond the scope of this dissertation and could easily constitute the subject of an entire dissertation. Such a treatment would undoubtedly necessitate the identification of nonlinear algorithms, since some of the basic partial differential equations governing unsaturated flow are nonlinear. However, the author believes that FSMs should be able to treat nonlinearity with less difficulty than PDE-based models. The formulation and validation of a three-dimensional FSM of unsaturated flow would be a major contribution to the science of hydrology.

9.5 Transport of Heat Energy

Finite-state models also possess the potential to model other types of energy transport in hydrologic systems. Next to the transport of hydraulic energy, the transport of heat is undoubtedly the most important type of energy transport. The practical applications of a hydrologic heat transport FSM are not difficult to visualize. The discharge of thermal wastewater into a surface water body is a critical factor in determining the future biological and physicochemical regimes of the water body. The movement of heat in soils is important since it may affect seed germination, plant growth, water movement, and chemical reactions in the soil. The modeling of heat flow in a ground-water reservoir may be especially relevant in this time of

possible energy shortages, since one could conceivably model geothermal reservoirs with a FSM.

The modeling of convective heat transport with a FSM might be accomplished by using an equation similar to Equation (4), although in the context of heat transport such an equation would be interpreted as describing the conservation of heat. Conductive heat transport might be accomplished by using this equation in conjunction with the exchange process. Appropriate algorithms would have to be formulated to account for the consumption and evolution of heat in the system. A substantial amount of research remains to be done in the area of finite-state modeling of heat transport in hydrologic systems.

9.6 Concluding Remarks on Finite-State Modeling of Energy Transport in Hydrologic Systems

This chapter presented a brief introduction to the modeling of fluid flow and heat transport in hydrologic systems using finite-state models. The flow algorithms in this chapter have not yet been validated in FSMs of real-world hydrologic systems, although most of them are based upon previous work in the general area of linear hydrologic systems. The algorithms are presented mainly as indications of the course to be followed in developing flow models based on FSM theory. The author does not doubt that new algorithms will have to be formulated, and that in some cases, the use of nonlinear algorithms might be dictated.

FSMs also have the potential to model heat transport in hydrologic systems, although the algorithms to describe this type of transport have yet to be formulated.

Although the FSM linear reservoir algorithm (Equation [62]) does not include threshold effects, these can be considered by rewriting this equation as:

$$VOL(N) - \phi = K*BDV(N) \tag{91}$$

where ϕ = cell threshold volume, below which the cell outflow is zero. If the left-hand side of Equation (91) is less than or equal to zero, the BDV will be zeroed and Equation (85) can be used to calculate changes in VOL. When the BDV $\neq$ zero, then

$$VOL(N+1) = \frac{K*(VOL(N) + BRV(N+1)) + \phi}{K + 1} \tag{92}$$

and

$$BDV(N+1) = \frac{VOL(N+1) - \phi}{K} \tag{93}$$

This capability has been incorporated into the author's computer program.

CHAPTER 10

SUMMARY, SUGGESTIONS FOR FUTURE RESEARCH, AND CONCLUDING REMARKS

10.1 Summary

The author developed a digital computer model capable of modeling transport phenomena in hydrologic systems whose basic algorithm for mass transport is a discrete form of the continuity equation. A discrete form of the storage equation is utilized to model flow in hydrologic systems. Although designed primarily for hydrologic systems, the model can be applied to any system in which these basic equations are valid. It was necessary to develop appropriate algorithms for mixing and flow in order to use the basic algorithms. One of the main advantages in using finite-state transport models is that they can easily model processes occurring in any number of spatial dimensions in addition to accounting for sources and/or sinks within the system. The distribution functions A(N) and T(N) were presented as properties of steady flow, steady volume FSMs. The concepts of mean age and transit numbers were introduced, and methods were given to calculate these parameters. The author also discussed non-steady flow, non-steady volume FSMs as well as the concepts of active and dead cells and exchanges of volumes.

After briefly discussing the uses of radioactive and other tracers in ground-water hydrology, the author designed and calibrated a three-dimensional, steady flow, steady volume FSM of the observed C-14 decay age distribution in a portion of the Tucson Basin Aquifer. This model provided information on the ages of the water in the system, the long-term average annual recharge to the system and the three-dimensional movement of water in the aquifer.

A FSM of tritium transport in the Edwards Aquifer yielded reasonable agreement between the observed and calculated tritium concentrations. The Edwards Aquifer FSM differs from the Tucson Basin FSM in that it is a non-steady flow, steady volume FSM. The Edwards Aquifer FSM provided information on the distribution of flow in the aquifer, and it will be of interest to compare it with a hydraulic model of the same system when such becomes available. Although there is much room for improvement in the Edwards Aquifer FSM, it is important to note that it was capable of modeling a highly anisotropic, nonhomogeneous aquifer system. The FSM should prove to be a valuable tool in the analysis of karst and fractured rock aquifers, in which the problems of anisotropy and nonhomogeneity may be compounded by the presence of non-Darcian flow regimes.

Brief attention was also devoted to the modeling of flow in a variety of hydrologic systems. Algorithms describing flow in saturated, unsaturated, and surface

water systems were developed using linear reservoir theory and that of other linear conceptual elements. In some cases it may be necessary to develop algorithms incorporating nonlinear relationships. The author hopes that his suggestions will provide the impetus for modeling flow in hydrologic systems using a combined FSM-systems approach. FSMs have the potential for modeling heat transport in hydrologic systems, although a great deal of research remains to be done in this area.

10.2 Suggestions for Future Research

There remains a considerable amount of research to be done, both in the theory of FSMs and in their applications to hydrologic and other systems. Below are listed those areas of investigation the author feels are important.

1. Explore the relationship between and the relative advantages of the MMC and SMC algorithms.
2. Perform sensitivity analyses on FSMs in order to assess quantitatively how changes in the input parameters effect changes in the output parameters. In short, determine whether FSMs are ill-conditioned or well-conditioned. The author's experience with mass transport FSMs leads him to believe that cell effective volumes are very important in effecting changes in the FSMs. A methodology should be

developed to evaluate how changes in cell effective volumes affect the performance of the entire FSM.

3. Investigate the uncertainties in the boundary and initial conditions of the FSM and how these uncertainties are propagated. This area is closely allied to the one above.
4. Apply FSMs to model mass transport in surface water and in soil systems.
5. Devise and validate algorithms to describe fluid flow in hydrologic systems other than those considered in this dissertation.
6. Investigate the modeling of heat and fluid transport in hydrologic systems, as, for example, geothermal reservoirs.
7. Investigate possible mathematical reformulations of FSM theory and alternate representations of the FSM cell network. Noting the recursive structures of the basic FSM algorithms, one might use a Markov chain model as suggested by Simpson and Duckstein (1975). Since the FSM cell network appears amenable to representation by a finite graph, the theory of finite graphs might prove useful in analyzing FSMs. The finite graph representation of a FSM composed of many cells might be awkward, though perhaps no more awkward than the current method of representation. The ordering of the FSM cells in a systematic

fashion might prove useful, as it has in analyzing channel networks (Smart, 1972). The ordering of cells in FSMs could prove helpful in discussing the relative proximity of a cell to a boundary cell. It might be better to order the flow paths and treat the cells as flow junctions, and then develop a method to add the ordered flow paths when they converge at a junction.

8. Derive and validate algorithms to model chemical reactions other than first-order reactions.
9. Derive and validate algorithms for the sink and source terms one might encounter in hydrologic systems.
10. Investigate the meaning and applicability of the FSM age number and transit number distributions to regimes other than the steady flow, steady volume regime.
11. The usefulness of other distribution functions in the literature of chemical engineering (Himmelblau and Bischoff, 1968, Chapter 4) to hydrologic systems should be investigated. These distribution functions would have to be discretized before they could be used in FSMs. Relationships among the discrete distributions might exist as they do among the continuous ones (Himmelblau and Bischoff, 1968, p. 64).

12. Compare the results obtained from mass and energy transport FSMs with those obtained from other models such as analytical and numerical solutions to partial differential equations.
13. Determine if and under what conditions the basic FSM algorithms for mass transport and energy transport converge to the partial differential equations describing these phenomena in hydrologic systems. It should also rigorously be demonstrated that for a given cell network, any existing analytical solution gives the same results as the FSM solution.
14. Couple FSMs to describe the various interrelationships among the different subsystems of the hydrologic cycle.
15. Apply FSMs to appropriate non-hydrologic systems.

10.3 Concluding Remarks

Finite-state models provide the hydrologist with a powerful tool. Using FSMs, a wide variety of hydrologic systems can be simulated. The simplicity and flexibility of FSMs may enable one to account for many processes occurring simultaneously in a particular system. The relatively low cost of the author's generalized computer model will enable users to model systems which otherwise might be too costly

to simulate. Networks of up to ten cells can be programmed on many desk-top programmable calculators.

FSMs are particularly useful in modeling decay age distributions of radioactive isotopes in aquifers. In addition, they should be able to account for distributions of environmental tracers, radioactive or not, in hydrologic systems. These types of FSMs will provide a great deal of useful information on the properties of the hydrologic systems, and may be helpful in predicting the contamination of a system by a pollutant before waiting for the actual pollution to reach undesirable levels. In areas of sparse hydrologic data, FSMs would be useful in giving a rough first approximation to the physicochemical processes occurring therein and in identifying areas where more data are required. As such, FSMs may serve as precursors to more sophisticated models, either FSM or not, and aid in developing sampling schemes.

Some may express doubts about the ability of the FSM to model large and complex systems. These doubts may be rooted in the seeming lack of physical and mathematical rigor in the basic equations of the FSM. Some of these doubts may be allayed by further research, as was suggested in Section 10.2. The author does not apologize for the relatively simple nature of the FSM, but would indicate that a FSM can be made as simple or as complex as befits the system it is simulating. One should not judge the FSM on

its lack of rigor, but rather on its ability to simulate real-world systems and to provide meaningful, hydrologically acceptable answers. No one should demand more, and no one should accept less.

APPENDIX A

LIST OF SYMBOLS AND ABBREVIATIONS

AARDIM	Edwards Aquifer average annual recharge-discharge model.
a-f	Acre-feet (L^3).
A	(a) Chemical species, and (b) Parameter in infiltration equations ($L^{-2}T^{-1}$).
$\bar{A}$	Average or mean age number (iterations or T).
A(N)	Age number distribution.
$A(N)_i$	Fraction of fluid elements in age number group i.
B	(a) Chemical species, and (b) Parameter in FSM infiltration equation (T^{-1}).
BDC( )	Boundary discharge concentration at iteration ( ) (ML^{-3}).
BDV( )	Boundary discharge volume at iteration ( ) (L^3).
BRC( )	Boundary recharge concentration at iteration ( ) (ML^{-3}).
BRV( )	Boundary recharge volume at iteration ( ) (L^3).
BRV_j	Boundary recharge volume flowing from cell j to one particular cell (L^3).
C( )	Concentration at iteration ( ) (ML^{-3}).
$C(N)_i$	Concentration as a function of iteration number at iteration i (ML^{-3}).

C	Concentration (ML^{-3}).
C'	Mass of tracer entering a particular set of boundary cells at the first iteration divided by the sum of the effective volumes of the cells (ML^{-3}).
C_{in}	Input concentration (ML^{-3}).
C_o	Average concentration of input pulse if distributed evenly throughout the entire system (ML^{-3}).
C_∞	Equilibrium or steady state concentration at infinite time (ML^{-3}).
C-12	Carbon-12.
C-14	Carbon-14.
CFSTR	Constant flow stirred tank reactor.
CO_3^{-2}	Carbonate ion.
CSTR	Continuous stirred tank reactor.
D	Deuterium.
D_L	Longitudinal dispersion coefficient (L^2T^{-1}).
D_T	Transverse dispersion coefficient (L^2T^{-1}).
E(t)	Exit age distribution of a fluid from a closed vessel.
EP	Effective porosity.
EXVOL	Volume of water exchanged between two cells (L^3).
f	Rate of infiltration capacity (LT^{-1}).

f_c	Ultimate rate of infiltration capacity (LT^{-1}).
F	Volume of infiltration (L^3).
F_c	Ultimate volume of infiltration (L^3).
F_p	Volume of potential infiltration (L^3).
FAC	Constant or function of some quantity.
FC	Effective volume of a cell at total saturation (L^3).
FOR	First-order reaction correction factor.
FP( )	Volume of potential infiltration at iteration ( ) (L^3).
FSM	Finite-state model.
g	Acceleration due to gravity (LT^{-2}).
h	Hydraulic head (L).
H	Hydrogen.
$_1H^2$	Deuterium.
$_1H^3$	Tritium.
H_2O^{18}	Water molecule with an atom of oxygen-18.
HCO_3^-	Bicarbonate ion.
HDO^{16}	Water molecule with one atom of hydrogen, one atom of deuterium, and one atom of oxygen-16.
HTO	Tritiated water.
i	(a) Index, (b) Group number, and (c) Iteration number (iterations).
I	Volumetric inflow to a stream reach (L^3).
I(t)	Internal age distribution of a fluid in a closed vessel.

j	Subscript
k_1	First-order reaction rate constant (T^{-1}).
K	Storage delay time (iterations or T).
K( )	Storage delay time at iteration ( ) (iterations or T).
K'	Storage constant in Muskingum equation (iterations or T).
K'( )	Storage constant in Muskingum equation at iteration ( ) (iterations or T).
MMC	Modified mixing cell.
n	(a) Index, (b) Exponent, and (c) Amount of material remaining after lapse of time t (M).
n_o	Amount of material present at time t = 0 (M).
N	Iteration number (iterations).
N'	Number of iterations required to purge a pulsed input of tracer from all cells in a finite-state model (iterations).
$\bar{N}$	Mean value of the concentration versus iteration number curve (iterations).
N_m	Maximum transit or age number (iterations).
O	Volumetric outflow from a stream reach (L^3).
O^{16}	Oxygen-16.
O^{18}	Oxygen-18.
p	Hydrostatic pressure ($ML^{-1}T^{-2}$).
ppm	Parts per million.
PDE	Partial differential equation.

Q	Volumetric flow rate (L^3T^{-1}).
Q( )	Volumetric rate of outflow from a linear storage element at time ( ) (L^3T^{-1}).
R( )	Mass or energy source/sink term at iteration ( ) (M or ML^2T^{-2}).
RD	Radioactive decay correction factor.
RVOL( )	Volumetric source/sink term at iteration ( ) (L^3).
S	Storage (L^3).
S( )	State of a cell at iteration ( ), the quantity of mass or energy in the cell (M or ML^2T^{-2}), and (b) Storage at time ( ) (L^3).
S'( )	State of a cell at iteration ( ) after both flow and radioactive decay changes (M).
SBDC( )	System boundary discharge concentration at iteration ( ) (ML^{-3}).
SBDV( )	System boundary discharge volume at iteration ( ) (L^3).
SBRC( )	System boundary recharge concentration at iteration ( ) (ML^{-3}).
SBRV( )	System boundary recharge volume at iteration ( ) (L^3).
SBRV'	Sum of the system boundary recharge volumes to a particular set of boundary cells at the first iteration (L^3).
SMC	Simple mixing cell.

SMOW	Standard Mean Ocean Water.
t	Time (T).
$\bar{t}$	Residence time (T).
$\bar{t}'$	Dimensionless residence time (iterations).
$t_{1/2}$	Half-life of a radioactive substance (T).
T	Tritium.
$\bar{T}$	Average or mean transit number (iterations or T).
$\hat{T}$	Estimator of average or mean transit number (iterations or T).
T(N)	Transit number distribution.
$T(N)_i$	Fraction of fluid elements in transit group number i.
TU	Tritium unit = one atom of tritium per 10^{18} atoms of hydrogen.
URV	Unit reference volume (L^3).
V	Volume (L^3).
V'	Volume of an individual mixing cell in a series of equi-volume cells (L^3).
VAR	Variance of concentration versus iteration number curve (iterations^2).
VAR'	Variance of the age number distribution (iterations^2 or T^2).
VOL( )	Effective volume of a cell at iteration ( ) (L^3).
VOL'	Sum of the effective volumes of a particular set of boundary cells receiving tracer at the first iteration only (L^3).

VOL" Effective volume of a cell designated as exchanging its volumetric amount first (L^3).

VOL"' Effective volume of the other cell participating in an exchange (L^3).

X Constant expressing the relative importance of inflow and outflow in determining the storage in a stream reach.

XVOL Decimal fraction of the effective volume of the cell designated as exchanging its volumetric amount first.

y Rate of application of water to a soil surface (LT^{-1}).

Y( ) Volumetric rate of application of water to a soil surface at iteration ( ) (L^3T^{-1}).

z Height relative to a datum (L).

* Multiplicative operator.

Δt Length of time represented by one iteration (T).

λ Radioactive decay constant (T^{-1}).

$\Lambda(t)$ Intensity function.

ρ Density of water (ML^{-3}).

Σ Summation operator.

τ Lag time (iterations or T).

$\tau_{1/2}$ Half-life of a chemical reaction (T).

ϕ Threshold volume for linear reservoir algorithm (L^3).

APPENDIX B

FORTRAN IV COMPUTER PROGRAM

The computer program written and used by the author consists of a main program, FISTMO, and eight subroutines: DECAY, VOLFAC, XCHANJ, FLOW, MIX, MAGEVO, MAGEIM, and PRINT. Subroutines DECAY, XCHANJ, MAGEVO, and MAGEIM may not be called depending upon the particular FSM used and/or the types of simulations conducted by the modeler. Instructions on the use of the program are contained within the listing and will not be discussed here.

The program is relatively inexpensive to operate. Each run of the Edwards Aquifer FSM cost a little over two dollars, whereas the Tucson Basin FSM, which required 50,000 years to reach steady state, cost approximately fifty dollars per run. The cost of running the Tucson Basin FSM could have been reduced substantially by increasing the size of the iteration interval from one year to five or ten years, although some loss in accuracy might have occurred.

As currently dimensioned, the program can accommodate a FSM of up to 101 cells, 20 of which are permitted to receive inputs from outside the FSM boundaries. The program

requires a central memory of 50600 (octal) on a Control Data Corporation 6400 computer.

```
      PROGRAM FISTMO (INPUT,OUTPUT)
C
C  FINITE-STATE MODEL (FSM) BY MICHAEL CAMPANA, DEPT. OF HYDROLOGY AND
C  WATER RESOURCES, UNIVERSITY OF ARIZONA, TUCSON, ARIZONA 85721, U.S.A.
C  AS CURRENTLY DIMENSIONED, THIS PROGRAM CAN MODEL A SYSTEM OF UP TO 101 CELLS,
C  20 OF WHICH CAN RECEIVE INPUTS FROM OUTSIDE THE FSM. ALL VOLUMES ARE
C  EXPRESSED AS MULTIPLES OF A UNIT REFERENCE VOLUME.
C  THIS PROGRAM WAS DESIGNED MAINLY FOR THE CASE OF A CONSTANT ITERATION
C  INTERVAL (DELT). HOWEVER, VARIABLE ITERATION INTERVALS CAN BE USED AS LONG
C  AS SUBROUTINES DECAY, MAGEVO AND MAGEIM ARE NOT USED. THESE SUBROUTINES
C  REQUIRE THAT DELT REMAIN CONSTANT THROUGHOUT THE OPERATION OF THE PROGRAM.
C  DATE OF LATEST REVISION - OCTOBER, 1975
C
      DIMENSION IPRIN(101),NOFRAC(40),BRECON(20),SRC(20)
      COMMON/ALPHA/RD,DELT,HALF,DATE,MAGE,MPUL,NCEL,ICEL,NUM,KZ
      COMMON/BETA/PHI(101)
      COMMON/   /NI(101),NC(101),NOIN(101),EXTI(101),EXTO(101),TI(101),
     $TO(101),EXVOL(101),KROUT(150,3),RI(150),RO(101),BRV(101),BDV(101),
     $STATE(2,101),VOL(2,101),FAC(101),T(101),ADD(101),SUMCON(101),
     $VAR(101),AGE(101),BDC(101),SBDV(101),SBRC(400,20),SBRV(40,20)
      COMMON/OMEGA/ITYPE,KM,LA,LB,LC,LD,IVAR,KNIT,ICON
C
C  READ NCEL, ICEL, NIT, MPUL, KZ, ISIT, NOREC
C  NCEL   =  TOTAL NUMBER OF CELLS IN THE FSM.
C  ICEL   =  NUMBER OF CELLS RECEIVING INPUTS FROM OUTSIDE THE FSM. THESE CELLS
C  MUST BE NUMBERED CONSECUTIVELY STARTING WITH NUMBER 1 THROUGH ICEL.
C  NIT    =  TOTAL NUMBER OF ITERATIONS.
C  MPUL   =  NUMBER OF ITERATIONS FOR WHICH THERE ARE CONCENTRATION INPUTS TO
C  THE FSM FROM OUTSIDE THE SYSTEM.
C  KZ   =  NUMBER OF ROWS IN KROUT(KZ,3) AND NUMBER OF ELEMENTS IN RI(KZ).
C  ISIT   =  NUMBER OF ITERATIONS FOR WHICH A CONCENTRATION OF SRC(J) IS INJECTED
C  INTO CELL J FROM OUTSIDE THE SYSTEM, WHERE J .LE. ICEL. ISIT MUST BE .LE. MPUL
C  NOREC = NUMBER OF CHANGES (UP TO 40) TO BE MADE IN THE SET OF SYSTEM BOUNDARY
C  RECHARGE VOLUMES DURING OPERATION OF THE FSM. IF THE SAME SET IS TO BE USED
C  AT EACH ITERATION, SET NOREC = 0.
      READ 100,NCEL,ICEL,NIT,MPUL,KZ,ISIT,NOREC
100   FORMAT (7I10)
      NUM = 1
      NN = NOREC + 1
C
C  READ MAGE, ITYPE, IVAR, ICON, NURD, IPI
C  MAGE   =  1 IF THE MEAN AGE NUMBERS AND VARIANCES ARE TO BE CALCULATED BY THE
C  IMPULSE-RESPONSE METHOD (SUBROUTINE MAGEIM). OTHERWISE, SET MAGE .NE. 1.
```

```
C ITYPE  =  2 FOR THE SMC ALGORITHM OR .NE. 2 FOR THE MMC ALGORITHM.
C IVAR   =  0 FOR THE STEADY VOLUME REGIME OR .NE. 0 FOR THE NON-STEADY VOLUME
C REGIME AS MODELED BY A LINEAR, TIME-INVARIANT RESERVOIR ALGORITHM.
C ICON   =  1 TO HAVE CELL STATES PRINTED OUT WITH CONCENTRATION DIMENSIONS OR
C .NE. 1 FOR PROPER (MASS OR ENERGY) STATE DIMENSIONS.
C NURD   = 1 IF INITIAL STATES ARE TO BE READ IN WITH CONCENTRATION DIMENSIONS.
C OTHERWISE, SET NURD .NE. 1.
C IPI    =  TOTAL NUMBER OF ITERATIONS AT WHICH DATA PRINTOUTS ARE DESIRED.
C IF PRINTOUTS ARE DESIRED AT EACH ITERATION, SET IPI = ANY NEGATIVE NUMBER.
      READ 120,MAGE,ITYPE,IVAR,ICON,NURD,IPI
120   FORMAT (6I10)
C
C IF NOREC.GT.0, READ NOFRAC(-), THE ARRAY STORING THE SPECIFIC ITERATION
C NUMBERS (IN ASCENDING ORDER) AT WHICH CHANGES IN THE SET OF SYSTEM BOUNDARY
C RECHARGE VOLUMES ARE TO BE MADE.
      IF(NOREC.GT.0) READ 160,(NOFRAC(J),J=1,NOREC)
C IF IVAR.NE.0, READ FAC(-), THE ARRAY STORING THE NON-STEADY VOLUME FACTORS.
C IF FAC(J) = 0.0, THEN A STEADY VOLUME REGIME IS SPECIFIED FOR CELL J.
C IF CELL J UNDERGOES PURE EXCHANGE ONLY, FAC(J) = 0.
      IF(IVAR.NE.0) READ 140,(FAC(J),J=1,NCEL)
140   FORMAT (10F8.4)
C IF IPI.GT.0,READ IPRIN(IPI), THE ARRAY STORING THE SPECIFIC ITERATION NUMBERS
C (IN ASCENDING ORDER) AT WHICH DATA PRINTOUTS ARE DESIRED.
      IF(IPI.GT.0) READ 160,(IPRIN(J),J=1,IPI)
160   FORMAT (10I8)
      NPI = 1
C
C READ HALF, DELT, DATE
C HALF   =  HALF-LIFE OF RADIOACTIVE TRACER. IF RADIOACTIVE DECAY IS NOT
C TO BE CONSIDERED, SET HALF = 0.0.
C DELT   =  REAL (CONSTANT) TIME BETWEEN ITERATIONS. IF REAL TIME IS NOT TO BE
C CONSIDERED OR THE REAL TIME BETWEEN ITERATIONS VARIES, SET DELT = 1.0.
C DATE   =  REAL TIME (DATE) AT TIME = 0. OTHERWISE, READ IN 0.
C NOTE - ANY TIME UNITS CAN BE USED AS LONG AS CONSISTENCY IS MAINTAINED
C THROUGHOUT THE PROGRAM.
      READ 180,HALF,DELT,DATE
180   FORMAT (F12.3,2F12.6)
C
C READ INITIAL STATE OF EACH CELL. INITIAL STATES CAN HAVE EITHER CONCENTRATION
C DIMENSIONS OR PROPER STATE (MASS OR ENERGY) DIMENSIONS.  IF STATES ARE READ
C IN WITH PROPER STATE DIMENSIONS, SET NURD .NE. 1 (STATEMENT NO. 120).
C STATE(1,X) IS THE STATE OF CELL X AT THE START OF ITERATION I.
C STATE(2,X) IS THE STATE OF CELL X AT THE END OF ITERATION I.
```

```
      READ 200,(STATE(1,J),J=1,NCEL)
200   FORMAT (8F10.3)
C
C READ INITIAL VOLUME OF EACH CELL. THESE VOLUMES WILL REMAIN CONSTANT UNLESS
C A NON-STEADY VOLUME REGIME IS SPECIFIED.
      READ 240,(VOL(1,J),J=1,NCEL)
C
C IF IVAR.NE.0, READ IN CELL THRESHOLD VOLUMES FOR THE LINEAR RESERVOIR
C ALGORITHM. THESE VOLUMES CAN BE ZERO IF NO THRESHOLDS ARE DESIRED. A CELL WILL
C NOT BE ALLOWED TO DISCHARGE UNTIL ITS VOLUME EXCEEDS THE THRESHOLD VOLUME.
      IF(IVAR.NE.0) READ 240,(PHI(J),J=1,NCEL)
C
C READ IN SBRV(-,-), THE SYSTEM BOUNDARY RECHARGE VOLUME ARRAY. ONLY THE FIRST
C ICEL CELLS CAN RECEIVE SYSTEM BOUNDARY RECHARGE VOLUMES.
      DO 220 I = 1,NN
220   READ 240,(SBRV(I,J),J=1,ICEL)
240   FORMAT (8F10.4)
C
C READ SYSTEM BOUNDARY RECHARGE CONCENTRATIONS. ONLY THE FIRST ICEL CELLS CAN
C RECEIVE THESE QUANTITIES. IF THE SAME SET OF INPUT CONCENTRATIONS IS TO BE
C USED FOR THE ICEL CELLS FOR A LARGE NUMBER OF ITERATIONS, ONE CAN READ IN
C THESE VALUES WITH THE SRC(-) ARRAY AND THE NUMBER OF ITERATIONS (ISIT) FOR
C WHICH IT IS TO BE USED. ADDITIONAL DATA CAN BE READ IN WITH THE SBRC(-,-)
C ARRAY ACCORDING TO STATEMENT NO. 300. IF ONE DOES NOT WISH TO USE THE
C ISIT-SRC(-) FEATURE, PUNCH IN A ZERO FOR ISIT (STATEMENT NO. 100) AND REMOVE
C ANY SRC(-) DATA CARDS FROM THE DECK. IF ONLY THE CASE WHERE ISIT = MPUL IS TO
C BE CONSIDERED, REMOVE ANY SBRC(-,-) DATA CARDS FROM THE DECK. NOTE THAT WHEN
C THE NUMBER OF ITERATIONS EXCEEDS MPUL, SBRC(-,-) IS ZEROED (STATEMENT NO. 580)
C
      IF(ISIT.EQ.0) GO TO 280
      READ 200,(SRC(J),J=1,ICEL)
      IF(ISIT.EQ.MPUL) GO TO 320
      DO 260 J=1,ICEL
      DO 260 I=1,ISIT
260   SBRC(I,J) = SRC(J)
280   IISIT = ISIT + 1
      DO 300 J=1,ICEL
300   READ 200, (SBRC(I,J),I=IISIT,MPUL)
C
C READ IN ARRAYS KROUT(-,-), RI(-) AND RO(-). THE FIRST TWO ARRAYS COMPLETELY
C DESCRIBE THE FLOW PATHS AMONG THE CELLS OF THE FSM. NOTING THAT EACH CELL HAS
C BEEN ASSIGNED A NUMBER FOR IDENTIFICATION PURPOSES, KROUT(1,1) THROUGH
C KROUT(ICEL,1) CONTAINS THE NUMBERS OF THE CELLS (IN ASCENDING ORDER)
C RECEIVING INPUTS FROM OUTSIDE THE FSM. KROUT(1,(2 AND 3)) THROUGH
```

```
C KROUT(ICEL,(2 AND 3)) AND RI(1) THROUGH RI(ICEL) ARE LEFT BLANK.
C KROUT(ICEL+1,(1 AND 2)) TO KROUT(KZ,(1 AND 2)) IS A LIST OF CELL PAIRS
C DESCRIBING THE FLOW PATHS. THE DISCHARGING CELL IS PLACED IN THE FIRST COLUMN
C AND THE CELL RECEIVING THE DISCHARGE IS PLACED IN THE SECOND COLUMN. RI(-)
C CONTAINS THE FRACTION OF THE OUTPUT OF THE CELL IN THE FIRST COLUMN THAT FLOWS
C TO THE CELL IN THE SECOND COLUMN. FOR EXAMPLE, SUPPOSE THAT CELL 3 DISCHARGES
C 40 PERCENT OF ITS TOTAL DISCHARGE TO CELL 8. 3 WOULD THEN BE PLACED IN THE
C FIRST COLUMN OF THE APPROPRIATE ROW OF KROUT(-,-) AND 8 WOULD BE ENTERED IN
C THE SECOND COLUMN. THE THIRD COLUMN OF KROUT(-,-) WOULD BE LEFT BLANK, AND THE
C NUMBER .40 WOULD BE PLACED IN THE RI(-) ARRAY IN THE POSITION CORRESPONDING
C TO THE ROW OF THE KROUT(-,-) ARRAY. IN FACT, ONE CAN THINK OF THE RI(-)
C ARRAY AS BEING THE FOURTH COLUMN OF THE KROUT(-,-) ARRAY. IF TWO CELLS ARE
C TO EXCHANGE EQUAL VOLUMES OF WATER, PROCEED AS BEFORE EXCEPT PLACE A 1 IN THE
C THIRD COLUMN OF KROUT(-,-). THE VOLUME EXCHANGED IS GIVEN AS A DECIMAL
C (.GT.0 AND .LE.1) OF THE VOLUME OF THE CELL IN THE FIRST COLUMN. THIS
C QUANTITY IS PLACED IN THE APPROPRIATE POSITION OF THE RI(-) ARRAY.
C NOTE - BEFORE A CELL CAN DISCHARGE SOME OF ITS CONTENTS, ALL INPUTS TO THAT
C CELL MUST BE LISTED. IF, FOR EXAMPLE, CELL 6, WHICH FLOWS TO CELL 8, RECEIVES
C INPUTS FROM CELLS 3 AND 5, THE PAIRS (3,6) AND (5,6) MUST BE LISTED IN THE
C KROUT(-,-) ARRAY BEFORE THE PAIR (6,8). IN THE CASE OF AN EXCHANGE, ALL
C NON-EXCHANGE INPUTS TO BOTH CELLS SHOULD BE LISTED BEFORE THE EXCHANGE OCCURS.
C IF THIS IS NOT POSSIBLE, ALL NON-EXCHANGE INPUTS TO THE CELL DEPICTED AS
C DISCHARGING ITS EXCHANGE VOLUME FIRST (THE CELL IN COLUMN 1) SHOULD BE LISTED
C BEFORE THE EXCHANGE OCCURS.
C IF ALL OF THE OUTPUT OF A CELL IS NOT ACCOUNTED FOR, THE PROGRAM ASSUMES
C THAT IT IS REMOVED FROM THE FSM. THE FRACTION OF A CELL OUTPUT THAT IS
C DISCHARGED OUTSIDE THE FSM SHOULD BE ENTERED IN THE POSITION OF THE RO(-)
C ARRAY CORRESPONDING TO THAT CELL. FOR EXAMPLE, IF 25 PERCENT OF THE OUTPUT
C OF CELL J IS DISCHARGED OUTSIDE THE FSM, ENTER .25 IN RO(J).  MAKE CERTAIN
C THAT EACH CELL DISCHARGES EXACTLY 100 PERCENT OF ITS OUTPUT (IGNORE ANY
C EXCHANGES) TO OTHER CELLS AND/OR OUTSIDE THE FSM.
C
320     DO 340 J = 1,3
340     READ 360,(KROUT(I,J),I=1,KZ)
360     FORMAT (20I4)
        READ 380, (RI(I),I=1,KZ)
        READ 380, (RO(J),J=1,NCEL)
380     FORMAT (16F5.3)
C
C READ NOIN(-), THE ARRAY CONTAINING THE NUMBER OF INPUTS TO EACH CELL. THESE
C ARE INPUTS FROM OTHER CELLS (INCLUDING ANY EXCHANGES) AND/OR FROM OUTSIDE
C THE FSM.
```

```
      READ 400, (NOIN(K),K=1,NCEL)
400   FORMAT (40I2)
C
      PRINT 1010, (NCEL,ICEL,ITYPE)
      PRINT 1020,(NIT,MPUL,ICON)
      PRINT 1030,(NOREC,DATE,IVAR)
      CALL DECAY
      PRINT 1040
      DO 420 M = 1,KZ
420   PRINT 1050,((KROUT(M,N),N=1,3),RI(M))
      PRINT 1060
      IF(IVAR.NE.0) PRINT 1070
      DO 460 J = 1,NCEL
      VOL(2,J) = 0.0
      STATE(2,J) = 0.0
      T(J) = 0.0
      ADD(J) = 0.0
      AGE(J) = 0.0
      VAR(J) = 0.0
      SUMCON(J) = 0.0
C
C NOTE - INITIAL STATES PRINTED OUT EXACTLY AS THEY WERE READ IN.
C
      PRINT 1080,(J,STATE(1,J),VOL(1,J),NOIN(J),RO(J))
      IF(IVAR.NE.0) PRINT 1090,(FAC(J),PHI(J),J)
C
C IF NECESSARY, CONVERT INITIAL STATES GIVEN WITH CONCENTRATION DIMENSIONS
C TO PROPER STATE DIMENSIONS (CONCENTRATION*UNIT REFERENCE VOLUME DIMENSIONS).
C
440   IF(NURD.EQ.1) STATE(1,J) = STATE(1,J)*VOL(1,J)
460   CONTINUE
C
C START ITERATING
C
480   DO 800 INIT = 1,NIT
      KNIT = INIT
C
C CHECK FOR CHANGES IN SYSTEM BOUNDARY RECHARGE VOLUMES
C
      IF(NUM.GE.NN) GO TO 500
      IF(KNIT.EQ.NOFRAC(NUM)) NUM = NUM + 1
C
```

```
C ZERO ARRAYS
C
500    DO 520 KZERO = 1,NCEL
       TI(KZERO) = 0.0
       TO(KZERO) = 0.0
       BRV(KZERO) = 0.0
       BDV(KZERO) = 0.0
       BDC(KZERO) = 0.0
       SBDV(KZERO) = 0.0
       EXTI(KZERO) = 0.0
       EXTO(KZERO) = 0.0
       EXVOL(KZERO) = 0.0
       NI(KZERO) = 0
520    NC(KZERO) = 0
C
C GO THROUGH KROUT(-,-) ROW-BY-ROW
C
       DO 660 IROW = 1,KZ
       KM = IROW
       LA = KROUT(KM,1)
       LB = KROUT(KM,2)
       LC = KROUT(KM,3)
C
C CHECK FOR FLOW TO ANOTHER CELL
C
       IF(LB.EQ.0) 540,600
C
C CHECK SYSTEM BOUNDARY RECHARGE CONCENTRATIONS
C
540    IF(ISIT.EQ.MPUL) GO TO 560
       BRECON(LA) = SRC(KNIT,LA)
       GO TO 580
560    BRECON(LA) = SRC(LA)
580    IF(KNIT.GT.MPUL) BRECON(LA) = 0.0
C
C CALCULATE BRV AND TOTAL AMOUNT OF MATERIAL (TI(-)) ENTERING CELL FROM OUTSIDE
C THE SYSTEM
C
       BRV(LA) = BRV(LA) + SBRV(NUM,LA)
       TI(LA) = TI(LA) + (BRV(LA)*BRECON(LA))
       NI(LA) = NI(LA) + 1
       GO TO 660
```

```
C
C  CHECK FOR EXCHANGE BETWEEN CELLS
C
600    IF(LC.EQ.1) 620,640
620    CALL XCHANJ
       GO TO 660
640    CALL FLOW
660    KM = 0
C
C  CHECK FOR RADIOACTIVE DECAY AND ADJUST STATES, IF NECESSARY
C
       IF(RD.EQ.1.0) GO TO 700
       DO 680 NZ=1,NCEL
680    STATE(2,NZ) = STATE(2,NZ)*RD
700    IF(MAGE.EQ.1) CALL MAGEIM
C
C  CHECK TO SEE IF PRINTOUTS ARE WANTED
C
       IF(IPI.LT.0) GO TO 740
       IF(NPI.GT.IPI) GO TO 760
       IF(KNIT.EQ.IPRIN(NPI)) GO TO 720
       GO TO 760
720    NPI = NPI + 1
740    CALL PRINT
760    DO 780 KS = 1,NCEL
       VOL(1,KS) = VOL(2,KS)
       VOL(2,KS) = 0.0
       STATE(1,KS) = STATE(2,KS)
780    STATE(2,KS) = 0.0
800    KNIT = 0
820    IF(IVAR.NE.0.OR.NOREC.GT.0) GO TO 9000
       CALL MAGEVO
       PRINT 1100
       DO 840 J = 1,NCEL
       SBDV(J) = RO(J)*BDV(J)
840    PRINT 1110,(J,VOL(1,J),BRV(J),BDV(J),EXVOL(J),SBDV(J),AGE(J),J)
1010   FORMAT (1H1,4X,*NUMBER OF CELLS =*,I5,10X,*NO. OF CELLS RECEIVING
      $INPUTS FROM OUTSIDE SYSTEM =*,I5,8X,*ITYPE =*,I3,*  (2 = SMC)*/)
1020   FORMAT (5X,*NO. OF ITERATIONS =*,I7,5X,*CONC. INPUTS FROM OUTSIDE
      $SYSTEM FOR *,I7,* ITERATIONS (= MPUL)*,5X,*ICON =*,I5,* (1 = CONC.
      $DIM.)*/)
1030   FORMAT (5X,*CHANGES IN SBRV =*,I4,15X,*STARTING TIME =*,F12.6,20X,
      $*IVAR =*,I5,*  (C = STEADY VOLUME CASE)*/)
```

```
1040   FORMAT (4(/)24X,*KROUT*,14X,*RI*/)
1050   FORMAT (/13X,3(4X,I3),8X,F5.3)
1060   FORMAT (6(/)2X,*CELL NO.*,5X,*INITIAL STATE OR CONC.*,5X,*INITIAL
      $VOLUME*,5X,*INPUTS*,5X,*RO*)
1070   FORMAT (1H+,83X,*FAC*,6X,*THRESHOLD*,4X,*CELL NO.*)
1080   FORMAT (/2X,I5,12X,F11.3,12X,F10.4,8X,I4,7X,F5.3)
1090   FORMAT (1H+,79X,F8.4,4X,F10.4,6X,I3)
1100   FORMAT (7(/)1X,*CELL NO.*,5X,*VOLUME*,9X,*BRV*,12X,*BDV*,9X,*EXVOL
      $*,10X,*SBDV*,8X,*MEAN AGE NO.*,5X,*CELL NO.*/)
1110   FORMAT (/3X,I3,1X,5(4X,F10.6),4X,F11.3,9X,I3)
9000   STOP
       END
```

```
      SUBROUTINE DECAY
C
C  THIS SUBROUTINE CALCULATES THE RADIOACTIVE DECAY CORRECTION FACTOR (RD).
C  THIS SUBROUTINE REQUIRES A CONSTANT DELT.
C
      COMMON/ALPHA/RD,DELT,HALF,DATE,MAGE,MPUL,NCEL,ICEL,NUM,KZ
      IF(HALF.NE.C.O) RD = EXP(-(ALOG(2.00)*DELT/HALF))
      IF(HALF.EQ.O.O) RD = 1.0
      PRINT 1000, (RD,DELT)
      IF(HALF.NE.C.O) PRINT 1001, HALF
1000  FORMAT (5X,*RADICACTIVE DECAY = *,E14.8,8X,*CNE ITERATION = *,E12.
     $6,* (TIME UNITS)*/)
1001  FORMAT (5X,*HALF-LIFE = *,E12.6,* (TIME UNITS)*/)
      RETURN
      END
```

```
      SUBROUTINE VOLFAC
C
C  THIS SUBROUTINE CALCULATES VOLUMES AND BOUNDARY DISCHARGE VOLUMES. IF IVAR =0,
C  A STEADY VOLUME REGIME WITH BRV = BDV IS SPECIFIED. IF IVAR .NE. 0, CHANGES
C  IN VOLUME AND BDV ARE CALCULATED BY THE FOLLOWING TWO EQUATIONS -
C
C     1)     VOL(I+1)   =  VOL(I) + BRV(I+1) - BDV(I+1)        (FSM STORAGE EQN.)
C     2)     BDV(I+1)   =  (VOL(I+1)-PHI(-))/FAC(-)          (LINEAR TIME-INVARIANT
C                                                              RESERVOIR EQN.)
C
C
C  NOTE THAT IF THE CELL EFFECTIVE VOLUME .LE. PHI, BDV IS SET EQUAL TO ZERO.
C  NOTE ALSO THAT IF FOR A GIVEN CELL, FAC(-) = 0.0, A STEADY VOLUME REGIME IS
C  ALWAYS SPECIFIED FOR THAT CELL.
C
      COMMON/BETA/PHI(101)
      COMMON/   /NI(101),NC(101),NOIN(101),EXTI(101),EXTO(101),TI(101),
     $TO(101),EXVOL(101),KROUT(150,3),RI(150),RO(101),BRV(101),BDV(101),
     $STATE(2,101),VOL(2,101),FAC(101),T(101),ADD(101),SUMCON(101),
     $VAR(101),AGE(101),BDC(101),SBDV(101),SBRC(400,20),SBRV(40,20)
      COMMON/OMEGA/ITYPE,KM,LA,LB,LC,LD,IVAR,KNIT,ICON
      IF(IVAR.EQ.0) GO TO 150
      IF(FAC(LD).EQ.0.0) GO TO 150
      VOL(2,LD) = VOL(1,LD) + BRV(LD)
      IF(VOL(2,LD).GT.PHI(LD)) GO TO 100
      BDV(LD) = 0.0
      RETURN
100   VOL(2,LD) = (FAC(LD)*(VOL(1,LD)+BRV(LD)) + PHI(LD))/(FAC(LD)+1.0)
      BDV(LD) = (VOL(2,LD) - PHI(LD))/FAC(LD)
      IF(BDV(LD).LE.(VOL(2,LD)-PHI(LD))) RETURN
      BDV(LD) = VOL(2,LD) - PHI(LD)
      VOL(2,LD) = VOL(1,LD) + BRV(LD) - BDV(LD)
      RETURN
150   BDV(LD) = BRV(LD)
      VOL(2,LD) = VOL(1,LD)
      RETURN
      END
```

```
      SUBROUTINE XCHANJ
C
C  THIS SUBROUTINE EXCHANGES EQUAL VOLUMES OF WATER BETWEEN TWO CELLS.
C
      COMMON/   /NI(101),NC(101),NOIN(101),EXTI(101),EXTO(101),TI(101),
     $TO(101),EXVOL(101),KROUT(150,3),RI(150),RO(101),BRV(101),BDV(101),
     $STATE(2,101),VOL(2,101),FAC(101),T(101),ADD(101),SUMCON(101),
     $VAR(101),AGE(101),BDC(101),SBDV(101),SBRC(400,20),SBRV(40,20)
      COMMON/OMEGA/ITYPE,KM,LA,LB,LC,LD,IVAR,KNIT,ICON
      IF(ITYPE.EQ.2) GO TO 100                                          MMC ONLY
      XV = RI(KM)*VOL(1,LA)                                             MMC ONLY
      EXTO(LA) = XV*(STATE(1,LA)/VOL(1,LA))
      EXTI(LB) = EXTI(LB) + EXTO(LA)                                    MMC ONLY
      EXTOLB = XV*(STATE(1,LB)/VOL(1,LB))
      GO TO 150                                                         SMC ONLY
100   XV = RI(KM)*(VOL(1,LA)+BRV(LA))                                   SMC ONLY
      EXTO(LA) = XV*(TI(LA)+STATE(1,LA))/(VOL(1,LA)+BRV(LA))
      EXTI(LB) = EXTI(LB) + EXTO(LA)
      EXTOLB = XV*(TI(LB)+EXTI(LB)+STATE(1,LB))/(VOL(1,LB)+BRV(LB)+XV)  SMC ONLY
150   EXTI(LA) = EXTI(LA) + EXTOLB
      EXTO(LB) = EXTO(LB) + EXTOLB
      NI(LA) = NI(LA) + 1
      NI(LB) = NI(LB) + 1
      LD = LA
C
C  CHECK TO SEE WHETHER ALL INPUTS ARE ACCOUNTED FOR
C
      DO 300 JILL = 1,2
      IF(NI(LD).EQ.NOIN(LD)) 200,250
200   CALL VOLFAC
      CALL MIX
C
C  EXVOL(J) CONTAINS CUMULATIVE EXCHANGE VOLUME FOR CELL J DURING THE ITERATION
C
250   EXVOL(LD) = EXVOL(LD) + XV
300   LD = LB
      EXTOLB = 0.0
      XV = 0.0
      RETURN
      END
```

```
      SUBROUTINE FLOW
C
C  THIS SUBROUTINE CALCULATES FLOW CHANGES.
C
      COMMON/   /NI(101),NC(101),NOIN(101),EXTI(101),EXTO(101),TI(101),
     $TO(101),EXVOL(101),KROUT(150,3),RI(150),RO(101),BRV(101),BDV(101),
     $STATE(2,101),VOL(2,101),FAC(101),T(101),ADD(101),SUMCON(101),
     $VAR(101),AGE(101),BDC(101),SBDV(101),SBRC(400,20),SBRV(40,20)
      COMMON/OMEGA/ITYPE,KM,LA,LB,LC,LD,IVAR,KNIT,ICON
C
C  CHECK TO SEE WHETHER CELL HAS BEEN MIXED AND VOLUMETRIC QUANTITIES CALCULATED
C  BEFORE ALLOWING IT TO DISCHARGE
C
      IF(NC(LA).GT.0) GO TO 100
      LD = LA
      CALL VOLFAC
      CALL MIX
C
C  CALCULATE TOTAL AMOUNT OF MATERIAL ENTERING CELL AND BRV
C
100   TI(LB) = TI(LB) + TO(LA)*RI(KM)
      BRV(LB) = BRV(LB) + BDV(LA)*RI(KM)
      NI(LB) = NI(LB) + 1
C
C  CHECK TO SEE WHETHER ALL INPUTS ARE ACCOUNTED FOR
C
      IF(NI(LB).EQ.NOIN(LB)) 150,200
150   LD = LB
      CALL VOLFAC
      CALL MIX
200   RETURN
      END
```

```
      SUBROUTINE MIX
C
C THIS SUBROUTINE MIXES THE CONTENTS OF A CELL ONCE IT HAS RECEIVED ALL OF
C ITS INPUTS. THE CELL STATE IS CALCULATED HERE, AS IS THE TOTAL AMOUNT OF
C MATERIAL MOVING OUT OF THE CELL (TO(-)).
C
      COMMON/   /NI(101),NC(101),NOIN(101),EXTI(101),EXTO(101),TI(101),
     $TO(101),EXVOL(101),KROUT(150,3),RI(150),RO(101),BRV(101),BDV(101),
     $STATE(2,101),VOL(2,101),FAC(101),T(101),ADD(101),SUMCON(101),
     $VAR(101),AGE(101),BDC(101),SBDV(101),SBRC(400,20),SBRV(40,20)
      COMMON/OMEGA/ITYPE,KM,LA,LB,LC,LD,IVAR,KNIT,ICON
      IF(ITYPE.EQ.2) GO TO 100
      TO(LD) = BDV(LD)*(STATE(1,LD)/VOL(1,LD))                          MMC ONLY
      GO TO 150
100   TO(LD) =BDV(LD)*(STATE(1,LD)+TI(LD)+EXTI(LD)-EXTO(LD))/(VOL(1,LD)+
     $BRV(LD))                                                          SMC ONLY
150   STATE(2,LD) = STATE(1,LD)+TI(LD)+EXTI(LD)-TO(LD)-EXTO(LD)
      NC(LD) = NC(LD) + 1
      RETURN
      END
```

```
      SUBROUTINE MAGEVO
C
C  THIS SUBROUTINE CALCULATES THE CELL MEAN AGE NUMBERS USING THE VOLUME METHOD.
C  THIS SUBROUTINE SHOULD NOT BE USED FOR A FSM IN WHICH EXCHANGES OCCUR, ELSE
C  ERRONEOUS ANSWERS WILL RESULT. THIS SUBROUTINE REQUIRES A CONSTANT DELT.
C
      COMMON/ALPHA/RD,DELT,HALF,DATE,MAGE,MPUL,NCEL,ICEL,NUM,KZ
      COMMON/   /NI(101),NC(101),NOIN(101),EXTI(101),EXTO(101),TI(101),
     $TO(101),EXVOL(101),KROUT(150,3),RI(150),RO(101),BRV(101),BDV(101),
     $STATE(2,101),VOL(2,101),FAC(101),T(101),ADD(101),SUMCON(101),
     $VAR(101),AGE(101),BDC(101),SBDV(101),SBRC(400,20),SBRV(40,20)
      COMMON/OMEGA/ITYPE,KM,LA,LB,LC,LD,IVAR,KNIT,ICON
      DO 100 M = 1,NCEL
      AGE(M) = 0.0
100   NI(M) = 0
      DO 300 J = 1,KZ
      LA = KROUT(J,1)
      LB = KROUT(J,2)
      LC = KROUT(J,3)
      IF(LB.NE.0) GO TO 200
      IF(ITYPE.EQ.2) GO TO 150
      AGE(LA) = VOL(1,LA)/BRV(LA)
      GO TO 300
150   AGE(LA) = (VOL(1,LA)+SBRV(NUM,LA))/BRV(LA)
      GO TO 300
200   IF(LC.EQ.1) GO TO 300
250   AGE(LB) = AGE(LB) + ((AGE(LA)*BDV(LA)*RI(J))/BRV(LB))
      NI(LB) = NI(LB) + 1
      IF(LB.GT.ICEL.AND.NI(LB).EQ.NOIN(LB)) AGE(LB) = AGE(LB) + (VOL(1,L
     $B)/BRV(LB))
300   CONTINUE
C
C  ACCOUNT FOR REAL TIME DELT
C
      DO 350 J = 1,NCEL
350   AGE(J) = AGE(J)*DELT
      RETURN
      END
```

```
      SUBROUTINE MAGEIM
C
CC THIS SUBROUTINE IS USED ONLY IN THE CASE OF AN IMPULSE-RESPONSE EXPERIMENT.
CC THE QUANTITIES CALCULATED HERE WILL CONVERGE TO THE MEAN (MEAN AGE NUMBER)
CC AND VARIANCE OF THE AGE NUMBER DISTRIBUTION OF EACH CELL AFTER A SUFFICIENT
CC NUMBER OF ITERATIONS. USE ONLY FOR A STEADY FLOW, STEADY VOLUME FSM.
CC THIS SUBROUTINE REQUIRES A CONSTANT DELT.
CC
      COMMON/ALPHA/RD,DELT,HALF,DATE,MAGE,MPUL,NCEL,ICEL,NUM,KZ
      COMMON/    /NI(101),NC(101),NOIN(101),EXTI(101),EXTO(101),TI(101),
     $TO(101),EXVOL(101),KROUT(150,3),RI(150),RO(101),BRV(101),BDV(101),
     $STATE(2,101),VOL(2,101),FAC(101),T(101),ADD(101),SUMCON(101),
     $VAR(101),AGE(101),BDC(101),SBDV(101),SBRC(400,20),SBRV(40,20)
      COMMON/OMEGA/ITYPE,KM,LA,LB,LC,LD,IVAR,KNIT,ICON
      KK = KNIT - MPUL + 1
      DO 100 I = 1,NCEL
      RATIO = STATE(2,I)/VOL(2,I)
      SUMCON(I) = SUMCON(I) + RATIO
      AGE(I) = T(I) + (FLOAT(KK)*RATIO)
      ADD(I) = ADD(I) + RATIO*(FLOAT(KK)**2)
      T(I) = AGE(I)
      IF(SUMCON(I).EQ.0.0) GO TO 100
      AGE(I) = AGE(I)/SUMCON(I)
      VAR(I) = (ADD(I)/SUMCON(I)) - AGE(I)**2
100   RATIO = 0.0
C
CC ACCOUNT FOR REAL TIME DELT
C
      DO 150 J = 1,NCEL
      AGE(J) = AGE(J)*DELT
150   VAR(J) = VAR(J)*(DELT**2)
      RETURN
      END
```

```
      SUBROUTINE PRINT
C
CC  THIS SUBROUTINE CONTROLS THE PRINTING ACTION
C
      COMMON/ALPHA/RD,DELT,HALF,DATE,MAGE,MPUL,NCEL,ICEL,NUM,KZ
      COMMON/    /NI(101),NC(101),NOIN(101),EXTI(101),EXTO(101),TI(101),
     $TO(101),EXVOL(101),KROUT(150,3),RI(150),RO(101),BRV(101),BDV(101),
     $STATE(2,101),VOL(2,101),FAC(101),T(101),ADD(101),SUMCON(101),
     $VAR(101),AGE(101),BDC(101),SBDV(101),SBRC(400,20),SBRV(40,20)
      COMMON/OMEGA/ITYPE,KM,LA,LB,LC,LD,IVAR,KNIT,ICON
      TIME = DATE + (FLOAT(KNIT)*DELT)
      PRINT 1001,(KNIT,TIME)
      PRINT 1002
      PRINT 1006
      IF(MAGE.EQ.1) PRINT 1003
      DO 200 J = 1,NCEL
      TI(J) = TI(J) + EXTI(J)
      SBDV(J) = RC(J)*BDV(J)
      IF(ITYPE.EQ.2) GO TO 100
      BDC(J) = STATE(1,J)/VOL(1,J)                                    MMC ONLY
      GO TO 150
100   BDC(J) = (STATE(1,J)+TI(J)-EXTO(J))/(VOL(1,J)+BRV(J))           SMC ONLY
C
C  ADD TOTAL OUT DUE TO EXCHANGE TO GET CUMULATIVE TOTAL OUT
C
150   TO(J) = TO(J) + EXTO(J)
      IF(ICON.EQ.1) STATE(2,J) = STATE(2,J)/VOL(2,J)
      PRINT 1004,(J,STATE(2,J),TI(J),TO(J),BDC(J))
      IF(ICON.EQ.1) STATE(2,J) = STATE(2,J)*VOL(2,J)
      PRINT 1007,(VOL(2,J),BRV(J),BDV(J),SBDV(J))
      IF(MAGE.EQ.1) PRINT 1005,(AGE(J),VAR(J))
200   CONTINUE
1001  FORMAT (4(/)15X,*ITERATION NO. *,I6,7X,*TIME = END OF *,F12.5//)
1002  FORMAT (1X,*CELL*,2X,*STATE OR CONC.*,3X,*TOTAL IN*,3X,*TOTAL OUT*
     $,5X,*BDC*)
1003  FORMAT (1H+,110X,*MEAN*,7X,*VARIANCE*)
1004  FORMAT (/1X,I3,3X,E11.5,3X,E11.5,1X,E11.5,2X,E11.5)
1005  FORMAT (1H+,106X,F11.3,2X,E12.6)
1006  FORMAT (1H+,61X,*VOLUME*,6X,*BRV*,9X,*BDV*,8X,*SBDV*)
1007  FORMAT (1H+,57X,2(2X,F8.4),2(4X,F8.4))
      RETURN
      END
```

REFERENCES

Abbott, P. L., 1975, On the hydrology of the Edwards Limestone, south-central Texas, Journal of Hydrology, v. 24, n. 3/4, pp. 251-270.

Anderson, T. W., 1972, Electrical-analog analysis of the hydrologic system, Tucson basin, southeastern Arizona, U. S. Geological Survey Water-Supply Paper 1939-C, 34p.

Banks, Robert B., 1974, A mixing cell model for longitudinal dispersion in open channels, Water Resources Research, v. 10, n. 2, pp. 357-358.

Bear, Jacob, and Todd, David K., 1960, The transition zone between fresh and salt waters in a coastal aquifer, University of California at Berkeley Water Resources Center Contribution 29, 156p.

Bennett, Richmond, 1965, Carbon-14 dating of groundwater in an arid basin, Proceedings, Sixth International Conference on Radiocarbon and Tritium Dating at Washington State University, Pullman, Washington, pp. 590-596.

Bolin, B., and Rodhe, H., 1973, A note on the concepts of age distribution and transit time in natural reservoirs, Tellus, v. 25, n. 1, pp. 58-62.

Bredehoeft, John D., and Pinder, George F., 1973, Mass transport in flowing groundwater, Water Resources Research, v. 9, n. 1, pp. 194-210.

Burkham, D. E., 1970, Depletion of streamflow by infiltration in the main channels of the Tucson basin, southeastern Arizona, U. S. Geological Survey Water-Supply Paper 1939-B, 36p.

Condes de la Torre, Alberto, 1970, Streamflow in the upper Santa Cruz River basin, Santa Cruz and Pima Counties, Arizona, U. S. Geological Survey Water-Supply Paper 1939-A, 26p.

Craig, H., 1957, The natural distribution of radiocarbon and the exchange time of carbon dioxide between atmosphere and sea, Tellus, v. 9, pp. 1-17.

Damon, Paul E., Long, Austin, and Grey, Donald C., 1966, Fluctuation of atmospheric C-14 during the last six millennia, Journal of Geophysical Research, v. 71, n. 4, pp. 1055-1063.

Davidson, E. S., 1973, Geohydrology and water resources of the Tucson basin, Arizona, U. S. Geological Survey Water-Supply Paper 1939-E, 81p.

Deans, H. A., and Lapidus, Leon, 1960, A computational model for predicting and correlating the behavior of fixed-bed reactors, parts I and II, Journal, American Institute of Chemical Engineers, v. 6, n. 4, pp. 656-668.

Dooge, James C. I., 1959, A general theory of the unit hydrograph, Journal of Geophysical Research, v. 64, n. 2, pp. 241-256.

Dooge, James C. I., 1960, The routing of groundwater recharge through typical elements of linear storage, International Association of Scientific Hydrology, Publication 52, General Assembly of Helsinki, v. 2, pp. 286-300.

Dooge, James C. I., 1973, Linear theory of hydrologic systems, Technical Bulletin 1468, Agricultural Research Service, U. S. Department of Agriculture, 327p.

Eliasson, Jonas, 1971, Mechanism of ground water reservoirs, Nordic Hydrology, v. 2, pp. 266-277.

Eliasson, Jonas, St. Arnalds, Sigurdur, Johannsson, Skuli, and Kjaran, Snorri P., 1973, Reservoir mechanism in an aquifer of arbitrary boundary shape, Nordic Hydrology, v. 4, pp. 129-146.

Eriksson, E., 1971, Compartment models and reservoir theory, Annual Review of Ecology and Systematics, v. 2, pp. 67-84.

Fan, L. T., Chen, Michael S. K., Ahn, Y. K., and Wen, C. Y., 1969, Mixing models with varying stage size, Canadian Journal of Chemical Engineering, v. 47, n. 2, pp. 141-148.

Freeze, R. Allan, 1969, Theoretical analysis of regional groundwater flow, Scientific Series n. 3, Inland Waters Branch, Department of Energy, Mines and Resources, Ottawa, Canada, 147p.

Garder, A. O., Peaceman, D. W., and Pozzi, A. L., Jr., 1964, Numerical calculation of multidimensional miscible displacement by the method of characteristics, Journal, Society of Petroleum Engineers, v. 4, n. 1, pp. 26-36.

Garland, George D., 1971, Introduction to geophysics-mantle, core and crust, W. B. Saunders Company, Philadelphia, Pa., 420p.

Garza, Sergio, 1962, Recharge, discharge, and changes in groundwater storage in the Edwards and associated limestones, San Antonio area, Texas, a progress report on studies, 1955-59, Texas Board Water Engineers Bulletin 6201, 41p.

Garza, Sergio, 1966, Ground-water resources of the San Antonio area, Texas, a progress report on studies, 1960-64, Texas Water Development Board Report 34, 31p.

Garza, Sergio, 1968, Aquifer characteristics from well-field production records Edwards Limestone, San Antonio area, Texas, unpublished M. S. Thesis, Department of Hydrology and Water Resources, University of Arizona, Tucson, 46p.

Gaspar, E., and Oncescu, M., 1972, Radioactive tracers in hydrology, Elsevier Publishing Company, Amsterdam, the Netherlands, 342p.

Gelhar, Lynn W., and Wilson, John L., 1974, Ground-water quality modeling, Ground Water, v. 12, n. 6, pp. 399-408.

Green, C. R., and Sellers, W. D., eds., 1964, Arizona climate, University of Arizona Press, Tucson, 503p.

Guymon, Gary L., 1970, A finite element solution of the one-dimensional diffusion-convection equation, Water Resources Research, v. 6, n. 1, pp. 204-210.

Guymon, Gary L., Scott, V. H., and Herrmann, L. R., 1970, A general numerical solution of the two-dimensional diffusion-convection equation by the finite element method, Water Resources Research, v. 6, n. 6, pp. 1611-1617.

Hastings, James R., and Turner, Raymond, 1965, The changing mile, University of Arizona Press, Tucson, 317p.

Himmelblau, David M., and Bischoff, Kenneth B., 1968, Process analysis and simulation: deterministic systems, John Wiley and Sons, New York, 348p.

Holtan, H. N., 1961, A concept for infiltration estimates in watershed engineering, ARS 41-51, Agricultural Research Service, U. S. Department of Agriculture, 25p.

Kirkham, Don, and Powers, W. L., 1972, Advanced soil physics, Wiley-Interscience, New York, 534p.

Knisel, Walter G., 1972, Response of karst aquifers to recharge, Hydrology Paper 60, Colorado State University, Fort Collins, 48p.

Kraijenhoff van de Leur, D. A., 1958, A study of non-steady ground-water flow with special reference to the reservoir coefficient, Ingenieur, n. 19, pp. 87-94.

Laney, R. L., 1972, Chemical quality of the water in the Tucson Basin, Arizona, U. S. Geological Survey Water-Supply Paper 1939-D, 46p.

Levenspiel, Octave, 1972, Chemical reaction engineering, John Wiley and Sons, New York, 2nd edition, 578p.

Libby, W. F., 1955, Radiocarbon dating, University of Chicago Press, Chicago, 2nd edition, 175p.

Linsley, Ray K., Kohler, Max A., and Paulhus, Joseph L. H., 1958, Hydrology for engineers, McGraw-Hill, New York, 340p.

Long, Austin, 1975, Department of Geosciences, University of Arizona, Tucson, personal communication.

Mandeville, A. N., and O'Donnell, T., 1973, Introduction of time variance to linear conceptual catchment models, Water Resources Research, v. 9, n. 2, pp. 298-310.

Moore, Walter J., 1972, Physical chemistry, Prentice-Hall, Inc., Englewood Cliffs, N. J., 4th edition, 977p.

Munnich, K. O., 1957, Messung des ^{14}C-Gehaltes von hartem Grundwasser, Naturwiss, v. 44, pp. 32-42.

Munnich, K. O., and Vogel, J. C., 1960, C^{14} age determination of deep ground-waters, International Association of Scientific Hydrology Publication 52, v. 2, General Assembly of Helsinki, pp. 537-541.

Nash, J. E., 1957, The form of the instantaneous unit hydrograph, International Association of Scientific Hydrology Publication 45, pp. 114-121.

Nelson, R. William, 1973, N-stream functions for three-dimensional flow in heterogeneous porous materials, unpublished report, Computer Sciences Corp., Richland, Washington, 24p.

Neuman, Shlomo P., and Witherspoon, Paul A., 1971, Analysis of non-steady flow with a free surface using the finite element method, Water Resources Research, v. 7, n. 3, pp. 511-523.

Nir, A., 1964, On the interpretation of tritium "age" measurements of groundwater, Journal of Geophysical Research, v. 69, n. 12, pp. 2589-2595.

Payne, Bryan R., 1972, Isotope hydrology, in Chow, Ven Te, ed., Advances in hydroscience, v. 8, pp. 95-138, Academic Press, New York, 359p.

Pearson, F. Joseph, Jr., 1974, Water Resources Division, U. S. Geological Survey, Reston, Virginia, written communication.

Pearson, F. Joseph, Jr., Rettman, P. L., and Wyerman, T. A., 1974, Environmental tritium in the Edwards Aquifer, central Texas, 1963-1971, unpublished report, Water Resources Division, U. S. Geological Survey, Reston, Virginia.

Pettit, B. M., Jr., and George, W. O., 1956, Ground-water resources of the San Antonio area, Texas, Texas Board of Water Engineers Bulletin 5608, parts 1 and 2.

Pinder, George F., 1973, A Galerkin-finite element simulation of groundwater contamination on Long Island, New York, Water Resources Research, v. 9, n. 6, pp. 1657-1669.

Pinder, George F., and Cooper, H. H., Jr., 1970, A numerical technique for calculating the transient position of the saltwater front, Water Resources Research, v. 6, n. 3, pp. 875-882.

Prickett, T. A., and Lonnquist, C. G., 1971, Selected digital computer techniques for groundwater resource evaluation, Bulletin 55, Illinois State Water Survey, Urbana, 62p.

Przewlocki, K., and Yurtsever, Y., 1974, Some conceptual mathematical models and digital simulation approach in the use of tracers in hydrological systems, paper presented at the Symposium on Isotope Techniques in Ground-water Hydrology, International Atomic Energy Agency, Vienna, March 11-15, 1974.

Reddell, Donald Lee, and Sunada, Daniel K., 1970, Numerical simulation of dispersion in groundwater aquifers, Hydrology Paper 41, Colorado State University, Fort Collins, 79p.

Remson, I., Hornberger, G., and Molz, F. J., 1971, Numerical methods in subsurface hydrology, John Wiley and Sons, New York, 389p.

Sagar, Budhi, 1973, Calibration and validation of aquifer models, Technical Report 17, Department of Hydrology and Water Resources, University of Arizona, Tucson, 175p.

Scheidegger, A. E., 1961, General theory of dispersion in porous media, Journal of Geophysical Research, v. 66, n. 10, pp. 3273-3278.

Simpson, Eugene S., 1970, unpublished lecture notes, Department of Hydrology and Water Resources, University of Arizona, Tucson.

Simpson, Eugene S., 1973, Finite-state mixing cell models, unpublished report, Department of Hydrology and Water Resources, University of Arizona, Tucson, 12p.

Simpson, Eugene S., 1974, Department of Hydrology and Water Resources, University of Arizona, Tucson, personal communication.

Simpson, Eugene S., and Duckstein, Lucien, 1975, Finite state mixing-cell models, paper presented at Bilateral United States-Yugoslavian Seminar in Karst Hydrology and Water Resources, Dubrovnik, Yugoslavia, June 1975.

Smart, J. S., 1972, Channel networks, in Chow, Ven Te, ed., Advances in hydroscience, v. 8, pp. 305-346, Academic Press, New York, 359p.

Smith, G. E. P., 1910, Ground water supply and irrigation in the Rillito Valley, Arizona, Bulletin 64, University of Arizona Agricultural Experiment Station, 244p.

Supkow, Donald J., 1973, Tucson Basin digital model user's manual, unpublished report, Department of Hydrology and Water Resources, University of Arizona, Tucson, 16p.

Thompson, G. M., Hayes, J. M., and Davis, S. N., 1974, Fluorocarbon tracers in hydrology, Geophysical Research Letters, v. 1, n. 4, pp. 177-180.

Thrailkill, John, 1972, Digital computer modeling of limestone ground-water systems, University of Kentucky Water Resources Institute Research Report n. 50, Lexington, 71p.

Vogel, J. C., 1967, Investigation of groundwater flow with radiocarbon, in Isotopes in hydrology, pp. 355-369, International Atomic Energy Agency, Vienna, 740p.

Wallick, Edward I., 1973, Isotopic and chemical considerations in radiocarbon dating of groundwater within the arid Tucson basin, Arizona, unpublished Ph. D. Dissertation, Department of Geosciences, University of Arizona, Tucson, 184p.

Wendt, I., Stahl, W., Geyh, M., and Fauth, F., 1967, Model experiments for ^{14}C water-age determinations, in Isotopes in hydrology, pp. 321-337, International Atomic Energy Agency, Vienna, 740p.

Wentworth, Chester K., 1948, Growth of the Ghyben-Herzberg transition zone under a rinsing hypothesis, Transactions, American Geophysical Union, v. 29, n. 1, pp. 97-98.